

INVESTIGATION INTO THE BIOISOSTERIC APPROACH IN THE DESIGN, SYNTHESIS AND EVALUATION OF MUSCARINIC RECEPTOR LIGANDS

A Dissertation
Submitted to
the Temple University Graduate Board

In Partial Fulfillment
of the Requirements for the Degree
DOCTOR OF PHILOSOPHY
(OF PHARMACEUTICAL SCIENCE)

by
Richie R. Bhandare
January 2013

Examining Committee Members:

Daniel J. Canney, Ph.D, Advisory Chair, Department of Pharmaceutical Sciences
Michael Borenstein, Ph.D, Department of Pharmaceutical Sciences
Magid Abou-Gharbia, Ph.D, Department of Pharmaceutical Sciences
Marc Ilies, Ph.D, Department of Pharmaceutical Sciences
Boyd L. Harrison, Ph.D, External Member (Pfizer, Retired)

ABSTRACT

INVESTIGATION INTO THE BIOISOSTERIC APPROACH IN THE DESIGN, SYNTHESIS AND EVALUATION OF MUSCARINIC RECEPTOR LIGANDS

Richie R. Bhandare

Doctor of Philosophy, Temple University, 2013

Doctoral Advisory Committee Chair: Daniel J. Canney, Ph.D., R.Ph.

The acetylcholine (ACh) receptor system belongs to rhodopsin GPCR family and is an integral membrane protein divided into two types: muscarinic and nicotinic. The naturally occurring neurotransmitter acetylcholine binds to these two receptor systems non-selectively. The regulatory effects of the neurotransmitter acetylcholine are diverse ranging from autonomic nervous system and the central nervous system through different types of neurons innervated by cholinergic inputs. Muscarinic acetylcholine receptors (mAChRs) are divided into five receptor subtypes (M_1 - M_5). In general, M_1 , M_3 and M_5 receptor subtypes are coupled *via* Gq like proteins; while M_2 and M_4 subtypes are coupled to Gi-proteins. Muscarinic receptors are widely distributed in the body where they mediate a variety of important physiological effects. mAChRs have been the target of drug development efforts for the treatment of various disorders including overactive bladder, Alzheimer's disease, pain, cognitive impairment, drug addiction, schizophrenia and Parkinson's disease. The development subtype selective ligands possess a challenge due to a high degree of homology among mAChR subtypes, however the recent availability of the X-ray crystal structure for the M_2 and M_3 receptor can be utilized for the design of new ligands. The pharmacophoric requirements for cholinergic ligands have been reported by numerous investigators based on structure-activity relationship (SAR) and/or molecular modeling data of known muscarinic ligands. These fundamental requirements are useful when designing muscarinic ligands but have provided little guidance in the design of subtype selective compounds. Our interest in developing novel muscarinic receptor ligands led to the design of lactone-based ligands using an approach similar to that reported by Kaiser *et al.* Preliminary binding studies of our

previously synthesized lactone based compounds indicated that several were nonselective, low affinity ($IC_{50} = \mu M$ range) muscarinic agonists (based on preliminary in vivo data). Hence based on the background information, we decided to utilize the previously synthesized lactone parent compound as lead molecule set out to investigate a new series of lactone based compounds in order improve the affinity and later the selectivity of ligands. Bioisosteric approach has been investigated for the metabolic lability of the lactone ring. Four probable bioisosteres have been evaluated: tetrahydrofuran, 1,3-benzodioxole, oxazolidinone and chromone. Thermal/microwave assisted synthesis has been utilized in the generation of intermediates as well as final compounds. Preliminary screening and further evaluation (IC_{50} / subtype selectivity) has resulted in the identification of promising fragments as bioisosteres for the lactone ring

ACKNOWLEDGEMENTS

It is with a deep sense of gratitude that I write this acknowledgement. First, I would like to thank my thesis advisor Dr. Daniel J. Canney for his support and guidance. I would not have overcome the challenges of my student life at Temple University School of Pharmacy without his support. The insightful discussions and literature review sessions we had together has changed my perspective of scientific research. I owe my gratitude to Dr. Magid Abou-Gharbia, Director of the Moulder Center for Drug Discovery Research (MCDDS) for allowing me to work in this lab (MCDDS). The instrumentation provided to me has been of utmost help in my project.

I would like to thank Mr. Rogelio Martinez, for training me on the instrumental techniques in the Moulder Center for Drug Discovery Research.

I would like to thank Dr. Benjamin Blass for his valuable suggestions and assistance in generation of patent application which has now given a new direction to the project.

I would like to thank Dr Jack Gordon for his timely help in this project

I would like to thank all the Scientists from MCDDS for their timely cooperation.

I would like to thank Dr. Marc Ilies, Director of the NMR facility for helping with the NMR data for the compounds.

I thank the Dean Dr. Peter Doukas for the continued financial support in the form of teaching assistantship.

I thank Ms. Almira Cutler and Sopon Din for their assistance with administrative matters.

I would like to thank my seniors Shyam Desai, and Sivakumar for teaching me lab techniques during my initial years in the lab and having a wonderful time in the lab.

I would like to thank my labmates Rong and Otito Iwuchukwu for their cooperation and support.

I would like to thank my friends Aditya, Siva, Silpa, Manali, Satish, Jyoti, Amir, Kalpana, Biji, Mayuri, Bharat and Narendra for all the nice times we had at Temple.

I would like to thank my good friends Dr. Anurag Mishra, Milind Ranade, Pushkar for being with me during my times at Temple.

Last but not the least I would like to thank my Parents who stood by me during my utmost difficult times in my life.

Finally I would like to thank my Almighty and Guru's (Subodh Guruji, Ravi Dada and Deepak Kaka) for their blessings in this journey.

Dedicated
to my
mother

TABLE OF CONTENTS

ABSTRACT	Page iii
ACKNOWLEDGEMENT	iv
LIST OF TABLES	viii
LIST OF FIGURES	ix
LIST OF SCHEMES	xi
CHAPTER 1	
INTRODUCTION AND BACKGROUND	
1.1 Cholinergic receptor system.....	1
1.2 G protein coupled receptor system.....	2
1.3 Muscarinic signal transduction.....	4
1.4 Distribution and functional role of muscarinic receptors.....	5
1.5 Muscarinic receptors as therapeutic targets.....	7
1.6 Subtype selective muscarinic ligands reported in literature.....	13
CHAPTER 2	
DESIGN CONSIDERATIONS FOR MUSCARINIC RECEPTOR LIGANDS.....	
	21
CHAPTER 3	
SPECIFIC AIMS OF THE STUDY	
3.1 Specific Aim 1	
Modification of lead lactone 34	
3.1.1 (a) Incorporate aromatic and heteroaromatic ring systems to improve the affinity and evaluate higher affinity ligands for subtype selectivity.....	28
3.1.2 (b) Evaluate suitable bioisosteric replacements for the hydrogen bonding lactone fragment.....	29
3.2 Specific Aim 2	
3.2.1 (a) Develop retrosynthetic schemes for intermediate scaffolds and target ligands.....	32
3.2.2 (b) Design synthetic routes for the preparation of target ligands	40
3.3 Specific aim 3	

3.3.1 (a) <i>In-vitro</i> evaluation of target ligands in muscarinic receptor binding assay.....	45
3.4 Specific Aim 4	
Utilize preliminary data from earlier target compounds to direct molecular modification of leads.....	46
CHAPTER 4	
RESULTS	
4.1.1. Synthetic routes for the preparation of H-bonding fragments.....	48
4.1.2 Synthetic routes used for the preparation of amine-containing fragments.....	54
4.1.3. Preliminary binding studies of target ligands.....	60
CHAPTER 5	
DISCUSSION	
5.1.1 Synthesis of ortho-substituted phenyl piperidines.....	73
5.1.2 Synthesis of N3-substituted oxazolidinones.....	78
5.2 Biological activity of target compounds.....	81
5.3 Future directions.....	94
CHAPTER 6	
EXPERIMENTAL SECTION.....	96
REFERENCES.....	129
APPENDIX	
A. NMR SPECTRA	
B. LC-MS SPECTRA	

LIST OF TABLES

	Page
Table 1. Antimuscarinic activity of 27	24
Table 2: Structure of representative lactone - based leads.....	25
Table 3: Preliminary binding data (% inhibition; 10 μ M) for target compounds 127-137	61
Table 4: Preliminary binding data (% inhibition; 10 μ M) for target ligands 138-145	62
Table 5: Preliminary binding data (% inhibition; 10 μ M) for target compounds 146 – 159	64
Table 6: Preliminary binding data (% inhibition at 10 μ M) for substituted tetrahydrofuran based compounds 160 – 161	65
Table 7: Preliminary binding data (% inhibition at 10 μ M) for chromone based compounds 162 – 174	69
Table 8: Subtype selectivity data at hM ₁ -hM ₅ for compounds 146, 148 and 151	71
Table 9: Solubility profile for target compounds.....	74
Table 10: Solubility profile for lactone based compounds	90
Table 11: Solubility profile for oxazolidinone based compounds.....	91
Table 12: Solubility profile for chromone based compounds.....	93

LIST OF FIGURES

	Page
Figure 1: Cartoon structure of acetylcholinergic receptor system.....	2
Figure 2: Putative structure of muscarinic acetylcholine receptor (GPCR).....	3
Figure 3: Signal transduction of muscarinic receptor subtype family.....	4
Figure 4: Structure of the non-selective muscarinic antagonist benactyzine and the anti-muscarinic activity of a lactone-based ligand designed by Kaiser et al.....	24
Figure 4: General structural features of the newly designed ligands.....	29
Figure 5: Current lactone-bioisostere based ligands.....	31
Figure 6: Proposed bioisosteres for the lactone.....	31
Figure 7: Oxazolidinone-based muscarinic ligand.....	32
Figure 8a: Retrosynthetic analysis for target compounds (lactone, tetrahydrofuran, 1,3-benzodioxole, oxazolidinone and chromone).....	33
Figure 8b: Retrosynthetic analysis for H-bonding group (lactone, tetrahydrofuran, 1,3-benzodioxole, oxazolidinone and chromone).....	37
Figure 8c: Retrosynthetic analysis for N-containing fragments.....	40
Figure 9: Routes to iodomethyl and hydroxymethyl lactone (39 , 40) and tetrahydrofuran (42).....	41

Figure 10: Suzuki promoted synthesis of phenylpiperidines/ piperazines.....	42
Figure 11: Synthesis of N3-substituted oxazolidin-2-one.....	43
Figure 12: Synthesis of N3-substituted oxazolidin-2-one.....	44
Figure 13: Proposed mechanism for the formation of N3-substituted oxazolidin-2-one.....	45
Figure 14: Synthesis of target ligands.....	46
Figure 15: Subtype selective profile of compound 146 (at 500 nM), 148 (at 100 nM) and 151 (at 500 nM).....	71

LIST OF SCHEMES

	Page
Scheme 1: Synthesis of iodolactone (39) and hydroxylactone (40)	49
Scheme 2: Synthesis of 4,4-Diethyl-2-iodomethyl-tetrahydrofuran (42)	50
Scheme 3: Synthesis of Toluene-4-sulfonic acid 2-(4,4-diethyl-tetrahydro-furan-2-yl)-ethyl ester (44)	50
Scheme 4: Synthesis of 5-(2-Iodo-ethyl)-benzo[1,3]dioxole (47) and 5-Iodomethyl-oxazolidin-2-one (48)	51
Scheme 5: Synthesis of toluene-4-sulfonic acid benzo[1,3]dioxol-2-ylmethyl ester (52)	51
Scheme 6: Synthesis of 3-(2-Hydroxy-ethyl)-oxazolidin-2-one (55)	52
Scheme 7: Synthesis of precursors 56 – 63	52
Scheme 8: Synthesis of 6,6,9,9-Tetramethyl-4-oxo-6,7,8,9-tetrahydro-4H-benzo[g]chromene-3-carbaldehyde (68)	53
Scheme 9: Synthesis of precursors 74 – 79	53
Scheme 10: Synthesis of 2-Hydroxymethyl-chromen-4-one (82)	54
Scheme 11: Synthesis of mesylate precursors (84-100)	55
Scheme 12: Synthesis of 2-(4-piperidinyl)-1H-benzimidazole (102)	56

Scheme 13: Synthesis of precursor 4- <i>o</i> -tolyl-piperidine (106).....	56
Scheme 14: Synthesis of 1-(2-Isopropyl-phenyl)-piperazine (109).....	57
Scheme 15: Synthesis of precursors 116 – 118 , 122 - 124 and 126	58
Scheme 16: Synthesis of target compounds 127-174	60

CHAPTER 1

INTRODUCTION AND BACKGROUND

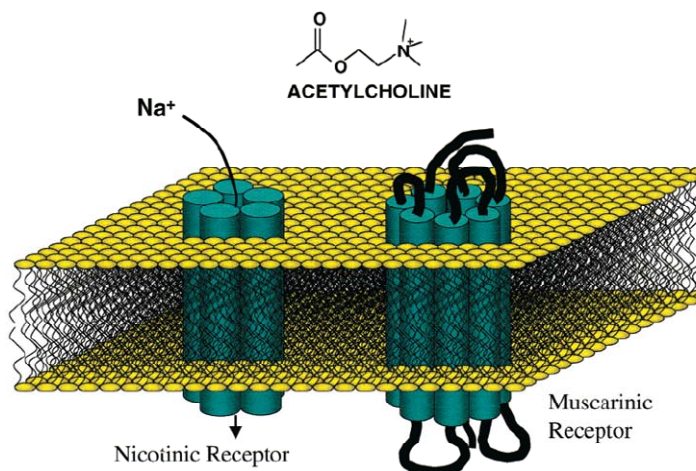
1.1 Cholinergic receptor system

Acetylcholine (ACh) is the neurotransmitter in the cholinergic system which binds to the muscarinic and nicotinic receptors. ACh binds to these two receptor systems non-selectively (**Figure 1**)⁴ to regulate a wide range of functions. It regulates peripheral activity through the autonomic nervous system and through different types of cholinergic inputs throughout the central nervous system (CNS). Nicotinic receptors belong to the superfamily of ligand-gated ion channels whereas muscarinic receptors belong to the G-protein (GTP binding proteins) coupled superfamily of receptors.³ Nicotine acetylcholine receptors (nAChRs) are pentameric membrane proteins that form cation channels and derive their name from their affinity for nicotine. These proteins consist of two to four distinct hydrophobic subunits that share a high degree of homology. Different combinations of subunits, including $\alpha_2\beta\gamma\delta$, $\alpha_2\beta\delta\epsilon$, $\alpha_2\beta_3$ have been observed in different tissues. Binding of nicotine to the receptor's α subunit results in opening of the cation channel. Like nicotine, acetylcholine (ACh) binds to α subunit of the nAChR resulting in opening of the ion channel.

The muscarinic acetylcholine receptor family was first discovered by its ability to bind muscarine, an alkaloid derived from the poisonous mushroom *Amanita muscaria*. In contrast to the nicotinic receptors, muscarinic receptors are single subunit proteins having seven transmembrane spanning regions and a large cytoplasmic domain between the fifth and sixth membrane - spanning regions. Different hydrophobic domains are involved in

the binding of acetylcholine to the mAChR. Binding results in a change in the conformation in the cytoplasmic regions which causes coupling to the G - protein.^{3,5}

Figure 1: Cartoon structure of acetylcholinergic receptor system⁴ [adapted with permission from Felder C. C, Bymaster F. P, Ward J and DeLapp N. (2000). Therapeutic opportunities for muscarinic receptors in central nervous system. *Journal of Medicinal Chemistry*, 43, 4333-4353].



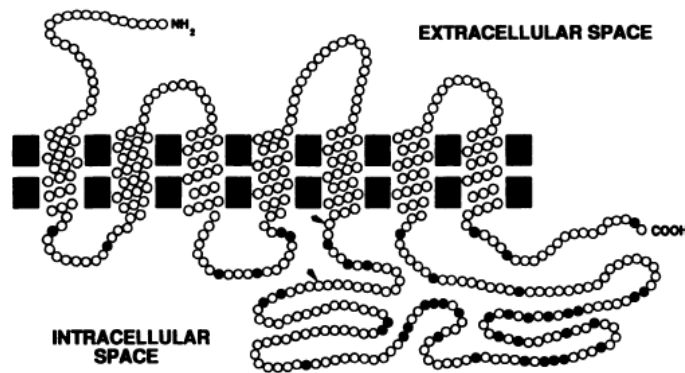
Muscarinic receptors are divided into five subtypes M₁ - M₅. Molecular cloning studies have now revealed the existence of molecularly distinct mammalian mAChR subtypes, M₁ - M₅. The physiological response to muscarinic receptor stimulation is a sequence of protein interactions that include G-protein interaction followed by stimulation or inhibition of effector channels or enzymes. Tissue localization and receptor subtype expression patterns influence the biological consequence of muscarinic receptor stimulation.^{3,4,6,7}

1.2 G protein coupled receptor system

One of the largest families of proteins found in nature is the G (guanine nucleotide) protein coupled receptor (GPCR) superfamily. Its primary mechanism of signaling is

such that the cells can sense changes in the external environment and convey this message to the interior part of the cell. Designing ligands for GPCRs for therapeutic purposes with agonists or antagonists has been successful with more than 50 % of drugs in the market. GPCRs can be activated by a number of different structural classes of extracellular ligands including neurotransmitters, hormones and drugs. The common structural criteria for the inclusion of receptors in the GPCR superfamily is the presence of seven transmembrane helical domains (TM I - VII) which are connected by three intracellular and three extracellular loops (**Figure 2**).^{1,2}

Figure 2: Putative structure of muscarinic acetylcholine receptor (GPCR)³. [adapted with permission from M. Marlene Hosey (1992). Diversity of structure, signaling and regulation within the family of muscarinic cholinergic receptors; *FASEB J* 6, 845-852.



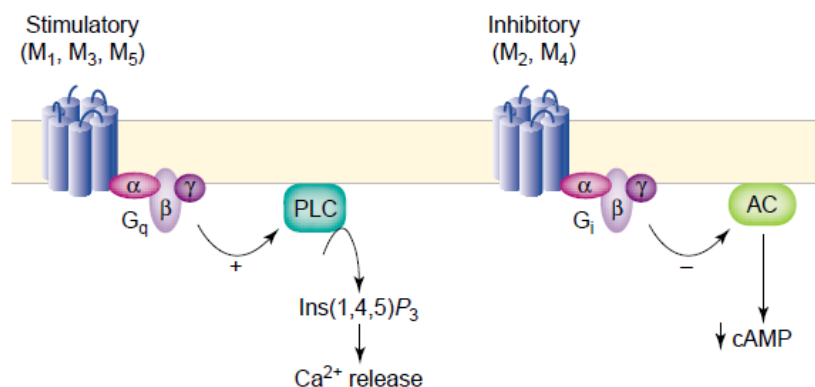
Upon activation by an agonist, GPCRs bind to the heterotrimeric GTP-binding proteins and cause GTP-GDP exchange. This results in dissociation of GTP-bound α -subunit and $\beta\gamma$ -dimer from the GPCR. Both $G\alpha$ and $G\beta\gamma$ subunits can modulate several downstream signaling pathways, including activation of phospholipases and phosphodiesterases and modulation of adenylate cyclases and ion channels. In addition to activating G-proteins, several GPCRs involve signaling molecules such as receptor serine/threonine kinases, tyrosine kinases, protein tyrosine phosphatases and adaptor proteins. The structures of

ligands that affect GPCRs are diverse and include small organic molecules, hormones, short and large polypeptides and glycoproteins. The human GPCRs can be classified into five distinct families: rhodopsin, glutamate receptor, adhesion receptor, taste2 receptor and secretin receptor.¹

1.3 Muscarinic signal transduction

In general, muscarinic receptor subtypes M_1 , M_3 and M_5 are coupled to Gq/11 stimulator proteins (**Figure 3**) and their activation by acetylcholine or suitable ligands stimulates the production of phospholipase C β . Activation of phospholipase C β results in the generation of diacylglycerol (DAG) and inositol triphosphate (IP₃) through hydrolysis of the membrane phospholipid phosphatidylinositol 4,5-bisphosphate. DAG binds and stimulates protein kinase C and IP₃ acts on the IP₃ ion channel receptor to liberate Ca²⁺ from intracellular compartments resulting in a transient cytosolic calcium flux.

Figure 3: Signal transduction of muscarinic receptor subtype family⁹ [adapted with permission from Eglen R. M., Choppin A. and Watson N. (2001). Therapeutic opportunities from muscarinic receptor research. *Trends in Pharmacological Sciences*, 22 409-414].



In addition to their ability to stimulate phospholipase C through G_q, M_1 , M_3 and M_5 have been shown to stimulate phospholipase A₂ (PLA₂) and phospholipase D (PLD) in various

cell lines and primary cultured cells. PLA₂ catalyzes the hydrolysis of membrane phospholipids which result in the generation of free arachidonic acid and the corresponding lysophospholipid.

M₂ and M₄ mAChRs are (**Figure 3**) generally coupled to Gi proteins and their activation results in decreasing concentrations of adenylyl cyclase. It is also proposed that M₂ and M₄ are involved in pre-activation of PLA₂.^{2,4,5,8,9,10,11} Other consequences of stimulating muscarinic receptors include activation of mitogen activated protein kinases, activation of calcium and potassium channels, activation of phospholipase A₂ and D, release of arachidonic acid, increase in intracellular calcium concentration, increase in inositol phosphates and activation of nitric oxide synthase pathways.^{13,14,15,16,17,18}

1.4 Distribution and functional role of muscarinic receptors

Muscarinic receptors are widely distributed in the human body. They are present centrally and peripherally thereby mediating a variety of physiological functions depending on their location. A brief discussion of the location and function of mAChRs is included below.^{19, 20}

Peripheral mAChRs:

i. Bladder:

The detrusor muscle of the human bladder has been shown to contain all five muscarinic subtypes with M₂ and M₃ predominating and bladder contractions controlled primarily by the M₃ subtype.

ii. Salivary glands:

The salivary glands contain M_1 and M_3 receptors. The M_3 receptors are involved in the control of high and low viscosity secretions and saliva volume whereas the M_1 receptor is involved in high viscosity lubrication.

iii. Gastrointestinal tract (GI):

The smooth muscle of the gastrointestinal tract contains all receptor subtypes; however the M_2 and M_3 subtypes appear to be functionally most relevant. In humans the M_2 receptor subtype is found in higher density than the M_3 receptor but both contribute towards contractility of the GI tract.

iv. Heart:

The M_2 receptor predominates in human heart where it is involved in maintaining pacemaker activity, atrioventricular conduction and the force of contraction in the atrium and the ventricle. The M_1 receptor has been shown to increase heart rate while the M_3 receptor influences cardiac movement.

mAChRs located in the CNS:

i. Brain:

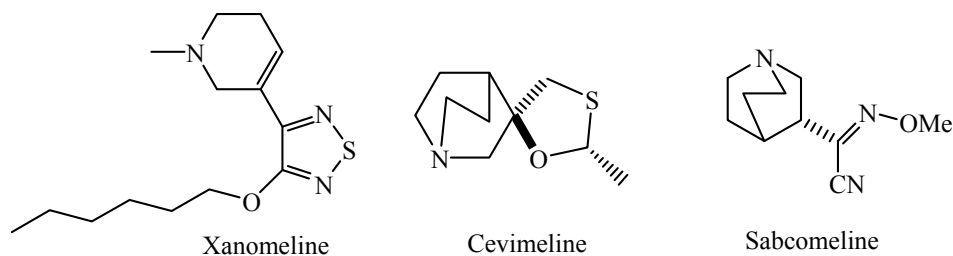
The human brain has been shown to express all five subtypes of mAChRs. They are believed to be involved in cognitive processes such as learning and memory. The M_1 receptors are found in neocortex, hippocampus and neostriatum. The M_2 subtypes are found in hippocampus and cortex while M_4 are present abundantly in neostriatum, cortex, hippocampus and striatum. The M_5 subtype is the only muscarinic receptor to be expressed by dopamine containing neurons of the substantia nigra pars compacta (provides principal dopamine innervations to the striatum). Activation of M_5 receptor

leads to dopamine release in that region of the brain. M₅ receptor is involved in maintenance of blood - brain barrier permeability caused by changes in the local blood flow. This effect has been associated with nitric oxide (NO) release induced by M₅ activation.

1.5 Muscarinic receptors as therapeutic targets

i. Alzheimer's disease and cognitive impairment^{6,11,22,23}:

mAChRs play a vital role in the process of learning and memory (cognition) and the M₁, M₂ and M₅ subtypes have been investigated as possible targets for anti-Alzheimer's therapy. Pharmacological evidence suggests that M₁ mAChR can mediate many of cognitive enhancing effects of ACh. The M₁ mAChR expressed in neocortex, hippocampus and neostriatum (memory and recognition region) is reported to be involved in the process of learning and memory as demonstrated in M₁ receptor knockout studies in mice. The M₂ autoregulatory receptor has also been implicated in the cognitive process. Hence blocking the centrally located M₂ autoreceptor may be a useful approach in improving cognition by increasing synaptic ACh levels. Centrally located M₅ receptors has been attributed to the cognitive enhancing effects of ACh and developing agonists for this receptor subtype can be a viable approach for the treatment of this disorder. Clinical candidates including xanomeline, cevimeline and sabcomeline have been evaluated for the treatment of Alzheimer's disease. Although they showed some level of clinical efficacy, they also exhibited adverse effects in clinical trials.



ii. Schizophrenia^{6,21}:

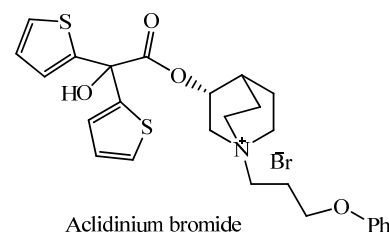
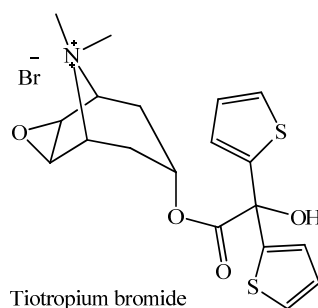
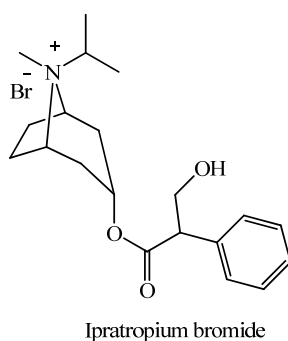
Schizophrenia is a complex disorder characterized by dopamine hyperactivity in subcortical areas such as the nucleus accumbens. The M_1 , M_4 and M_5 subtypes appear to play a role in schizophrenia. Human studies have shown that the density of M_1 and M_4 receptors in the brains of schizophrenic patients (postmortem and PET scans) are decreased in the basal ganglia and prefrontal cortex. Mice that are deficient in M_1 receptors have increased extracellular dopamine concentrations in the striatum. Hence activating the centrally located M_1 receptor can be considered a useful strategy. A deficiency of M_4 auto receptors in the midbrain of mice has been associated with an increase in the dopamine efflux in the nucleus accumbens. Hence developing an agonist for centrally located M_4 receptors may prove useful in the treatment of schizophrenia. Lastly, stimulation of the M_5 receptor has been shown to cause release of dopamine in striatum where they are found in higher density. M_5 knockout mice show a decrease in dopamine release suggesting that M_5 antagonist may be a rationale approach for the treatment of the disorder.

iii. Pain⁶:

Central and peripheral mAChRs have been shown to be involved in nociception. Current research suggests that the M_2 receptor is the predominant subtype involved in analgesia.

iv. COPD/bronchial asthma^{6,22}:

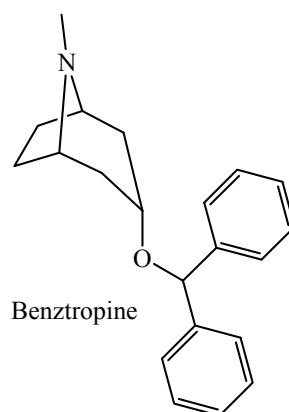
Some of the symptoms of chronic obstructive pulmonary disorder (COPD) and asthma are caused by increase in the vagal activity in the pulmonary tract. Contractions of airway smooth muscles are mediated predominantly by M_3 receptors. Other subtypes such as the airway M_1 receptors are also shown to be involved in mediating COPD/asthma. Compounds (nonselective) in clinical use include ipratropium, tiotropium and the recently approved aclidinium bromide. Both drugs are administered by inhalation.



v. Parkinson's disease^{6,27}:

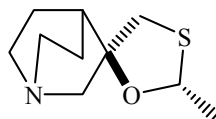
Parkinson's disease is characterized by degeneration of dopaminergic neurons located in the substantia nigra pars compacta that provide dopaminergic innervations to the striatum. Proper locomotor control requires a balance in muscarinic cholinergic and dopaminergic neurotransmission in the striatum. The M_4 receptors are expressed along with dopamine D_1 receptors in the striatum and this subpopulation of neurons gives rise to the striatonigral pathway. Activation of this pathway has been shown to lead to improvement in locomotor activity. Consequently selective M_4 receptor antagonists have been proposed as a possible treatment for the disorder. Similarly, M_1 knockout mice

models cause an increase in dopamine levels in the striatum. Hence blockade of centrally located M_1 receptors or M_4 receptors or mixed M_1/M_4 antagonists may a useful approach in the development of anti-Parkinson's agents. The nonselective anticholinergic agent currently in clinical use for the treatment of tremors and rigidity observed in Parkinson's disease is benzotropine.



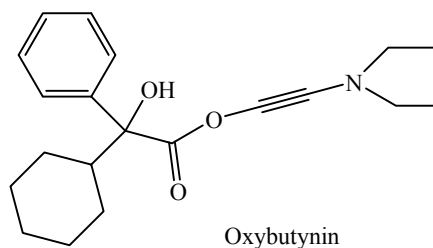
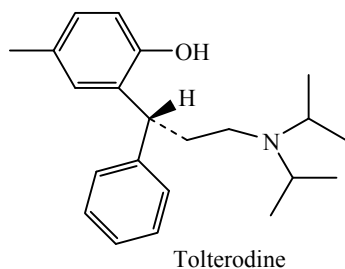
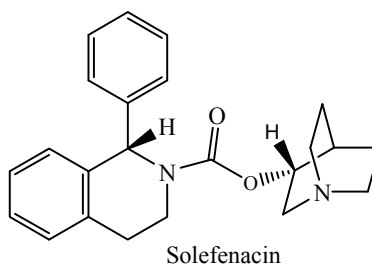
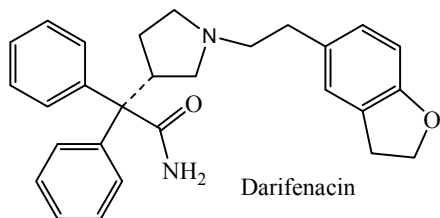
vi. Impaired salivary secretions^{6,22}:

Oral dryness or xerostomia is a condition caused by decrease in the salivary secretion due to malfunctioning of the salivary glands. Salivary secretion is mediated primarily by the glandular mAChRs. Studies on mAChR - mutant mice show that M_3 and M_1 subtypes are primarily responsible for salivary gland secretions. Hence, developing dual M_1/M_3 receptor agonists may be useful in treating oral dryness. Cevimeline (M_1/M_3 agonist) is in clinical use for the treatment of dry mouth.



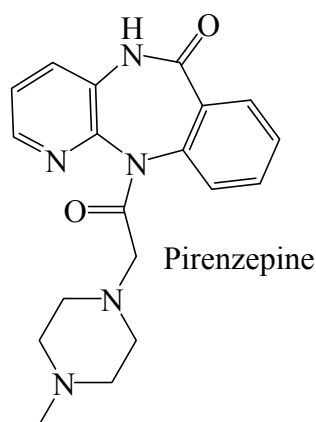
vii. Gastrointestinal (GI) and Urinary bladder disorders^{6,19,22,24,25,26}:

Nonselective muscarinic antagonists are useful in treating GI (irritable bowel syndrome, IBS) and urinary bladder (overactive bladder; OAB) disorders characterized by an increase in smooth muscle contractile activity. These nonselective agents are known to exhibit undesirable adverse effects related to their actions at nontarget receptor subtypes. The GI tract and urinary bladder predominantly express M₂ and M₃ receptor subtypes. Hence blockade of these two receptor subtypes would be anticipated to lead to agents useful in the treatment of GI and urinary bladder disorders with more favorable adverse effect profiles. Compounds in clinical use for the treatment of OAB include darifenacin, and solifenacin, both of which are M₃ selective agents. Tolterodine and oxybutynin (nonselective antagonists) are used for the treatment of urinary incontinence.



viii. Peptic ulcer^{6,40}:

An important mechanism for gastric acid secretion is vagal activity associated with stimulation of gastric mAChRs. Hence blockade of mAChRs can be a strategy of treating peptic ulcer disease. Studies show that M_1 and M_3 receptors are involved in basal gastric acid secretion. The M_5 receptor has also been implicated in increased gastric acid secretion. Pirenzepine is an M_1 selective agent in clinical use for the treatment of peptic ulcer.



ix. Type 2 diabetes⁶:

Type 2 diabetes is characterized by an inability of the pancreatic beta cells to deliver insulin in the blood following increases in blood glucose concentrations. Studies have shown that ACh, following its release from intrapancreatic parasympathetic nerve endings, can stimulate beta cell mAChRs leading to increases in glucose stimulated insulin secretion (GSIS). Furthermore, it is the M_3 subtype that is involved in cholinergic amplification of GSIS as evident from studies of M_3 knockout mice models where GSIS is found to be decreased. Hence developing M_3 agonists may prove effective in the treatment of this disorder.

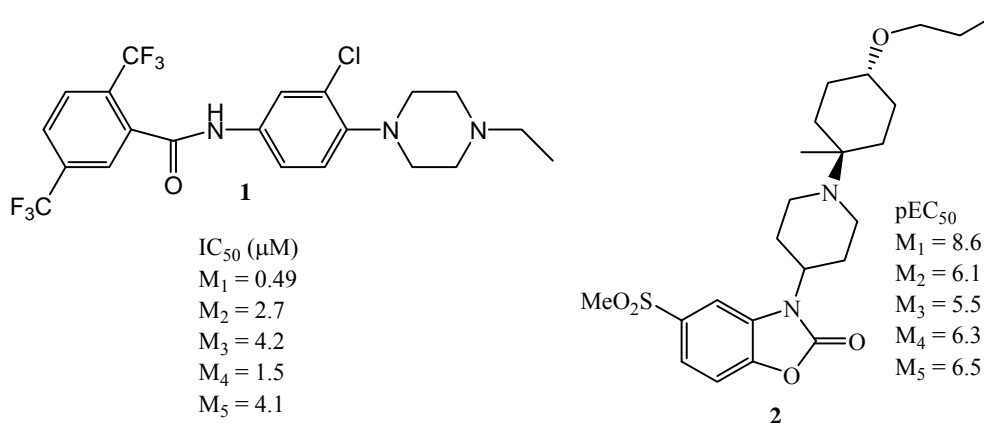
The following section describes selected muscarinic ligands for varying subtypes (agonists and antagonists) that have been reported in the literature.

1.6 Examples of subtype selective muscarinic ligands reported in the literature

A variety of approaches have been utilized in the development of subtype selective mAChR agonists and antagonists. The following section presents examples of muscarinic ligands with an eye toward highlighting molecular fragments present in the compounds.

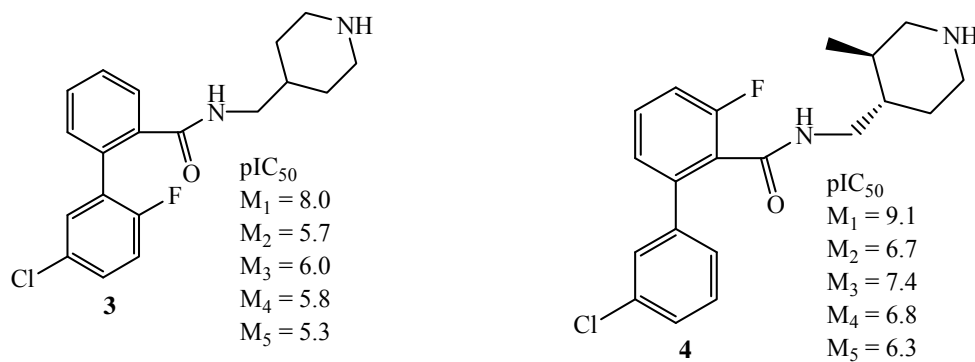
(a) Ligands exhibiting a preference for the M₁ receptor subtype.

A high throughput screen identified benzamide containing lead molecule. A detailed investigation of SAR study lead to the identification of compound **1** having 3-8 fold selectivity for M₁ subtype. Virtual screening of an in-house compound collection at GlaxoSmithKline led to the discovery of a series of benzoxazolidinones as muscarinic ligands. SAR studies identified **2** as a ligand with good potency and agonist activity at M₁ receptors.^{28, 29}

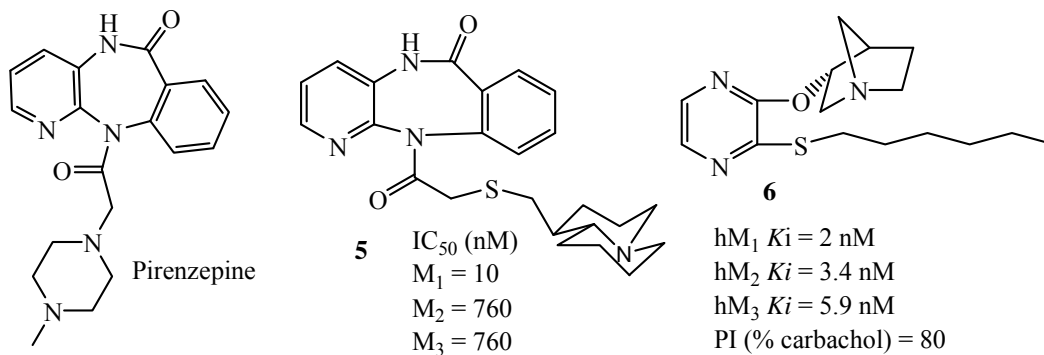


Jin et. al at GlaxoSmithKline analyzed corporate databases and identified a biaryl amide series of compounds (**3**, **4**) that exhibited potent agonist properties and M₁ selectivity.³⁰

31

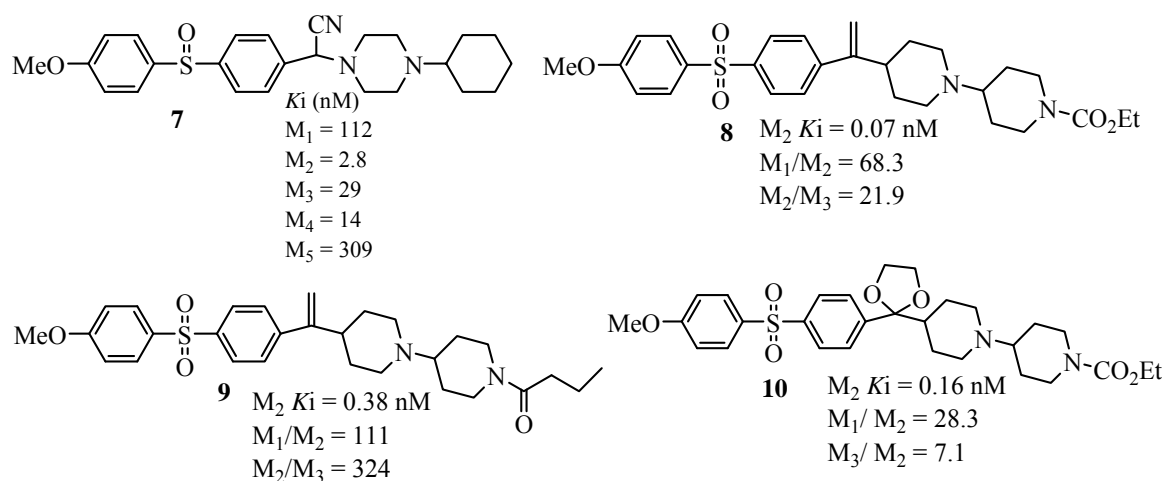


Varying the spacial location of the quinolizidine nitrogen relative to the tricyclic system characteristic of the antagonist pirenzepine resulted in the discovery of **5** that shows good selectivity for the M₁ receptor. Investigations at Wyeth on a lead M₂ selective agonist led to the identification of a series of pyrazine ether / thioether-based ligands. Compound **6** was shown to be an M₁ agonist with good affinity and efficacy.^{32, 42}



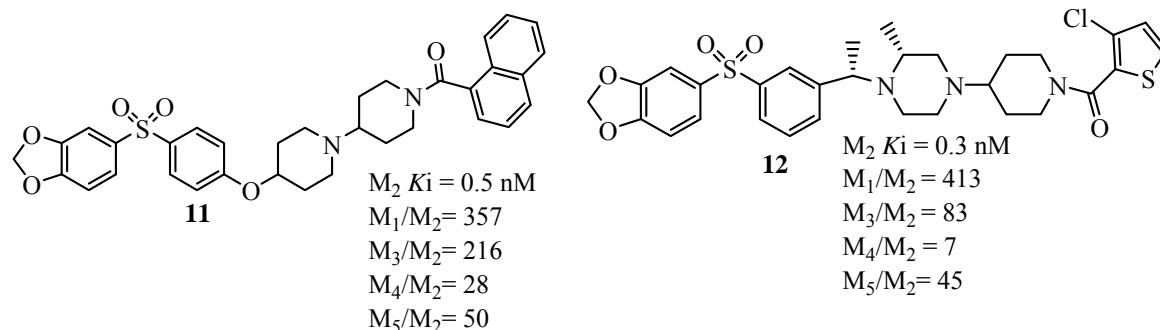
b) Ligands exhibiting preference for the M₂ receptor subtype.

Compound **7** is an antagonist with excellent affinity and selectivity for the M₂ subtype over M₁ and M₃ subtypes. The rationale behind elongating the cyclohexyl unit is to allow additional sites for interactions (steric/ hydrogen bonding) with the receptors. Hence molecular modifications of **7** and SAR studies led to the identification of three additional M₂ antagonists (**8**, **9** and **10**) with further improvements in affinity and selectivity for the M₂ subtype. Due to the metabolic instability of the styrene group and chemical reactivity of the benzylic cyano group, a stable ketal functionality (bioisosterism) was introduced at the benzylic position resulting in compound **10**.^{33, 34, 35a, 39, 41}

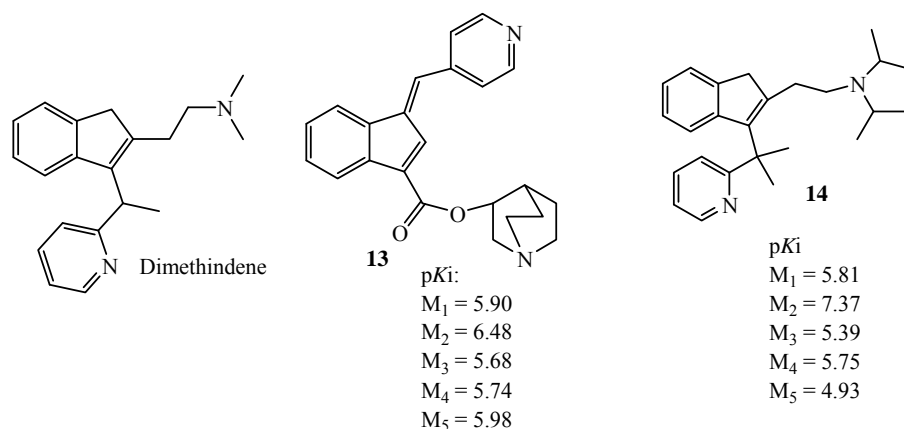


In a similar approach, the metabolically labile ethylidene moiety (compound **8**) and *p*-methoxy phenyl ring in compounds **8** and **9** was substituted with ether linkage and the *p*-methoxy phenyl ring was replaced by much stable benzodioxole that provided compound **11**. Compound **11** is an antagonist with excellent affinity for the M₂ subtype and improved selectivity over M₁ and M₃ subtypes. Taking into the consideration the SAR parameters required to have good affinity and selectivity, the same group incorporated appropriate features such as substitution of sulfoxide (prone to racemization) with

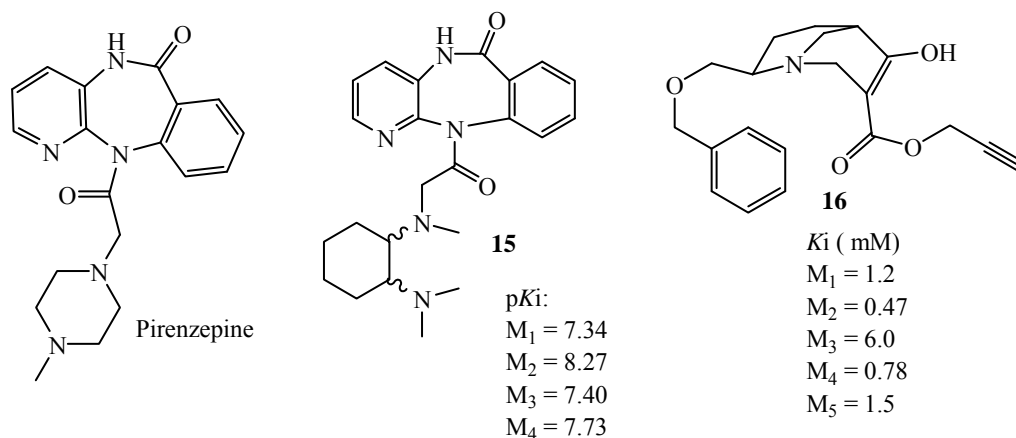
sulfone, replacement of *p*-methoxy phenyl ring with metabolically stable benzodioxole and ethylidene moiety with substituted methylene unit, a series of compounds were synthesized and resulted in the identification of 1-[4-(4-arylsulfonyl)phenylmethyl]-4-(1-aryloxy-4-piperidinyloxy) piperazine skeleton based compound **12**. Appropriately positioned and configured methyl groups at the benzylic center and at the piperazine 2-position were crucial for in selectivity and affinity for the M₂ subtype.^{34, 35b}



Dimethindene is an H₁ receptor antagonist that also possesses antimuscarinic properties. In an effort to increase the affinity and selectivity of dimethindene for M₂ muscarinic receptors and diminish H₁ binding, structural modification were made on the indene nucleus. These modifications led to the discovery of **13** and **14**. The quinuclidine analog **13** was the most promising compound in terms of receptor affinity and M₂ -subtype selectivity.^{36, 38}



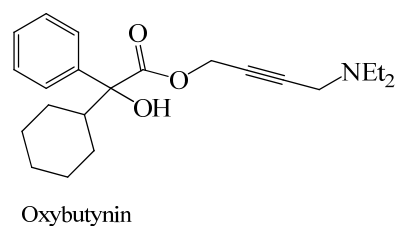
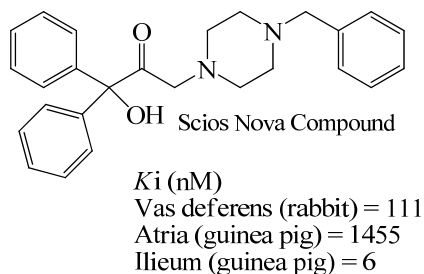
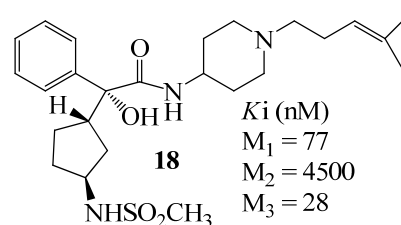
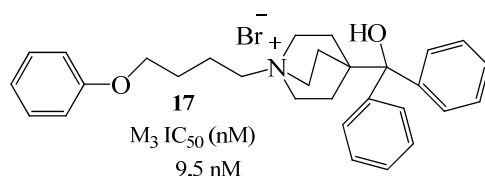
Modification of the known M_1 antagonist pirenzepine with a cyclohexane-1,2-diamine moiety provided compound **15** with M_2 affinity and selectivity. Additional SAR studies conducted on pirenzepine analogs provided the [3.3.1]-bicyclic amine, **16** which was shown to be an antagonist with modest selectivity for M_2 over M_1 , M_3 - M_5 subtypes.^{37, 40}



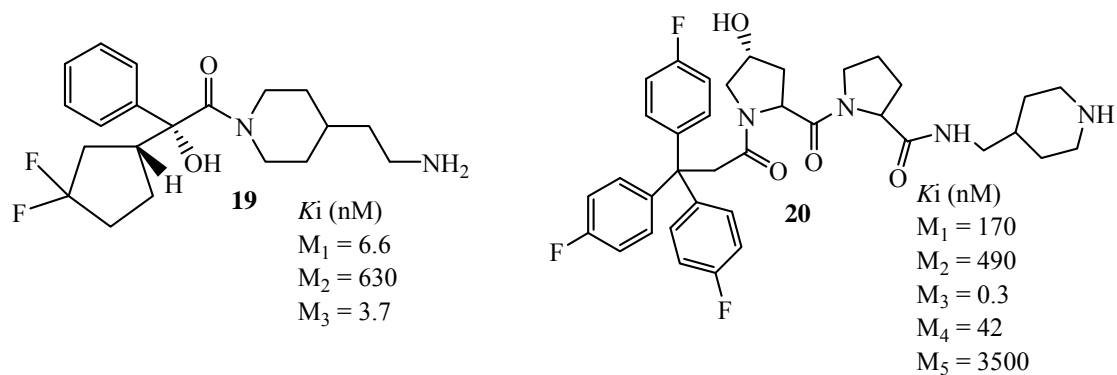
(c) Ligands exhibiting preference for the M_3 receptor subtype.

Optimization of a lead compound identified by high throughput screening (HTS) provided a novel series of 4-hydroxyl(diphenyl)methyl substituted quinuclidines which ultimately led to the discovery of **17** as a promising M_3 antagonist. Compound **18**

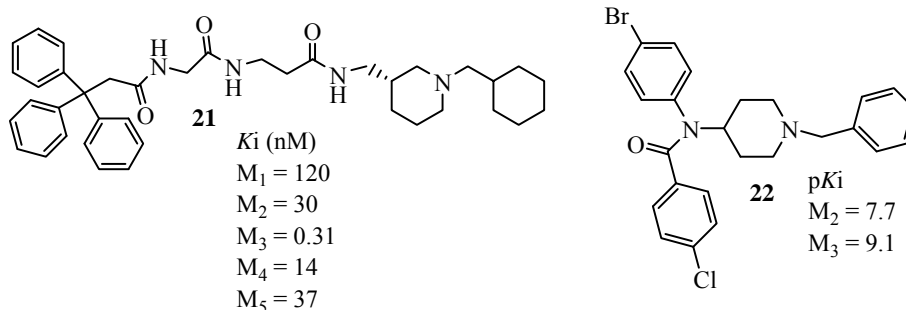
belongs to class of 4-acetamidopiperidine series identified by Merck. This molecule was designed with 4-acetamidopiperidine nucleus as core entity using structural features of two compounds; Scios Nova compounds and oxybutynin. The presence of amide region prevents the metabolism issues exhibited by esterases enzymes in the liver. Compound **18** was shown to exhibit good selectivity for the M₃ over the M₂ subtype.^{43, 44}



During the course of a project aimed at developing metabolically stable M₃ receptor antagonists, Mitsuya et. al in collaboration with scientists at Merck, discovered a series of (2*R*)-2-[(1*R*)-3,3-difluorocyclopentyl]-2-hydroxy-2-phenylacetamides having a variety of diamine functionalities. This work led to the identification of **19** as an M₃ selective antagonist. The compound was shown to have metabolic stability in rats, dogs and human liver microsomes. Compound **20** is a M₃ antagonist with a novel piperidine moiety and a terminal triphenylpropionamide moiety separated by a proline spacer.^{45, 46}



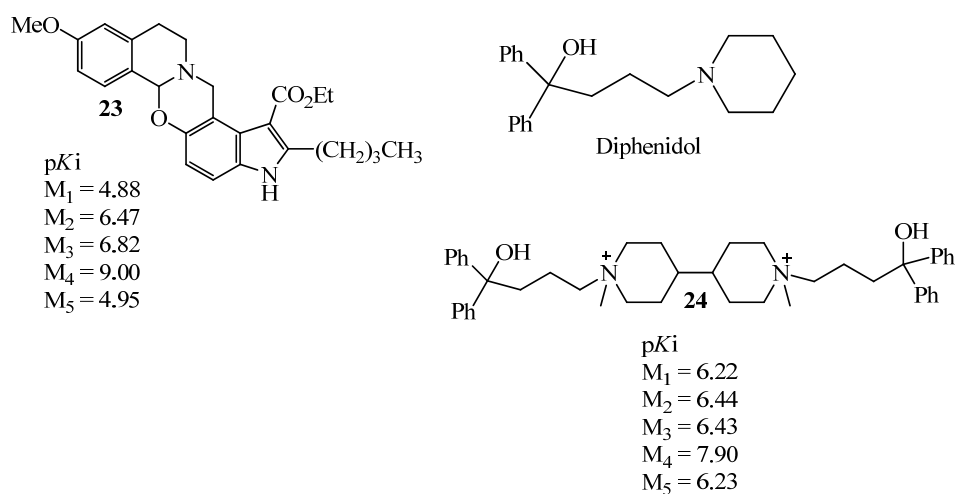
Application of a combinatorial chemistry approach led to the synthesis of a library that resulted in the identification of a ligand (**21**) possessing an amino acid spacer (glycine and β -alanine). *In-vitro* screening of **21** showed antagonist activity with high selectivity for M_3 over other subtypes. The 4-aminopiperidine scaffold was utilized in the synthesis of series of analogs which led to the discovery of **22**. Compound **22** had high affinity and good selectivity for M_3 subtype.^{47, 48}



(d) Ligands exhibiting a preference for the M_4 receptor subtype.

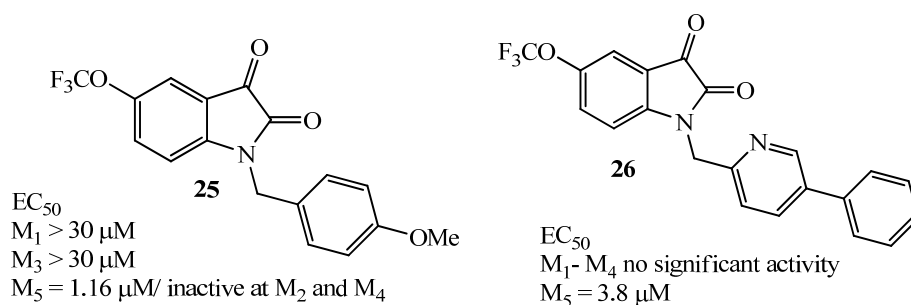
The benzoxazine nucleus was identified in the mass screening of compounds acting on muscarinic receptor subtypes. Structure activity relationship studies led to the identification of **23** as the first selective ligand for M_4 receptor subtype. Another M_4 selective antagonist identified was the quaternary ammonium derivative **24**, derived

from diphenidol, an antiemetic agent used to treat vomiting and vertigo. Diphenidol shows non-selective binding to muscarinic receptors. Compound **24**, a diphenidol dimer possesses a diphenidol moiety separated by bi-piperidinyll framework, and exhibits good potency and selectivity for the M₄ muscarinic subtype.^{49, 50}



(e) Ligands exhibiting preference for the M₅ receptor subtype.

Currently there are no M₅ selective muscarinic ligands reported in the literature. However novel allosteric modulators for this receptor have been recently reported. Identification of the lead compound by HTS and subsequent SAR study led to the discovery of the first selective allosteric modulator of the M₅ receptor. Compound **25** shows 1 μM affinity for M₅ receptor as shown in Ca²⁺ mobilization assay and > 30 μM affinity for M₁ and M₃ subtypes. No binding was observed for M₂ and M₄ receptor subtypes.⁵¹ Compound **25** was subjected to lead optimization efforts using iterative parallel synthesis which resulted in the identification of **26** as a potent M₅ allosteric modulator.



CHAPTER 2

DESIGN CONSIDERATIONS FOR MUSCARINIC RECEPTOR LIGANDS

To date, efforts to develop subtype selective ligands for muscarinic acetylcholine receptors (mAChRs) have been hampered by the lack of an X-ray crystal structures of the proteins and the high degree of homology among the receptor subtypes.^{4,6} A recent report provided the availability of X-ray crystal structure for M₂ receptor (human) bound to 3-quinuclidinylbenzilate and M₃ receptor (rat) bound to tiotropium. A phage T4 lysozyme was utilized for the crystallization of these receptors. The information from the binding characteristics can now be explored in the design of new ligands.^{54a,b} This report was not available at the time of the present work and will therefore not be considered herein. The pharmacophoric requirements for cholinergic ligands have been reported by numerous investigators based on structure-activity relationship (SAR) and/or molecular modeling data of known muscarinic ligands. In general, the models propose that the pharmacophoric elements to be present in muscarinic ligands include: a) a quaternary ammonium group or its equivalent, b) an unshared pair of electrons that can mediate a hydrogen (H)- bond, c) an appropriate distance between the H -bonding moiety and the center of the positive charge, and d) the presence of a suitably located lipophilic/alkyl

group.^{52,53} These fundamental requirements have aided in the development of high affinity muscarinic ligands but have provided little guidance in the design of subtype selective compounds.

The pharmacophoric model like the one described above along with binding site models for individual muscarinic receptor subtype can be a useful tool for the design of subtype preferring ligands. The binding site model for the M₁, M₂ and M₃ has been previously reported. In one study of the M₁ receptor, a model was constructed by taking into account the structural similarity between bacteriorhodopsin and G-protein coupled receptors. Docking of the known M₁ receptor agonists such as acetylcholine, muscarine was performed in order to study the interactions in the active site and thereby define the binding site.^{54c} In another study, a three dimensional M₁ receptor binding site was constructed utilizing agonists and antagonists for the M₁ receptor. The predicted binding site provided structural data regarding differences in the binding modes of agonists and antagonists at the protein.⁵⁵ The model for the M₂ receptor has been constructed using the crystal structure of bovine rhodopsin. The orthosteric and allosteric binding site was studied using N-methyl scopolamine and caracurine V derivatives.⁵⁶ A model for the M₃ receptor has been constructed using bovine rhodopsin as the template and the binding site was explored by docking agonists and antagonists into the receptor. The study also proposed pharmacophoric patterns for agonist and antagonist binding at the sites.⁵⁷

Homology modeling and molecular docking analysis of ACh in five muscarinic receptor subtypes have been investigated. Testa et.al have applied 3D molecular modeling techniques and docking studies using a homology model of bovine rhodopsin to reveal

unique interactions between acetylcholine (ACh) and the binding pockets of M₁ - M₅ receptors.⁵⁸ The study reports various interactions of ACh within the orthosteric binding pocket of each of the five muscarinic subtypes. For example, the binding of ACh to the M₁ receptor subtype is mediated by Thr192 (TM5) and Asn382 (TM6) [H-bonding to the ester group of ACh], Asp105 (TM3) is involved in ionic interactions with the cationic center [ammonium head of ACh] and the aromatic residues in the pocket are involved in the auxiliary binding of ACh.^{54,55,57} These binding of the aromatic groups to auxiliary sites contribute to increase affinity and potentially could increase selectivity for muscarinic ligands.⁵⁸ Similar residues involved in the interaction of ACh in the orthosteric binding sites of M₁-M₅ receptors are also found to be interacting with the agonists and antagonists in the M₁-M₃ receptor models.⁵⁴⁻⁵⁷ Romanelli et.al conducted another study that involved docking analysis of muscarinic receptors (M₁, M₂ and M₅) using known agonists from the literature. This study utilized the binding site geometry of the three receptors to design subtype selective ligands.⁵⁹

Like the pharmacophoric models described above, information available from SAR data of known muscarinic receptor ligands (see **Sec 1.6**) can be utilized in the design of new muscarinic ligands. A fragment based approach can be applied for the design of new ligands which will include H-bonding centers (lactone, benzodioxoles etc), cationic center (eg. piperazine/ piperidine) and aromatic centers (substituted phenyl/ biphenylmethyl). Using a fragment based drug design approach, a combination of fragments can be used that are complimentary to the amino acid residues identified in the models above. The goal of the approach is to design novel ligands with improved affinity and ultimately subtype selectivity.

Our early interest in developing novel muscarinic receptor ligands led to the design of lactone-based ligands using an approach similar to that reported by Kaiser et al (**Table 1**).⁶¹ Kaiser et. al applied the principle of increasing conformational rigidity in a lead in an attempt to retain or improve affinity and improve subtype selectivity. Using a known non-selective muscarinic antagonist (benactyzine; see **Figure 4**) as lead compound, a series of constrained analogs of benactyzine were designed, synthesized and tested as muscarinic ligands. These biphenyl lactone-based compounds with an N-substituted imidazole ring led to the discovery of **27** as M₃ antagonist.⁶⁰ Several of these compounds were identified as potential leads for the development of drugs for the treatment of urinary incontinence.

Figure 4: Structure of the non-selective muscarinic antagonist benactyzine and the anti-muscarinic activity of a lactone-based ligand designed by Kaiser et al.⁶⁰

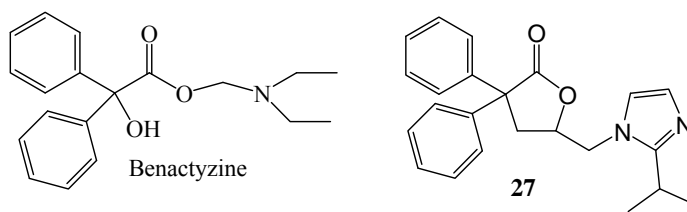
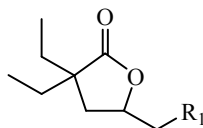


Table 1: Antimuscarinic activity of **27**

Antimuscarinic activity		
Vas deferens rabbit <i>Ki</i> (nM) M ₁	atria, guinea pig <i>Ki</i> (nM) M ₂	ileum, guinea pig <i>Ki</i> (nM) M ₃
133	115	8

The lactone ring used in the “Kaiser ligands” was utilized to design a novel series of 5-substituted 4,5-dihydro-3,3-diethyl-2(3H)-furanones in which the α -diphenyl groups were replaced with ethyl groups. The newly designed semi-rigid muscarinic ligands had the lactone oxygens serving as H-bond acceptors while several nitrogen containing heterocycles provided the requisite cationic group. Preliminary *in - vitro* binding data for the test compounds indicated that several compounds were low affinity, nonselective muscarinic ligands (**Table 2**).⁶¹

Table 2: Structure of representative lactone-based leads reported by Canney et. al.⁶¹



Compound #	R ₁	% Initial inhibition at 10 μ M		
		M ₁ [³ H]-pirenzepine (<i>K</i> _i = 2.2 nM)	M ₂ [³ H]-AF-DX 384 (<i>K</i> _i = 6.4 nM)	M ₃ [³ H]-NMS (<i>K</i> _i = 1.4 nM)
28		63.2	83.8	53.2
29		17	58.7	38.6
30		17.8	64.4	19.1
31		60.36	35.36	0.1
32		53.32	32.56	15.59
33		66.86	22.31	13.96
34		81.65	38.62	17.89

^aPreliminary binding data supplied by NOVASCREEN. ^bAssays were performed in triplicate or duplicate and presented as supplied by NOVASCREEN as averages representing % inhibition at 10 μ M. NOVASCREEN suggests that 50 % is the most common cut-off value for further investigation (determination of IC₅₀ or EC₅₀ values from concentration response curves).

Compound **34** was investigated further and found to have IC₅₀ value 1.56 μ M. *In-vivo* analysis performed on some of the above lactones (**Table 2**) to determine the functional activity in reciprocal hindlimb scratching assay in mice suggested that compound **34** was an agonist at the M₁ subtype.⁶¹

Based on this background information, we set out to design, synthesize and evaluate a new series of lactone-based compounds. The goal of the present work was to improve the affinity of our lead lactones, evaluate subtype selectivity and explore replacements for the hydrogen bonding lactone ring (bioisosteres).

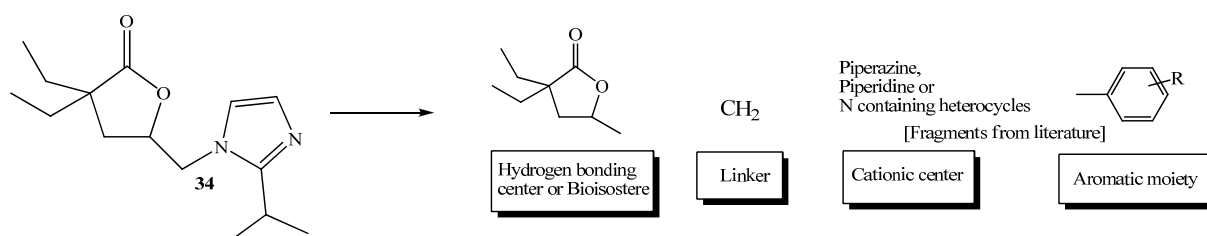
CHAPTER 3

SPECIFIC AIMS OF THE STUDY

Literature evidence and previous reports from our lab indicate that the lactone fragment is a suitable H-bonding center for the design of muscarinic ligands. A goal of the present work is to couple the lactone nucleus to heterocyclic rings attached or fused to aromatic and heteroaromatic systems. The specific aims of the project are described below.

3.1 Specific aim 1:

Modification of lead lactone **34**



3.1.1 (a) Incorporate aromatic and heteroaromatic ring systems to improve the affinity and evaluate higher affinity ligands for subtype selectivity.

3.1.2 (b) Evaluate suitable bioisosteric replacements for the hydrogen bonding lactone fragment.

3.2 Specific aim 2:

3.2.1 (a) Develop retrosynthetic schemes for intermediate scaffolds and target ligands.

3.2.2 (b) Design synthetic routes for the preparation of target ligands.

3.3 Specific aim 3:

3.3.1 (a) *In-vitro* evaluation of target ligands in muscarinic receptor binding assay

3.4.0 Specific aim 4:

Utilize preliminary data from earlier target compounds to direct molecular modification of leads.

3.1.1 Specific aim (1a)

Modification of lead lactone 34 by incorporating aromatic and heteroaromatic ring systems to improve the affinity and evaluate higher affinity ligands for subtype selectivity.

Lactone based compounds fulfill the pharmacophoric requirements for muscarinic ligands and have been reported by us and others to exhibit affinity for mAChR's. Based on the pharmacophoric requirements for known muscarinic ligands and the presence of aromatic residues in the binding pocket, this project was based on the hypothesis that appropriately positioned functional groups (e.g. substituted and unsubstituted aromatic rings and N-containing heterocycles) exhibiting a wide range of physicochemical properties on lead lactone-based molecules may provide improved affinity towards muscarinic receptors. Structure-activity relationship (SAR) data and molecular modeling experiments in the recent literature have been considered for the fragment based approach used in the design of the novel compounds. The ligands thus contain the following features:

(1) H-bond accepting moiety in the form of a lactone ring (or bioisostere)

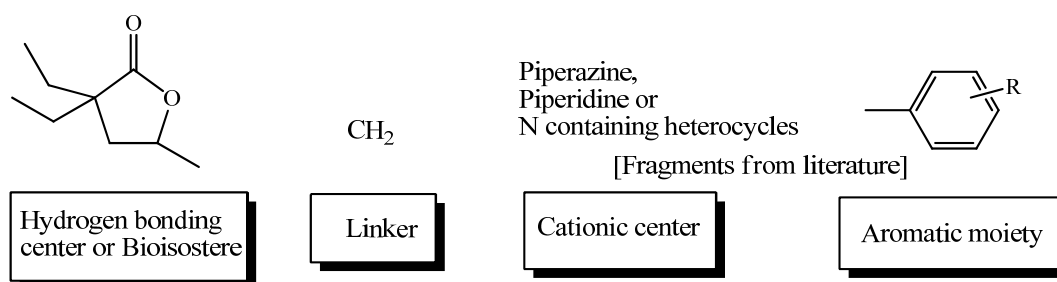
(2) A linker (CH₂ in the present series)

(3) A cationic center in the form of nitrogen containing piperazine/ piperidine or other heterocycles

(4) Substituted aromatic moiety

The newly designed ligands contain an H - bond accepting moiety in the form of the lactone ring, a linker (CH_2 in the present series), a cationic center in the form of nitrogen containing piperazine/ piperidine (or other heterocycles) and aromatic rings. The cationic group is expected to interact with aspartate residues in the receptor while substituted aromatic groups may interact with the known aromatic amino acids in the binding pocket.^{35,45,61,62}

Figure 4: General structural features of the newly designed ligands



An important distinction between the newly designed ligands and the lead lactones is the presence of substituted or unsubstituted aromatic systems that provide opportunities for interactions with auxiliary binding sites of the mAChR's.

3.1.2 Specific aim (1b)

Modification of newly identified lead lactones by evaluation of bioisosteric replacements for the hydrogen bonding lactone fragment

The first part of the project focused on the improvement in the affinity of the lead lactone (from μM to the in nM range). Compound **144** was identified as the highest affinity ligand in the series with IC_{50} value of 340 nM. Efforts were then undertaken to find a replacement for the lactone fragment of the new lead compound (**144**). Bioisosterism is a strategy used in medicinal chemistry for the rational design of new drugs in order to favourably alter pharmacokinetic or pharmacodynamic properties of lead molecules. Bioisosteres are typically not exact structural mimics but rather produce similar biological properties. The use of bioisosteres frequently introduces structural changes that may be beneficial depending on the context. Changes in substituent size, shape, electronic distribution, polarizability, polarity, lipophilicity, and pK_a play key roles in molecular recognition. The application of bioisosteric replacement in drug design is wide spread and may be used for:^{69, 70}

- i. extending or improving activity,
- ii. enhancing selectivity,
- iii. altering physicochemical properties,
- iv. reducing or redirecting metabolism,
- v. eliminating or modifying toxicophores and
- vi. acquiring novel intellectual property

In case of lactone-based ligands, the lactone ring was viewed as a possible liability due to the in-vivo stability of the cyclic ester. Hence, substituted tetrahydrofuran, 1,3-benzodioxoles, oxazolidinones and chromones were chosen as possible bioisosteres (**Figure 6**). While modifying the H-bonding portion of the ligands, the cationic and

aromatic moieties were held constant. Therefore, for our second series of compounds (**Figure 5**) the two fragments that were used as the aromatic cationic centers were the biphenylmethylpiperazine and the *o*-isopropyl phenyl tetrahydro-pyridine fragments. These groups were chosen due to the high % inhibition values observed for lactone-based compounds that contained them.

Figure 5: Current lactone-bioisostere based ligands

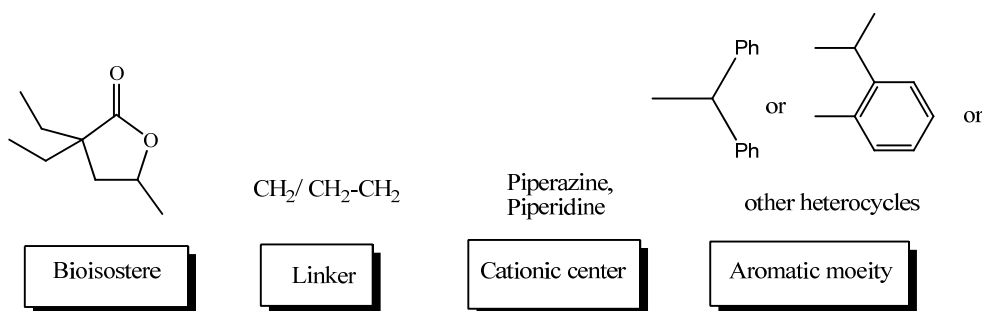
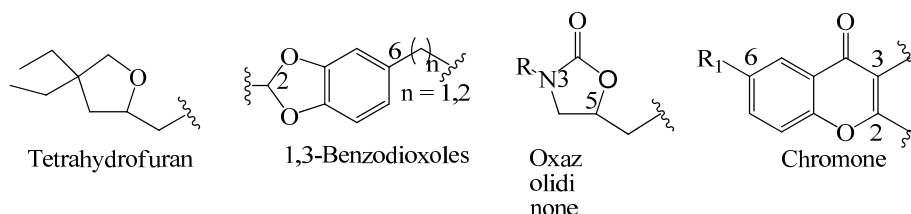


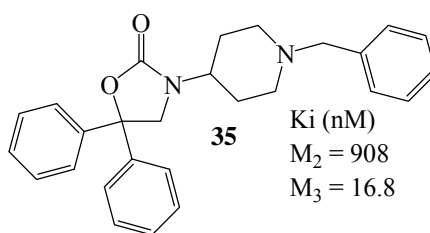
Figure 6: Proposed bioisosteres for the lactone



The substituted tetrahydrofurans differ from γ -butyrolactones due to the absence of carbonyl oxygen. This strategy was adopted to avoid the metabolic lability of the lactone nucleus. The role of the carbonyl oxygen in the binding affinity of the lactone-based ligands can also be investigated using this nucleus. The 1,3-benzodioxole nucleus is a widely reported H-bond acceptor fragment in muscarinic ligands [see compounds **11** and **12**].^{34,35b} The fragment provides the opportunity to explore positions 2 and 6 as points of

attachment for the linker, cationic center and aromatic moieties. The substituted oxazolidinone has been reported also as a H-bond acceptor (**Figure 7**) for ligands binding to muscarinic receptor subtypes.⁷¹ Compound **35** was reported to be 54 fold selective (M_3 K_i = 16.8 nM vs M_2 K_i = 908 nM). The oxazolidinone ring is structurally similar to the lactone ring with nitrogen in place of carbon. Side chains on the oxazolidinone may be attached to the N3 or the C5 positions.

Figure 7: Oxazolidinone-based muscarinic ligand⁷¹



Finally, the chromone nucleus is a fragment found in the design of ligands for retinoic acid receptors (RAR's) as well as in many natural products.^{77,81} This nucleus has a combination of H-bonding ability and a degree of aromaticity/lipophilicity. The aromatic groups on the proposed ligands may provide interactions with aromatic residues in the muscarinic binding pocket.

3.2.1 Specific aim (2a)

Develop retrosynthetic schemes for intermediate scaffolds and target ligands.

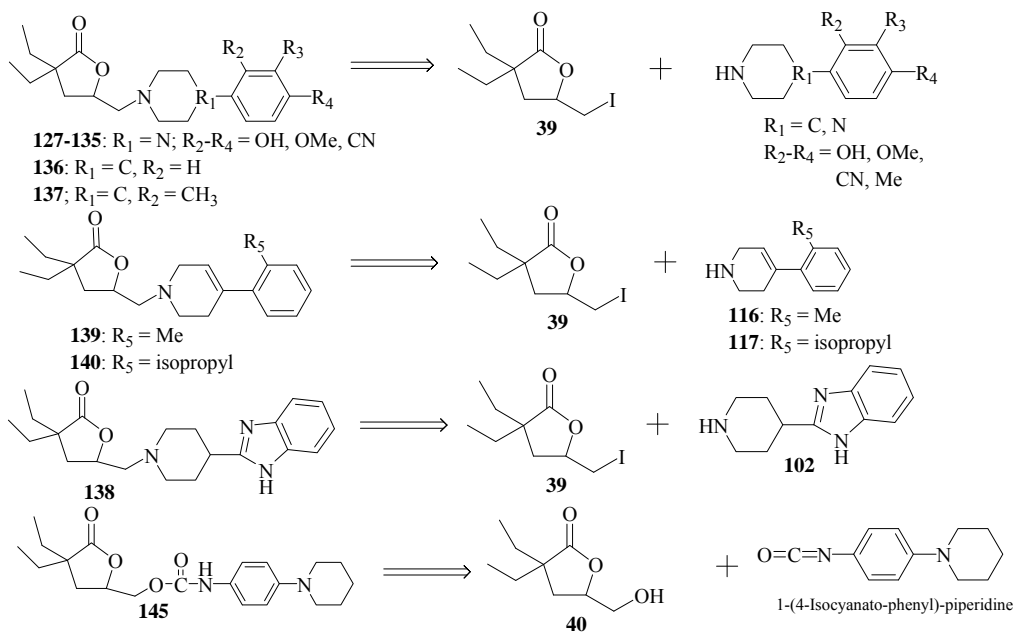
Figure 8a shows the retrosynthetic analysis of the target compounds **127-174**. **Figures 8b** and **8c** are the retrosynthetic analysis for the intermediate scaffolds required for the

synthesis of target ligands. The intermediates **39**, **40**, **42**, **44**, **52**, **85**, **86-93**, **94-100**, **102**, **106**, **109**, **116-118**, **121-123** and **126** could be prepared as outlined in **Figure 8a and 8b**.

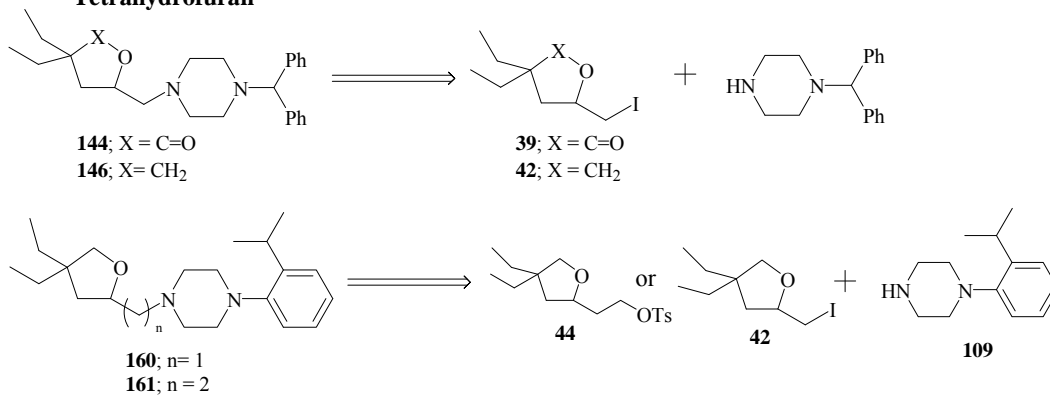
It was our contention that target ligands could be synthesized using either thermal or microwave methods. The lactone and 1,3-benzodioxole-based ligands were likely to be synthesized by thermal methods whereas the bioisostere-based ligands (e.g., oxazolidinone, tetrahydrofuran and chromone) would be prepared using microwave enabled synthetic techniques.

Figure 8a: Retrosynthetic analysis for target compounds (lactone, tetrahydrofuran, 1,3-benzodioxole, oxazolidinone and chromone).

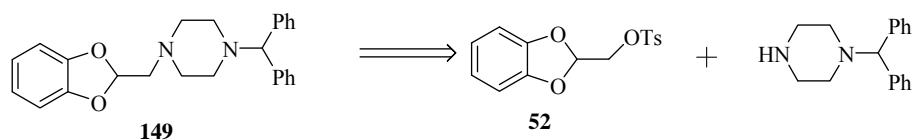
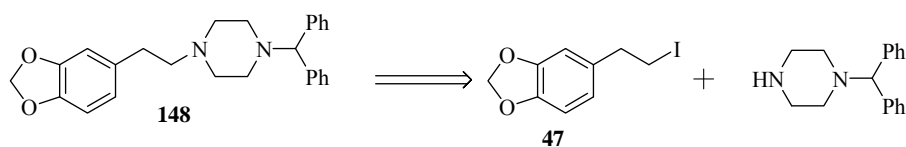
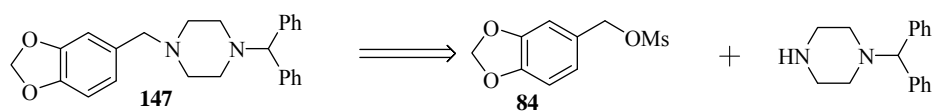
Lactone



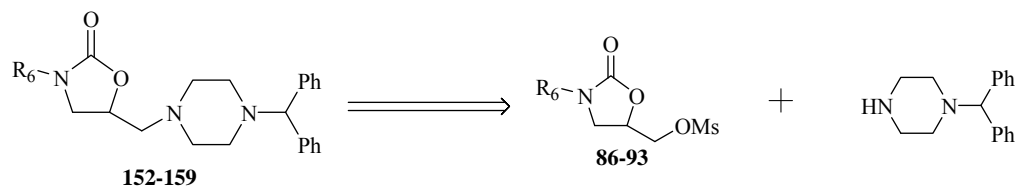
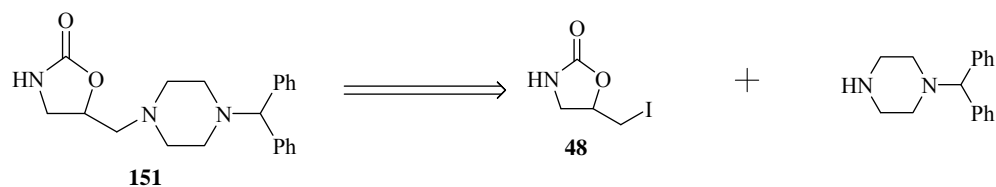
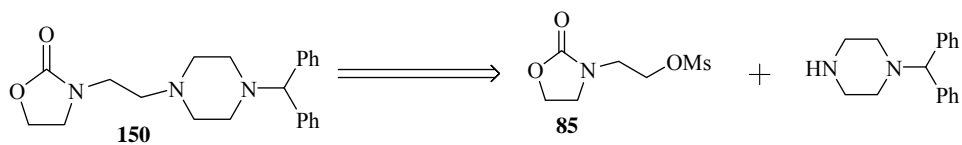
Tetrahydrofuran



1,3-Benzodioxoles



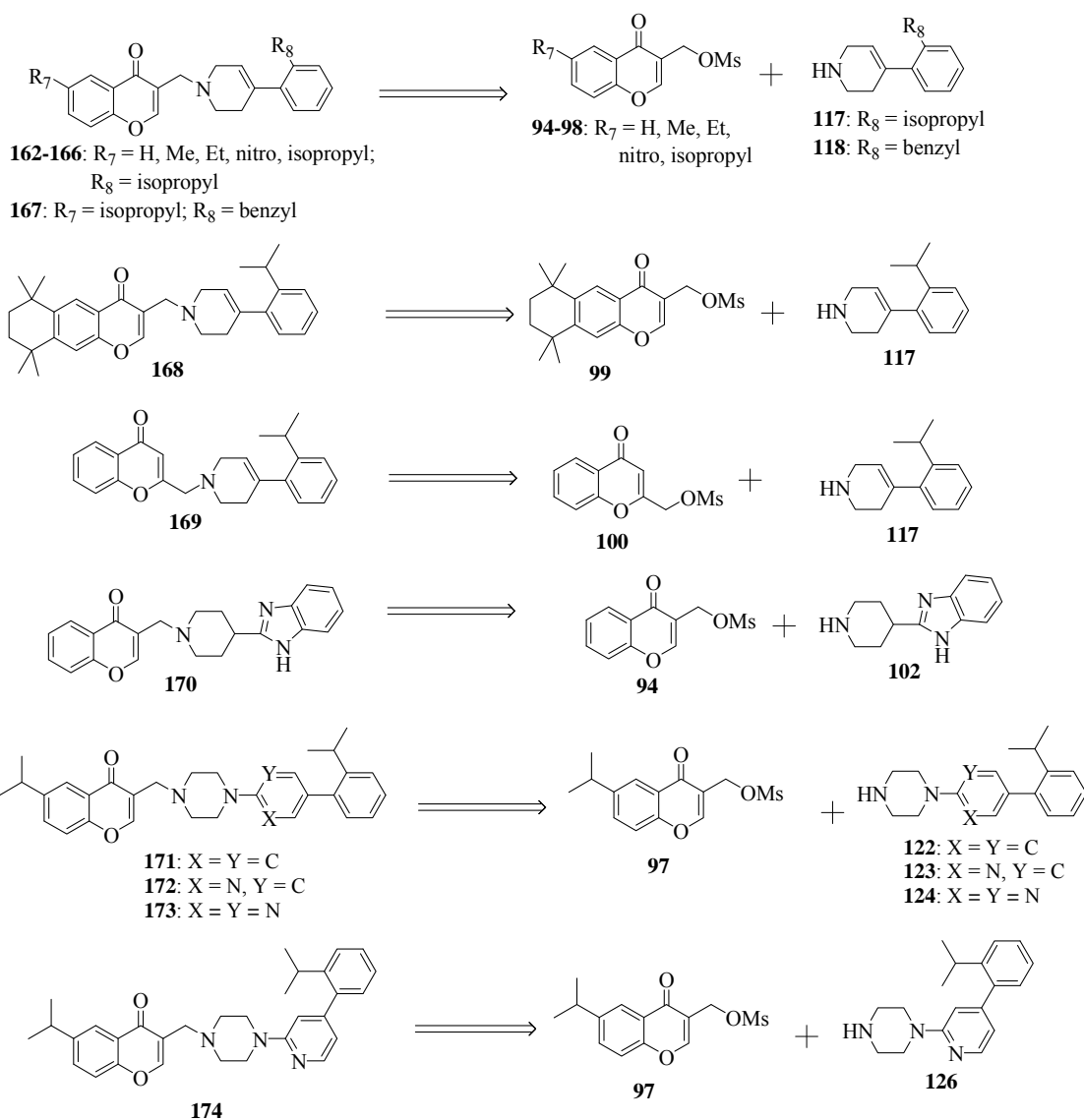
Oxazolidinone



R₆ = allyl (**152**), benzyl (**153**), isopropyl (**154**), *t*-butyl (**155**), cyclobutyl (**156**), cyclopentyl (**157**), cyclohexyl (**158**), cyclopropyl (**159**)

R₆ = allyl (**86**), benzyl (**87**), isopropyl (**88**), *t*-butyl (**89**), cyclobutyl (**90**), cyclopentyl (**91**), cyclohexyl (**92**), cyclopropyl (**93**)

Chromone



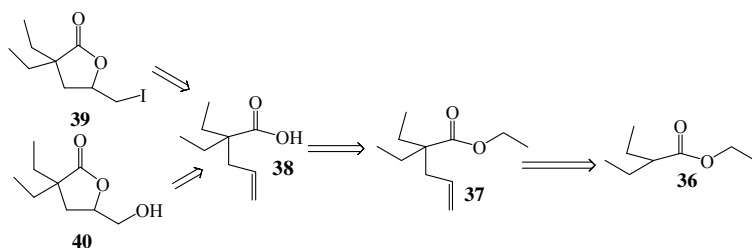
Much of the chemistry required for the preparation of lactone precursors had been worked out in our laboratory and is depicted in **Figure 8B** below. Thus, C-alkylation of ester **36** provides **37** which is hydrolyzed to acid **38** and then iodolactonized or epoxylactonized to afford lactones **39** and **40**, respectively. 1,3-benzodioxole **52** could be prepared via the *o*-alkylation of catechol **49** with methyl dichloroacetate followed by reduction of ester **50** to alcohol **51** which is subsequently tosylated to obtain **52**.

The preparation of oxazolidinone **85** was envisioned to involve the N-alkylation of oxazolidin-2-one **53** with ethyl bromoacetate to afford ester **54** followed by reduction (**55**) and mesylation (**85**). An efficient synthesis of the N-substituted oxazolidinones **56-63** was thought to involve a one pot cyclization reaction of epibromohydrin and the corresponding amines under mildly basic conditions followed by mesylation (**86-93**).

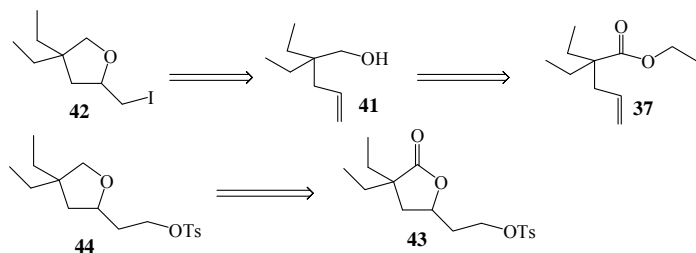
Much of the chemistry required for the preparation of chromone-based intermediates **94-100** had been worked out in our laboratory (**Figure 8B**). The chromone aldehydes **68-73** would be reduced to the corresponding alcohols **74-79** using 9-borabicyclo [3.3.1] nonane (9-BBN; 0.5 M solution in THF). Diol **64** will be converted to **65** which undergoes Friedel Crafts alkylation with phenol to provide **66**. Subsequent Friedel Crafts acylation of **66** affords keto alcohol **67** which is cyclized to chromone aldehyde **68** and then reduced to alcohol **79**. Chromone-2-carboxylic acid **111** is esterified to obtain the methyl ester **112** which is subsequently reduced to alcohol **113**. The chromone alcohols are later mesylated to obtain intermediates **94-100**.

Figure 8b: Retrosynthetic analysis for H-bonding group (lactone, tetrahydrofuran, 1,3-benzodioxole, oxazolidinone and chromone).

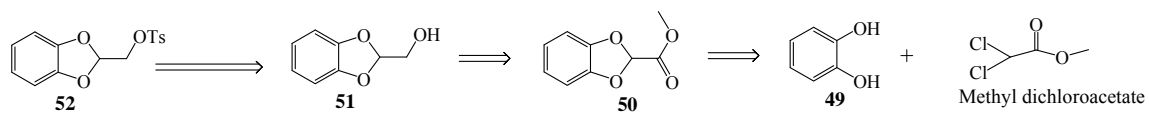
Lactone



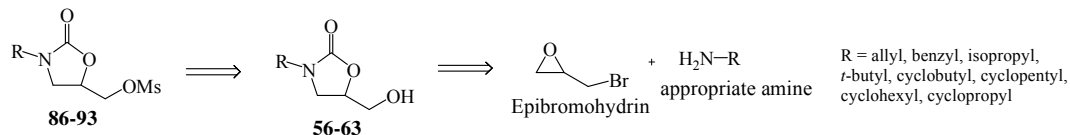
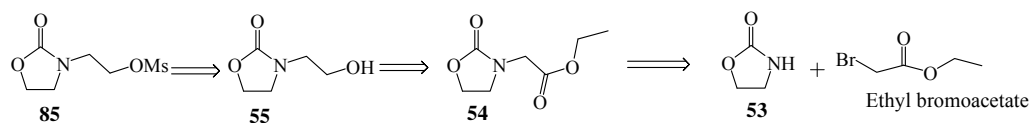
Tetrahydrofuran



1,3-benzodioxole

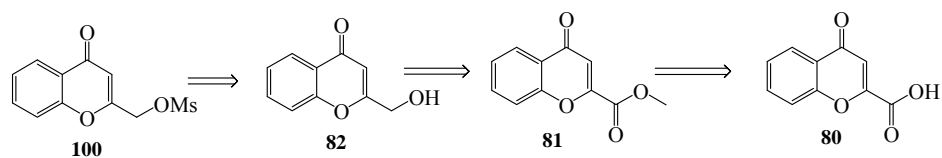
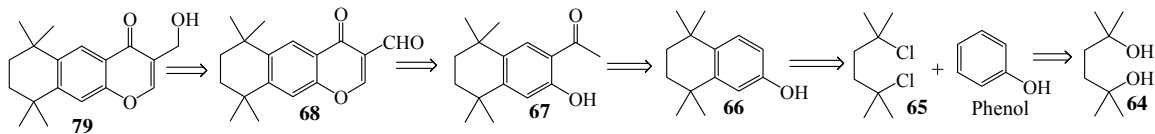
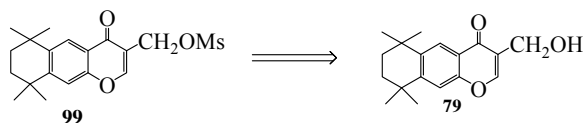
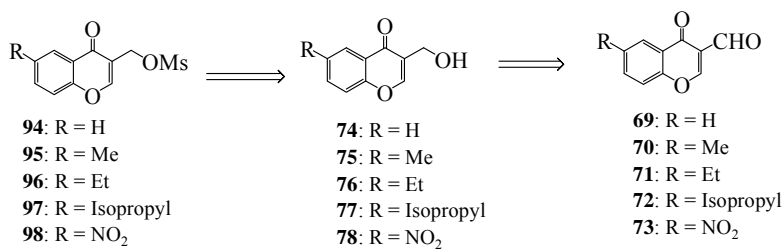


Oxazolidinone



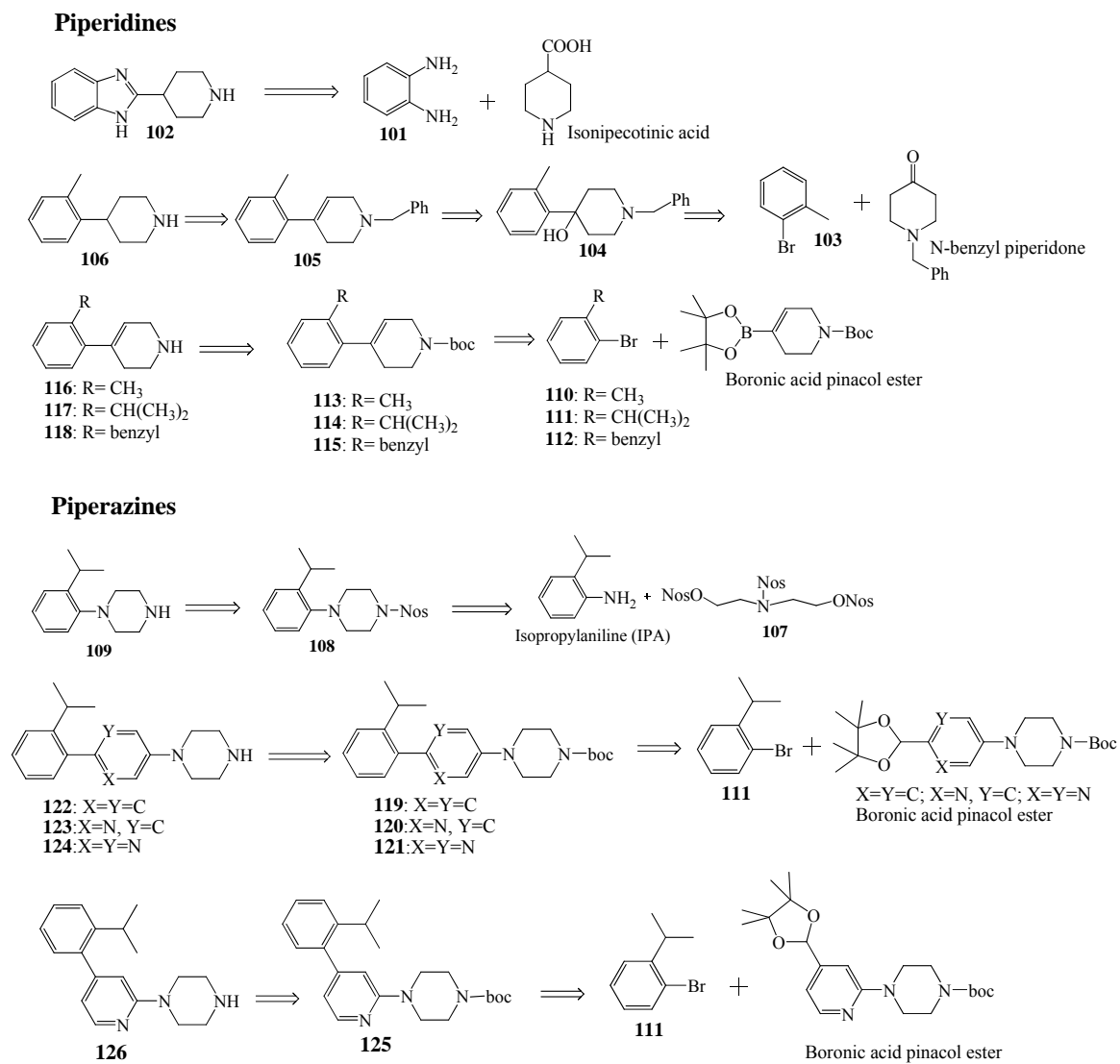
R_1 = allyl, benzyl, isopropyl, *t*-butyl, cyclobutyl, cyclopentyl, cyclohexyl, cyclopropyl

Chromone



The N-containing fragments consisted of two types; ortho substituted arylpiperidines and ortho substituted arylpiperazines/pyrido-pyrimido piperazines. The synthesis We envisioned preparing the benzimidazole piperidine **102** was prepared by treating 1,2-diaminobenzene **101** with isonipecotinic acid in the presence of polyphosphoric acid. Reacting 2-bromotoluene **103** with N-benzyl piperidone in the presence of n-BuLi yields alcohol **104** which is dehydrated (**105**) and hydrogenated to give *o*-methyl phenylpiperidine **106**. Suzuki coupling of **110-112** with boronic acid pinacol ester under thermal conditions yields **113-115**. Subsequent deprotection affords *o*-substituted phenyl piperidines **116-118**. Isocumene **111** and boc-protected pyrido/pyrimidopiperazine undergo microwave assisted Suzuki coupling of to provide intermediates **119-121** which were deprotected (TFA in DCM) to obtain secondary amines **122-124**. The same approach was used in the synthesis of intermediates **125** and **126** using isocumene **111**. Microwave irradiation of 2-isopropyl aniline (IPA) with nosyl protected amine **107** provides the nosyl protected *o*-substituted phenylpiperazine **108** which was deprotected to give secondary amine **109**.

Figure 8c: Retrosynthetic analysis for N-containing fragments



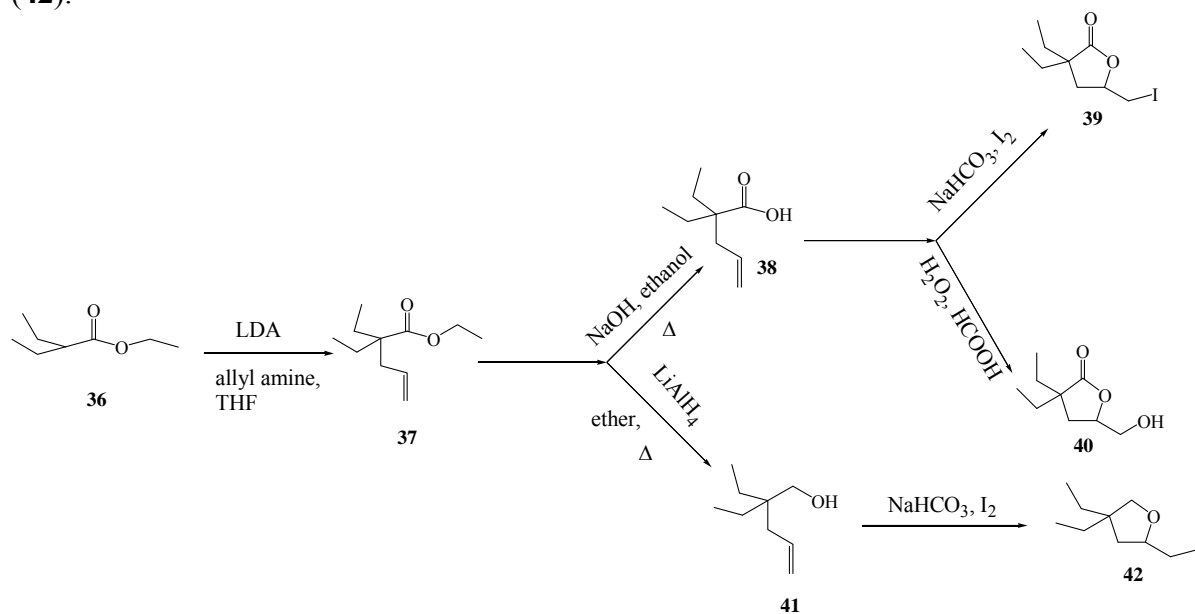
3.2.2 Specific aim (2b)

Design synthetic routes for the preparation of target ligands.

3.2.2.1 Synthesis of the lactone scaffold.

The first series of target compounds included substituted phenylpiperazines and piperidines coupled to the lactone nucleus. Hence, the facile synthesis of sufficient quantities of the iodolactone and hydroxylactone precursors was required. Previous work in our lab⁶¹ provided a useful synthetic route as mentioned above and depicted below. The reaction involved alkylating the ester **36** using lithium diisopropylamide (LDA) to obtain **37**. The alkylated ester **37** then undergoes basic hydrolysis to an olefinic acid **38**. The olefinic acid **38** is later epoxylactonized afforded hydroxy lactone **40** or iodolactonized to provide iodolactone **39**. The tetrahydrofuran **42** was synthesized from olefinic ester **37** by reducing the ester to an alcohol **41** using lithium aluminum hydride (LAH) in refluxing ether. The alcohol **41** undergoes cyclisation to five membered furan using iodine under basic conditions using sodium bicarbonate in tetrahydrofuran to obtain intermediate **42**.^{63, 72}

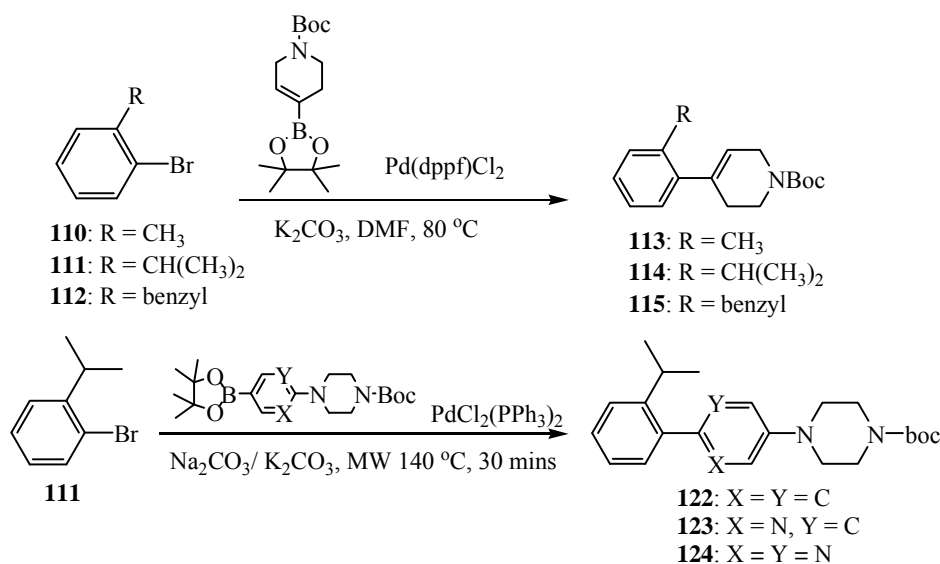
Figure 9: Routes to iodomethyl and hydroxymethyl lactone (**39**, **40**) and tetrahydrofuran (**42**).



3.2.2.2 Microwave/thermal promoted synthesis of substituted phenylpiperidines/piperazines.

Some of the secondary amines that were coupled to the iodolactone were commercially available, while others required synthesis. During the course of our work, binding data indicated that ortho substituted piperidines and piperazines had higher affinity for muscarinic receptors than some of the other substitution patterns evaluated. Based on these observation, it became necessary to prepare these ortho-substituted secondary amines. These compounds were synthesized in-house using Suzuki-Miyaura coupling involving substituted boronic esters in the presence of palladium catalysts using thermal or microwave methods.

Figure 10: Suzuki promoted synthesis of phenylpiperidines/ piperazines.



The boronic acids utilized in this process will bring about the desired structural modification of the piperidine/piperazine intermediate which will then be coupled to the hydrogen bonding centers (lactone, THF, chromone, oxazolidinone). The Suzuki-

Miyaura cross coupling reaction is the widely used method for C-C bond formation utilized in the synthesis of natural products, drugs and organic intermediates.

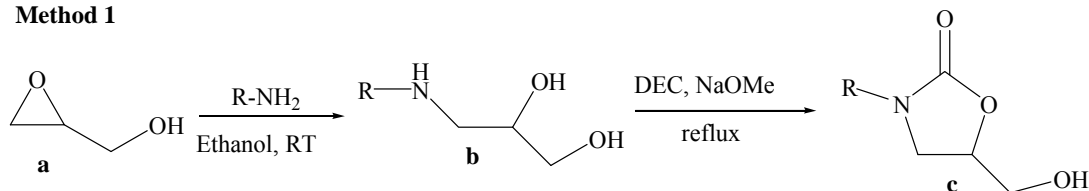
3.2.2.3 Synthesis of N3-substituted oxazolidin-2-ones

The promising preliminary binding data for unsubstituted oxazolidinone based compound **151** (87 % inhibition) warranted the synthesis of a series of N3-substituted oxazolidin-2-ones. The N3 position would be substituted with structurally diverse groups ranging from alkyl, cycloalkyl and aryl substituents. Two routes were investigated for the synthesis of the N3-oxazolidin-2-ones. **Figures 11** and **12** show the routes used for the synthesis of N3-substituted oxazolidin-2-ones which would later be coupled to biphenylmethylpiperazines.

Method 1 requires two steps, the first of which involves reaction of glycidol with a primary amine to afford the binary alcohol **b**. The second step involves a cyclization reaction of **b** using diethylcarbonate in presence of anhydrous sodium methoxide to obtain the target N3-substituted oxazolidin-2-ones.

Figure 11: Synthesis of N3-substituted oxazolidin-2-one.

Method 1

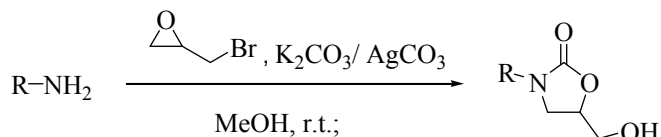


Method 2 involves a one step reaction between epibromohydrin and primary amines in the presence of base (e.g., potassium carbonate) in anhydrous methanol at room temperature. A variety of amines having alkyl, cycloalkyl, and aryl groups can be utilized

to obtain this intermediate in modest to high yields. This one step cyclisation process to obtain a variety of substituted oxazolidinones was found to be preferable to the other method and was used for future syntheses.

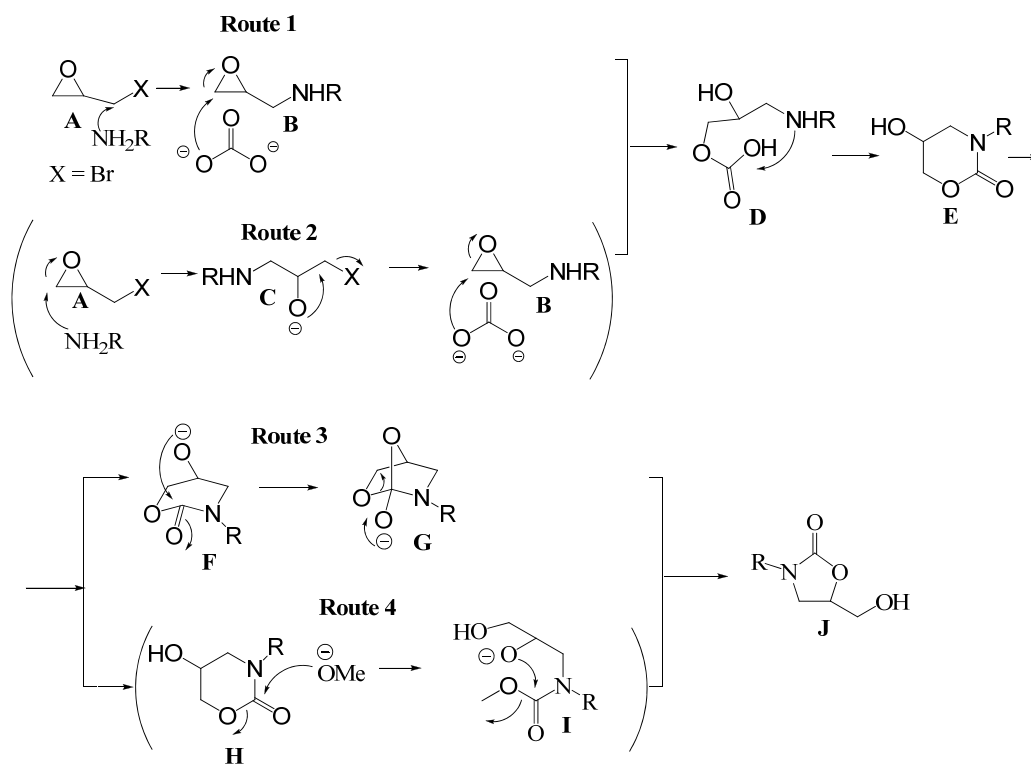
Figure 12: Synthesis of N3-substituted oxazolidin-2-one.

Method 2



Proposed mechanisms for the formation of N3-substituted oxazolidin-2-one are shown in **Figure 13** below. Two routes **1** and **2** could result in the formation of intermediate **D**. The resulting amino nitrogen in **D** attacks the carbonyl carbon to cyclize intramolecularly to obtain the six-membered oxazinanone **E**. Two routes are also considered for the conversion of intermediate **D** to the oxazolidinone **J**.

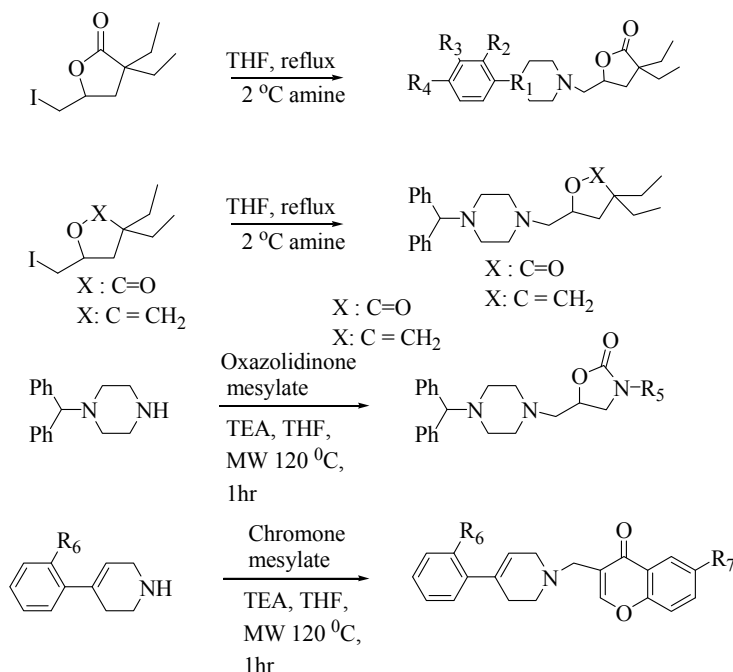
Figure 13: Proposed mechanism for the formation of N3-substituted oxazolidin-2-one



3.2.2.3 Coupling of the lactone or lactone bioisosteres with the amine containing fragment.

Lactone or lactone bioisostere will be coupled to commercially available piperazines or the synthesized piperidine/piperazines in the presence of triethyl amine under thermal or microwave conditions.

Figure 14: Synthesis of target ligands.



3.3.1 Specific aim

In-vitro evaluation of target ligands in muscarinic receptor binding assay

The target compounds **127 - 174** were evaluated in radioligand binding assays performed by CEREP, 86600 CELLE L'EVESCAULT, France using rat cerebral cortex membranes expressing muscarinic receptor subtypes $M_1 - M_5$. The competitive binding assays were performed according to the previously reported method.⁶⁸ The assays were done in duplicate and are presented as supplied by CEREP. Briefly, [3H]- quinuclidylbenzilate [QNB] (0.05 nM) and the test compounds (10 μ M) were incubated with rat cerebral cortex membranes for 90 mins at room temperature. Following incubation, the reaction was terminated by filtration. Atropine (1 μ M) was used to determine non-specific binding. The bound radioactivity was measured with a scintillation counter. For

interpretation of this type of preliminary data, CEREP suggests the following guidelines: 50 % inhibition or higher represent significant effects (i.e. 50 % is a common cut-off value for further investigation; determination of IC_{50} or EC_{50} values from concentration response curves). Results showing an inhibition between 20 and 50 % indicate weak to moderate effects; inhibition less than 20 % are considered inactive.

Preliminary data presented in **Tables 3 - 7** represent the percent inhibition of specific binding of radioligand at a single concentration (10 μ M) of test compound. Compounds showing % inhibition values of ≥ 95 % were chosen for further analysis to determine IC_{50} values and % inhibition at specific receptor subtypes. Solubility assays were performed at the high throughput screening facility, Moulder Center for Drug Discovery Research, Temple University.

3.4.0 Specific aim 4:

Utilize preliminary data from earlier target compounds to direct molecular modification of leads.

The project was based on promising preliminary binding data for a set of lead lactones developed in our lab. Using these compounds as leads, molecular modifications were made and the compounds evaluated in binding assays in an effort to improve affinity and ultimately to develop novel subtype selective ligands. During these efforts, the structure-activity relationship (SAR) data acquired for each series of compounds was used to design future compounds. Design efforts also considered pharmacophoric requirements of muscarinic ligands and SAR information from the literature. Based on these considerations bioisosteric replacements (1,3-benzodioxole, THF, oxazolidinones,

chromones) for the lactone ring were synthesized and evaluated. Once again, structure-activity relationship (SAR) data acquired for each series of compounds was used to design future compounds. The very recent availability of X-ray crystal structures for the M₂ and M₃ receptors will no doubt enable a better understanding of the binding interactions of.^{54a,b} Future efforts using these newly reported crystal structures along with molecular docking analysis should aid in the design of higher affinity, more selective ligands at these important receptors.

CHAPTER 4

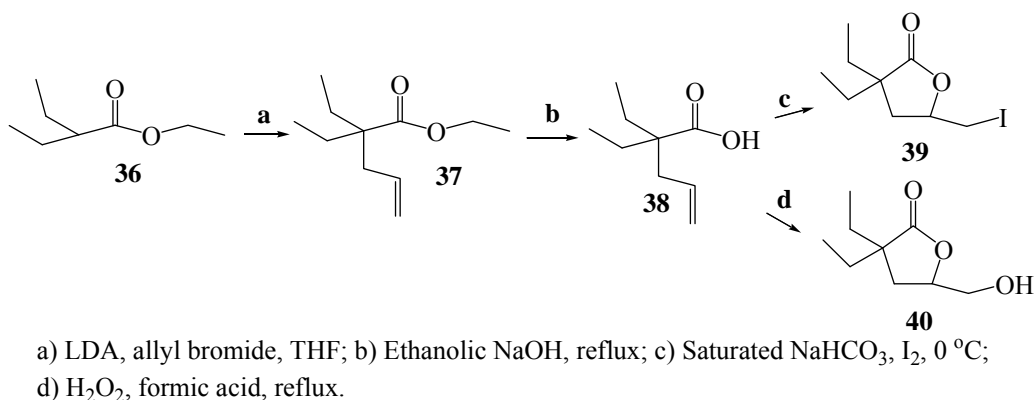
RESULTS

The present work focuses on the design, synthesis and evaluation of muscarinic ligands containing the lactone ring or lactone bioisosteres. The lactone fragment was chosen as a lead fragment in the design of these ligands based on previous work reported by our group and by other researchers. Bioactive amine-containing fragments found in muscarinic ligands from the literature have been incorporated in the design of our compounds. Thermal/ microwave promoted Suzuki coupling reactions have been utilized for the synthesis of phenyl piperidines/ piperazines. The secondary amines were coupled with iodolactone and mesylates of 1,3-benzodioxoles, oxazolidinones and chromones using thermal and/or microwave methods. The synthesized compounds were evaluated in solubility assays, preliminary binding assays, and subtype selectivity assays.

4.1.1. Synthetic routes for the preparation of H-bonding fragments

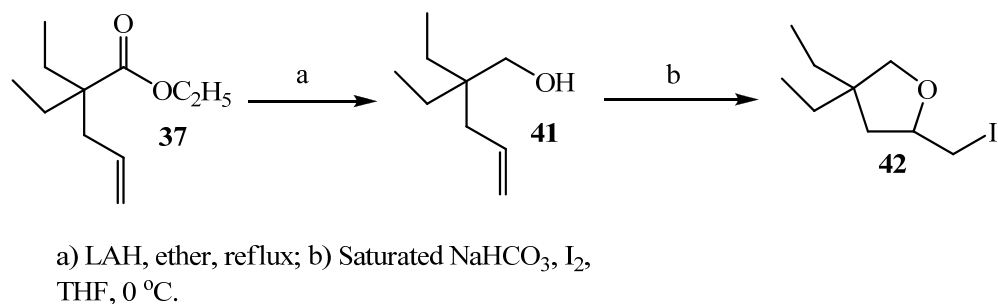
Precursors **39** and **40** were synthesized as described in **Scheme 1** from commercially available ester **36**. Alkylation of **36** with allyl bromide in the presence of lithium diisopropylamide (LDA) provided **37** which was hydrolyzed to olefinic acid **38**. Epoxylactonization or iodolactonization of olefinic acid **38** afforded hydroxy lactone **40** or iodolactone **39**, respectively, in 46-84 % yields.⁶³

Scheme 1: Synthesis of iodolactone (**39**) and hydroxylactone (**40**)



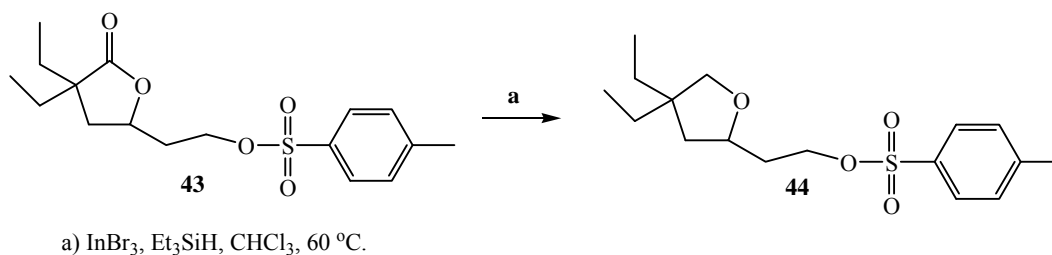
Precursor **42** (**Scheme 2**) was synthesized from olefinic ester **37** by reducing the ester to an alcohol (**41**) using lithium aluminum hydride (LAH) in refluxing ether. The alcohol was cyclized using iodine in THF under basic conditions (sodium bicarbonate) to afford furan **42** in 90 % yield.^{63, 72}

Scheme 2: Synthesis of 4,4-Diethyl-2-iodomethyl-tetrahydrofuran (**42**)



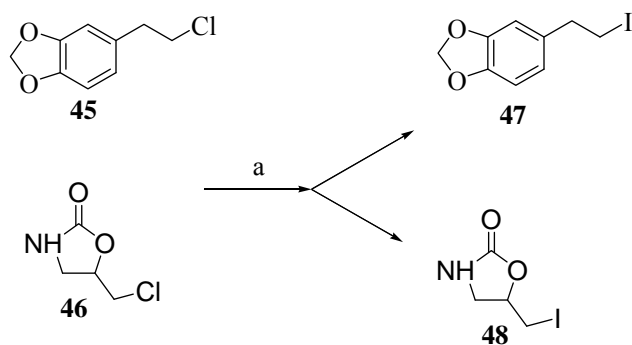
Deoxygenation of tosylated lactone **43** (**Scheme 3**) using triethylsilyl hydride and catalytic amounts of indium bromide in chloroform (CHCl₃) at 60 °C afforded **44** in 43 % yield.⁷⁸

Scheme 3: Synthesis of Toluene-4-sulfonic acid 2-(4,4-diethyl-tetrahydro-furan-2-yl)-ethyl ester (**44**)



A Finkelstein reaction was utilized to introduce the iodine (**Scheme 4**) in precursors **47** and **48** which were used directly for the synthesis of target compound **148** and **151**.^{63, 72}

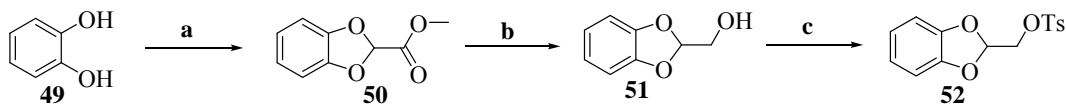
Scheme 4: Synthesis of 5-(2-Iodo-ethyl)-benzo[1,3]dioxole (**47**) and 5-Iodomethyl-oxazolidin-2-one (**48**)



Intermediate **51** (**Scheme 5**) was synthesized as per a previously published method.⁷³ *o*-alkylation of catechol **49** using methyl dichloroacetate in the presence of sodium methoxide (30 % wt in methanol) afforded methyl ester **50**, which was reduced to alcohol **51** using Lithium aluminum hydride (LAH). The alcohol was tosylated using *p*-

toluene sulfonylchloride in the presence of triethylamine in dichloromethane to obtain **52** in 85 % yield.⁶³

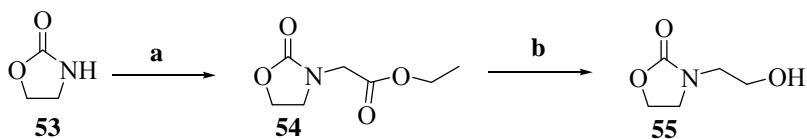
Scheme 5: Synthesis of toluene-4-sulfonic acid benzo[1,3]dioxol-2-ylmethyl ester (**52**)



a) NaOMe 30 % wt in MeOH, Cl₂CHCO₂CH₃, MeOH, reflux; b) LAH 1M in THF, THF, reflux; c) Triethyl amine, tosyl chloride, DCM, 0 °C to r.t.

Compound **55** was prepared as described in Scheme 6. Treatment of 2-oxazolidinone **53** with ethyl bromoacetate in presence of sodium hydride (60% dispersion in mineral oil) provided ethyl ester **54** (**Scheme 6**) which was reduced to alcohol **55** in 24 % yield.^{63,74,75}

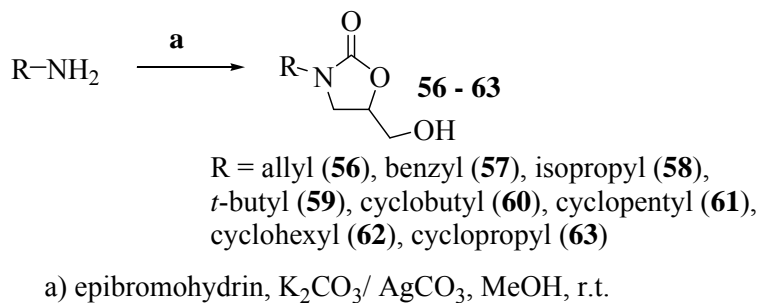
Scheme 6: Synthesis of 3-(2-Hydroxy-ethyl)-oxazolidin-2-one (**55**)



a) BrCH₂CO₂Et, NaH 60% mineral oil dispersion, THF 0 °C; b) NaBH₄, ethanol, 0 °C.

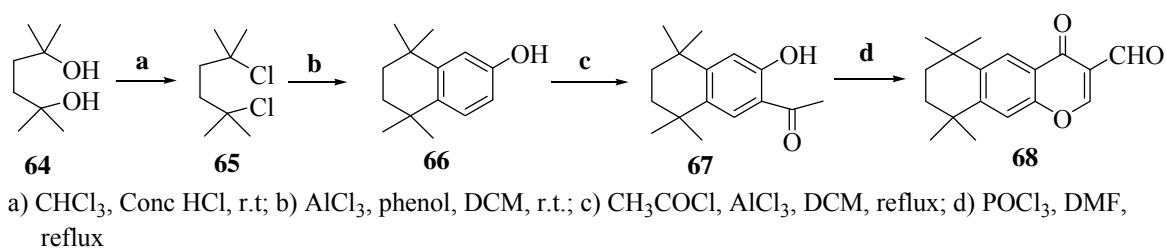
Reaction of primary amines with bromomethyloxiranes in presence of base afforded the N-substituted oxazolidinones **56 - 63** (**Scheme 7**) in 11-87 % yields.⁷⁶

Scheme 7: Synthesis of precursors **56 - 63**.



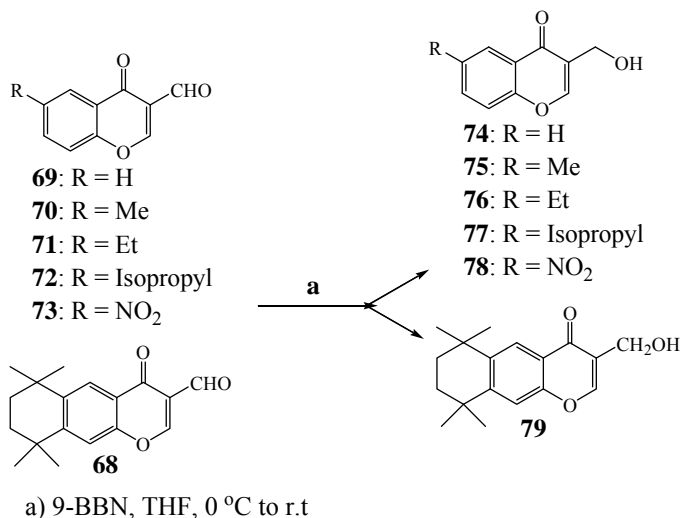
Synthesis of aldehyde **68** (**Scheme 8**) began with the dehydrohalogenation of 2,6-dimethyl-hexane-2,6-diol **64** to provide **65** which underwent a Friedel-Craft alkylation reaction with phenol in the presence of anhydrous AlCl₃ to give **66**. Phenol **66** then underwent Friedel-Craft acylation with acetyl chloride in the presence of AlCl₃ to afford **67**. Cyclization of **67** to chromone aldehyde **68** was accomplished using freshly distilled POCl₃ in refluxing dimethyl formamide (DMF) in 51 % yield.⁸⁰

Scheme 8: Synthesis of 6,6,9,9-Tetramethyl-4-oxo-6,7,8,9-tetrahydro-4H-benzo[*g*]chromene-3-carbaldehyde (**68**)



The chromone aldehydes **68 - 73** (**Scheme 9**) were reduced to the corresponding alcohols **74 - 79** using 9-borabicyclo [3.3.1] nonane (9-BBN; 0.5 M solution in THF) in 37-55 % yields.^{77, 63}

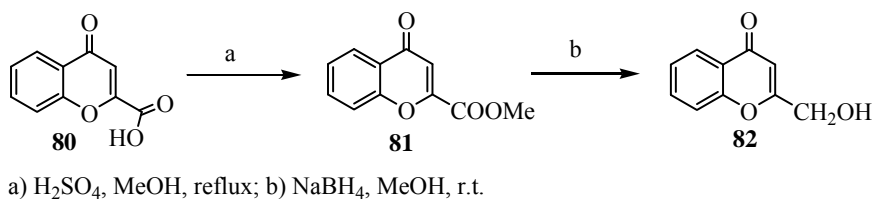
Scheme 9: Synthesis of precursors **74 - 79**.



Synthesis of chromone **82** (**Scheme 10**) began with commercially available acid **80**.

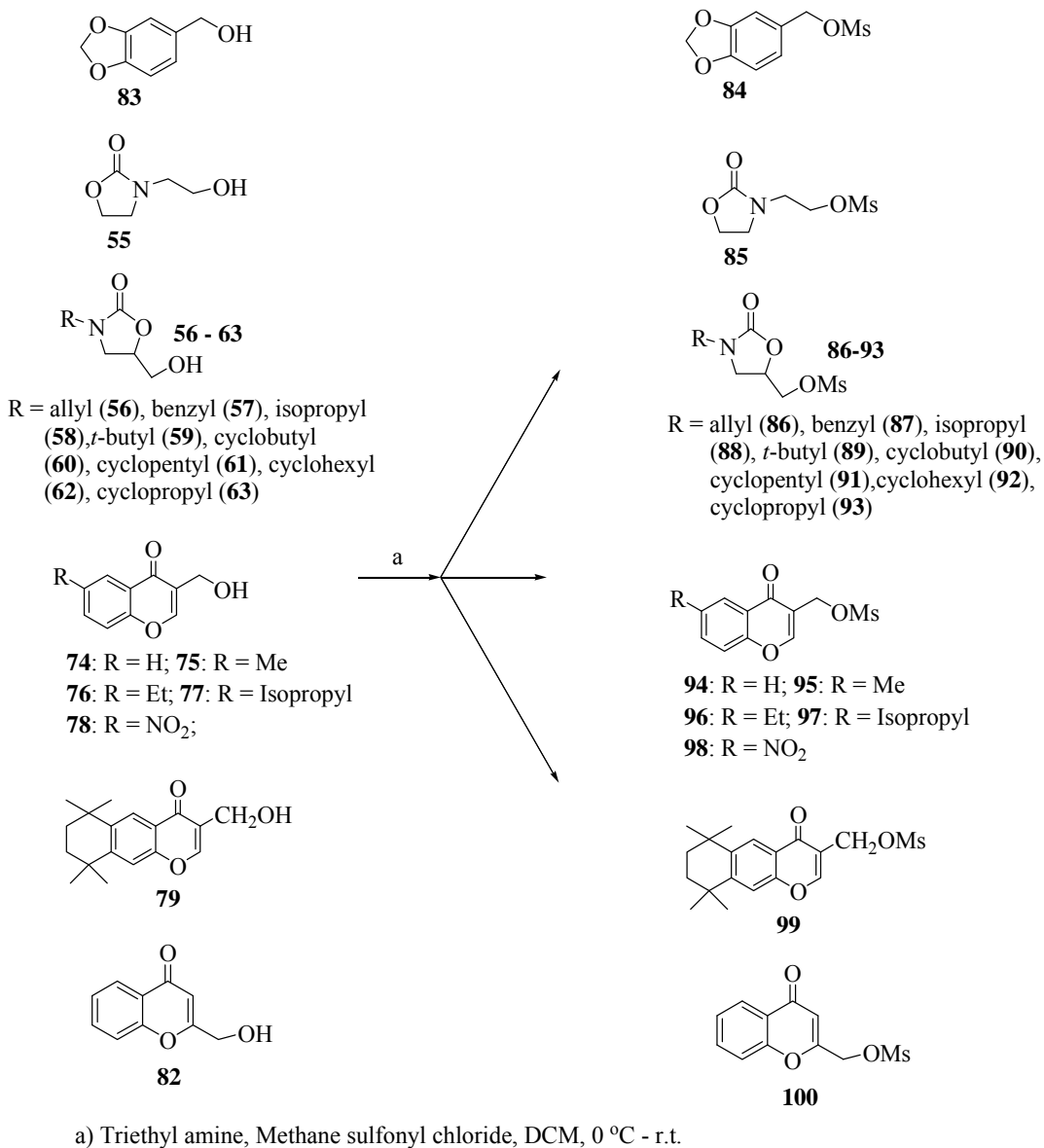
The acid was esterified (refluxing in methanol/H₂SO₄) and then reduced (NaBH₄) to the corresponding alcohol (**82**) in methanol (MeOH) in 45 % yield.^{82, 83, 84}

Scheme 10: Synthesis of 2-Hydroxymethyl-chromen-4-one (**82**)



Mesylation of alcohols **55-63**, **74-78**, **79**, **82** and **83** using triethylamine and methanesulfonyl chloride in dichloromethane (DCM) (**Scheme 7**) gave precursors **84-100** which were used directly for the synthesis of target compounds **147**, **150-174**.⁶³

Scheme 11: Synthesis of mesylate precursors (84-100)

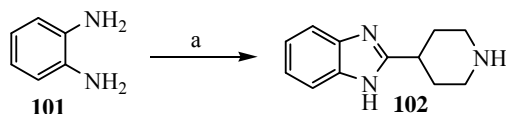


4.1.2 Synthetic routes used for the preparation of amine-containing fragments

Benzimidazole piperidine **102** served as an intermediate for the synthesis of target **138** (**Scheme 12**) and was prepared by treating 1,2-diamino benzene **101** with 4-piperidine

carboxylic acid (isonipecotinic acid) in presence of polyphosphoric acid (PPA) in 21 % yield.⁶⁴

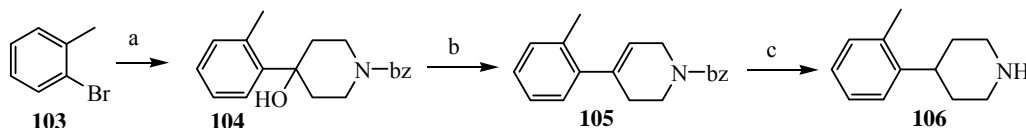
Scheme 12: Synthesis of 2-(4-piperidiny)-1H-benzimidazole (**102**)



a) Isonipecotinic acid, polyphosphoric acid, 180 °C.

The ortho substituted phenylpiperidine **106** was prepared (**Scheme 13**) by reacting 2-bromotoluene **103** with N-benzylpiperidone in the presence of nBuLi at -78 °C to provide alcohol **104**. The tertiary alcohol **104** was dehydrated to provide **105** which was reduced and deprotected (10 % Pd/C at 50 psi) to yield intermediate amine **106**. The amine was used in subsequent coupling reactions (see **Scheme 16**) without purification.⁶⁵

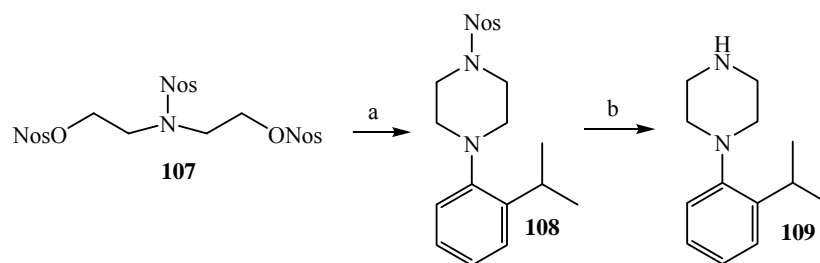
Scheme 13: Synthesis of precursor 4-*o*-tolyl-piperidine (**106**)



a) n-BuLi, N-benzyl-4-piperidone, THF, -78 °C; b) Conc. HCl, 95% ethanol; c) H₂, 50 psi, 10% Pd/C

Synthesis of *o*-isopropyl phenylpiperazine **109** (**Scheme 14**) was accomplished by reacting nosyl protected amine **107** with isopropyl aniline (IPA) in the presence of diisopropyl ethyl amine (DIEA) in acetonitrile under microwave irradiation followed by deprotection using thiophenol under mild basic conditions (59 % yield).⁷⁹

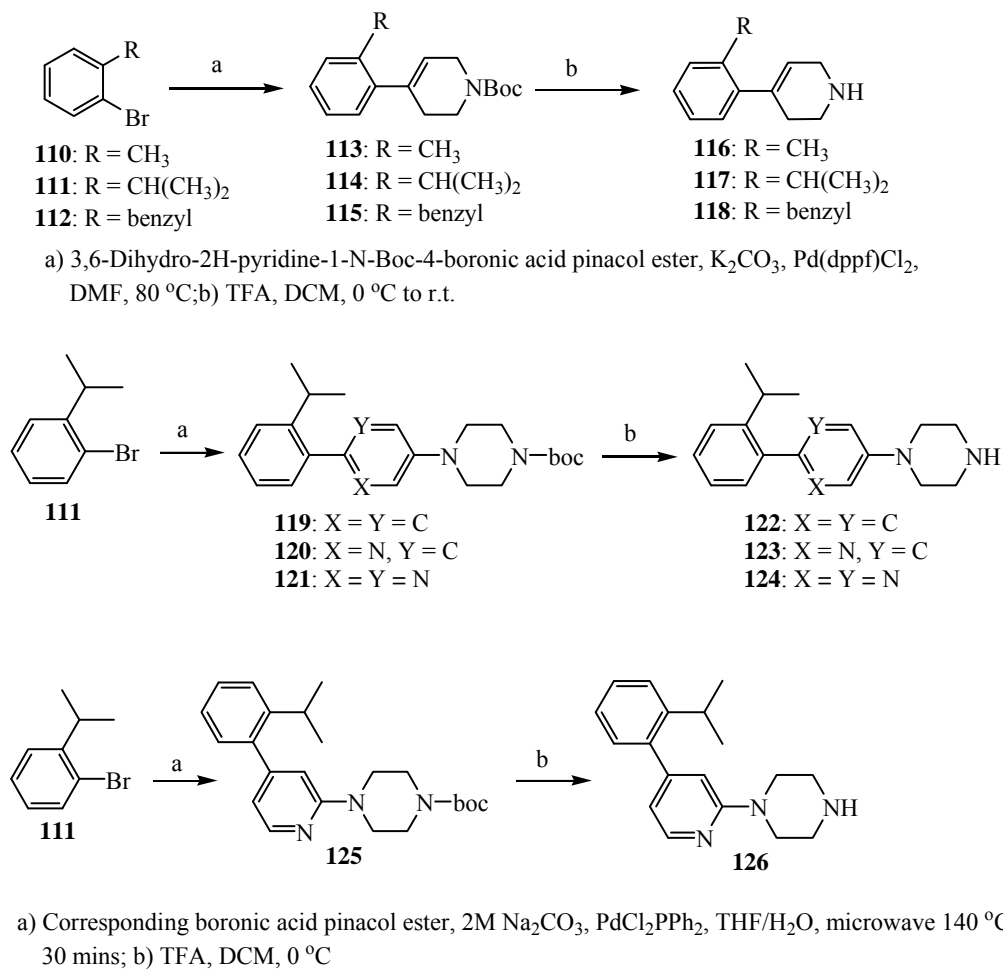
Scheme 14: Synthesis of 1-(2-Isopropyl-phenyl)-piperazine (**109**)



a) DIEA, IPA, CH₃CN, microwave, 175 °C, 1hr; b) thiophenol, K₂CO₃, CH₃CN, 2% DMSO, 60 °C.

Suzuki coupling of ortho substituted bromobenzenes **110-112** with appropriate boronic acid esters (**Scheme 15**) under thermal or microwave conditions in DMF or THF/water gave boc protected intermediates **113-115**, **119-121** and **125**. The *t*-Boc protecting group was removed using trifluoroacetic acid (TFA) in DCM to obtain the secondary amines **116-118**, **122 - 124** and **126** in 27-98 % yields (**Scheme 15**).^{66, 89}

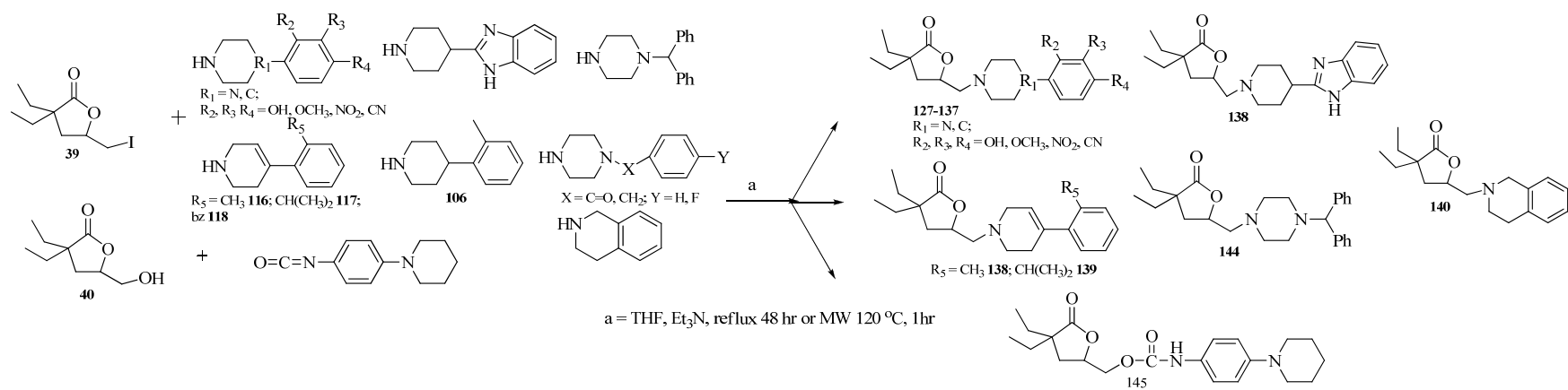
Scheme 15: Synthesis of precursors **116-118**, **122-124** and **126**.



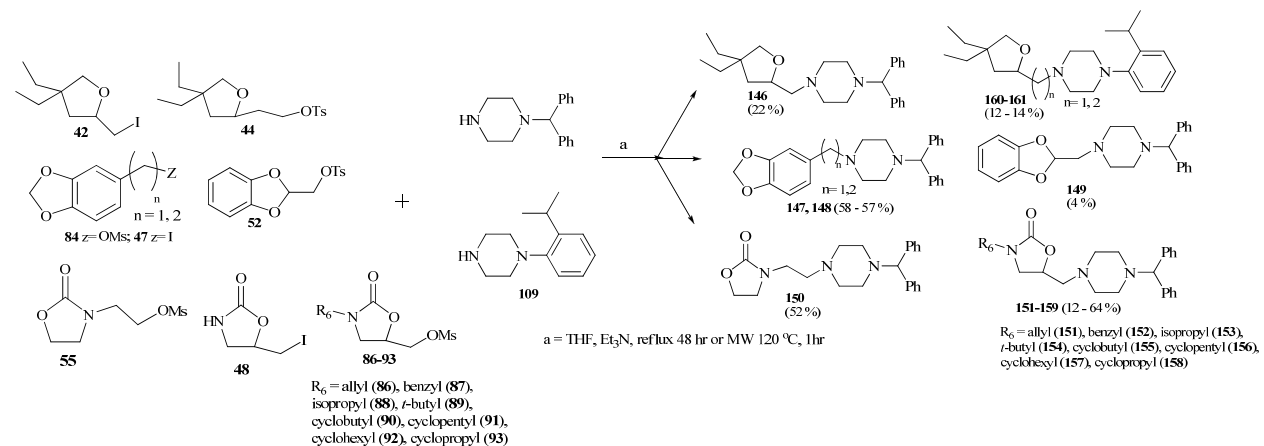
Displacement reactions involving the H-bonding fragments [lactones (e.g., **39**), furans (e.g., **42**), 1,3-benzodioxoles (e.g., **47**), oxazolidinones (e.g., **48**) and chromones (e.g., **94**)] and secondary amines (**Scheme 16**) under thermal/microwave conditions afforded the target compounds **127-174** in 4-83 % yields. Reacting alcohol **40** with the commercially available 1-(4-isocyanato-phenyl) piperidine afforded carbamate **145** in 52 % yields.^{61,63,67} The ligands synthesized as described above were then evaluated in

solubility assays, preliminary binding assays, and subtype selectivity assays. The results of those assays are included below.

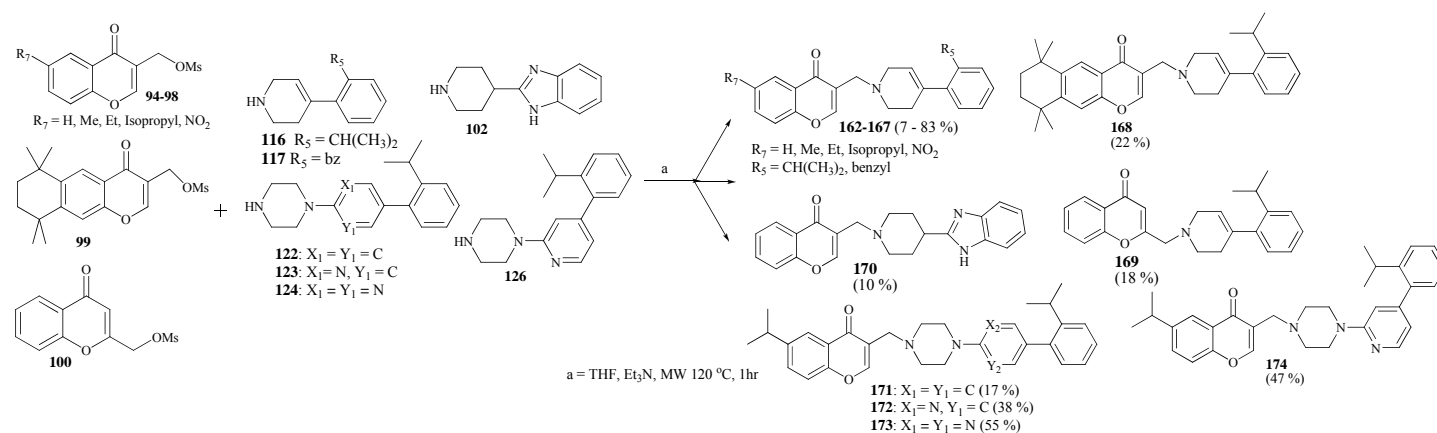
Scheme 16a: Synthesis of lactone based target compounds **127-145**.



Scheme 16b: Synthesis of 1,3-benzodioxole, oxazolidinone and tetrahydrofuran based target compounds **146-161**.



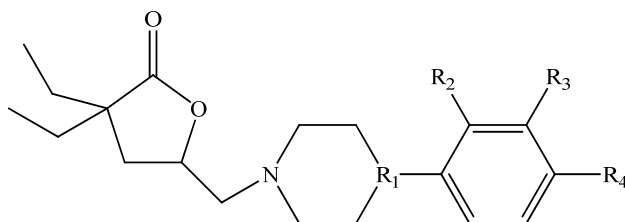
Scheme 16c: Synthesis of chromone based target compounds **162-174**.



4.1.3. Preliminary binding studies of target ligands.

Preliminary binding studies performed for the lactone-based test compounds at 10 μ M revealed that both piperidine and piperazine containing compounds exhibited modest affinity for muscarinic receptors (see **Tables 3** and **4**). Piperazines **127**, **132**, **135** and **143** and piperidinyl phenylcarbamate **145** inhibited [3 H]-Quinuclidyl benzilate (QNB) binding to rat cerebral cortex membranes by 26 to 32 %. Piperazine **134**, piperidines (unsubstituted, substituted and benzimidazole) **136-140** and 1,2,3,4-tetrahydroisoquinoline **141** inhibited specific binding with % inhibition values ranging from 44 to 68 %. In the present series of lactone-based ligands, compounds **136** and **144** exhibited the highest % inhibition values (68 % and 97 %, respectively). Based on the guidelines suggested for interpretation of these data (baseline = -20 - 20 %, considered inactive; 20 % - 49 %, considered marginally active; > 50 % considered active), the remaining piperazines (**128 - 131**, **133**) were considered inactive.

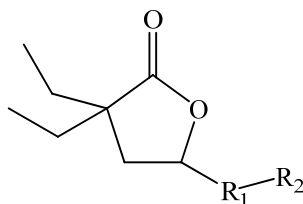
Table 3: Preliminary binding data (% inhibition; 10 μ M) for target compounds **127-137**.



Compound #	R ₁	R ₂	R ₃	R ₄	% specific inhibition at 10 μ M
127	N	H	H	OCH ₃	26
128	N	H	H	CN	18
129	N	H	H	NO ₂	18
130	N	H	H	OH	7
131	N	H	H	H	16
132	N	OCH ₃	H	H	32
133	N	H	OCH ₃	H	9
134	N	OH	H	H	46
135	N	CN	H	H	31
136	C	H	H	H	68
137	C	CH ₃	H	H	57

Data supplied by CEREP. Assays performed in duplicate and presented as averages representing % inhibition at 10 μ M. Guidelines for interpretation: baseline = -20 - 20 %, considered inactive; 20 % - 49 %, considered marginally active; > 50 % considered active.

Table 4: Preliminary binding data (% inhibition; 10 μ M) for target ligands **138-145**.



Compound #	R ₁	R ₂	% specific inhibition at 10 μ M
138			46
139			57
140			67
141			44
142			5
143			28
144			97
145			31

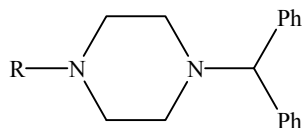
Data supplied by CEREP. Assays performed in duplicate and presented as supplied as averages representing % inhibition at 10 μ M. Guidelines for interpretation: baseline = -20-20 %, considered inactive; 20 % - 49 %, considered marginally active; > 50 % considered active.

Within the current series of test compounds, diphenylmethylpiperazine **144** was found to exhibit the highest % inhibition (97 % at 10 μ M). Determination of the IC₅₀ value for

144 revealed that this compound was the highest affinity lactone-based ligand identified thus far ($IC_{50} = 340$ nM).

For the next series of compounds (see **Tables 5-7**), four different bioisosteric replacements for the H-bonding lactone ring were investigated and the biphenylmethyl piperazine (**144**), the *o*-isopropyl phenylpiperazine (**140**) or the *o*-isopropyl phenyl tetrahydropyridine (**140**) fragments were retained. Two of the proposed bioisosteres (tetrahydrofuran and oxazolidinone) were structurally related to the lactone ring whereas the 1,3-benzodioxoles and substituted chromones were structurally unrelated but had the H-bonding feature required for binding to muscarinic receptors. The THF-based compound **146** (**Table 5**) retained activity similar to lactone **144** at 98 % inhibition. The 1,3-benzodioxoles **147** and **148** with substitution at 6 position (**Table 5**) also showed high % inhibition values of 98 and 97 %. However, the related analog **149** was found to be inactive (% inhibition = 17 %). Oxazolidinone **150** (**Table 5**) with an amine side chain coupled directly to the nitrogen of the heterocyclic ring inhibited specific binding by 81 %. Oxazolidinones **152-159** have amine side chains attached to the five (5) position while the three (3) position has different substituents (e.g., alkyl, cycloalkyl and aryl). This series of 3-,5-substituted oxazolidinones (**Table 5**; **152-159**) showed % inhibition values between 46-80 %. Among the 3-cycloalkyl substituted oxazolidinones, cyclopentyl analog **158** showed the highest % inhibition value (80 %). Among the oxazolidinone series evaluated herein, the unsubstituted compound **151** was found to have the highest % inhibition value (87 %).

Table 5: Preliminary binding data (% inhibition; 10 μ M) for target compounds **146** - **159**.

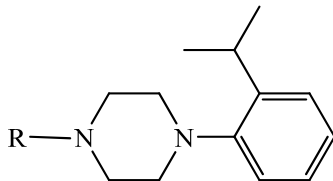


Compound #	R	% specific inhibition at 10 μ M	Compound #	R	% specific inhibition at 10 μ M
146		98	153		66
147		98	154		58
148		97	155		74
149		17	156		46
150		81	157		65
151		87	158		80
152		53	159		73

Data supplied by CEREP. Assays performed in duplicate and presented as supplied as averages representing % inhibition at 10 μ M. Guidelines for interpretation: baseline = -20-20 %, considered inactive; 20 % - 49 %, considered marginally active; > 50 % considered active.

In an effort to increase the structural diversity of the compound library, the *o*-isopropyl phenylpiperazine fragment was utilized in the design of furan-based and some chromone-based compounds. Tetrahydrofuran **160** showed modest affinity for muscarinic receptors with a % inhibition of 54 % while homolog **161** inhibited binding by 89%. The % inhibition observed for homolog **161** (89 %) indicates homologation was successful in improving affinity and that a 2 carbon spacer may be preferred for future ligands in this series.

Table 6: Preliminary binding data (% inhibition at 10 μ M) for substituted tetrahydrofuran based compounds **160** - **161**.



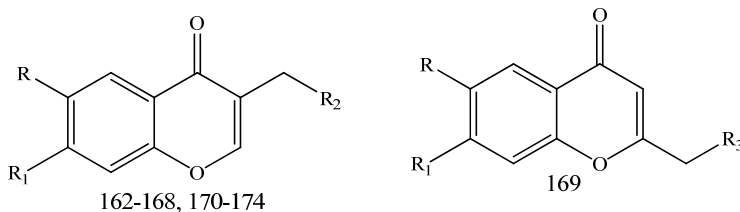
Compound #	R	% specific inhibition at 10 μ M
160		54
161		89

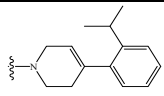
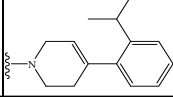
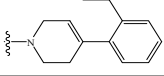
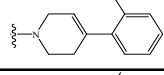
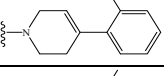
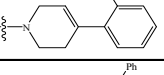
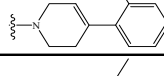
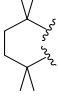
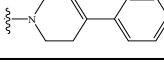
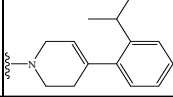
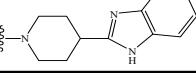
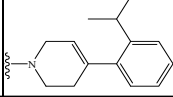
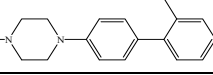
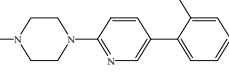
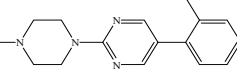
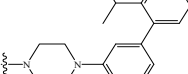
Data supplied by CEREP. Assays performed in duplicate and presented as averages representing % inhibition at 10 μ M. Guidelines for interpretation: baseline = -20-20 %, considered inactive; 20 % - 49 %, considered marginally active; > 50 % considered active.

The chromone fragment is capable of serving as an H-bond acceptor at both carbonyl or ether oxygens. In addition, it possesses an aromatic ring and a degree of lipophilicity that could contribute to improved binding to muscarinic receptors. An ortho substituted phenylpiperidine ring was chosen as the cationic fragment to couple to the chromone nucleus because it gave 67 % inhibition in the lactone-based compound **140** and had positive effects on binding in related muscarinic ligands. The chromone - based ligands **162-169** differ from each other in terms of lipophilicity, conformational rigidity and steric bulk (**Table 7**). Compound **170** has a benzimidazolepiperidine attached to the chromone ring while compounds **171 - 174** have ortho phenyl attached to aryl or pyridine or pyrimidopiperazine ring attached to a chromone ring. Compounds **162-168** and **170-174** have the aryl cationic center attached at the three (3) position of the chromone ring whereas in **169** the aryl cationic center is attached to the two (2) position of the chromone

ring. The chromone-based ligands were found to have % inhibition values between 14 – 90 %. The unsubstituted chromone **162** inhibited specific binding by 82 %. The methyl, ethyl and isopropyl analogs **163-165** were found to have similar % inhibition values of 82, 75 and 90 %, respectively. Further increasing lipophilicity, steric bulk and rigidity in **168** brought a decrease in binding (74 %) as compared to **162-164**. Substituting an *o*-benzyl (**167**) for the *o*-isopropyl group (see **165**) caused a decrease in binding (61 %). Moving the attachment point of the cationic center from the 3 position of the chromone ring in compound **162** to the 3 position in **169** resulted in a decrease in inhibition from 82% to 50%.

Table 7: Preliminary binding data (% inhibition at 10 μ M) for chromone based compounds **162 - 174**.



Compound #	R	R ₁	R ₂	R ₃	% specific inhibition at 10 µM
162	H	H			82
163	CH ₃	H			82
164	C ₂ H ₅	H			75
165	(CH ₃) ₂ CH	H			90
166	NO ₂	H			80
167	(CH ₃) ₂ CH	H			61
168					74
169	H	H			50
170	H	H			23
171	(CH ₃) ₂ CH	H			14
172	(CH ₃) ₂ CH	H			33
173	(CH ₃) ₂ CH	H			38
174	(CH ₃) ₂ CH	H			15

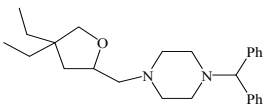
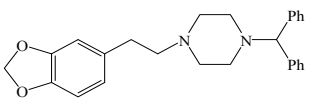
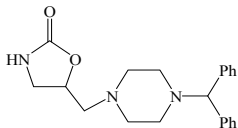
Data supplied by CEREP. Assays performed in duplicate and presented as supplied as averages representing % inhibition a 10 µM. Guidelines for interpretation: baseline = -20-20 %, considered inactive; 20 % - 49 %, considered marginally active; > 50 % considered active.

In the chromone series, the unsubstituted and isopropyl substituted compounds provided the highest % inhibition values (e.g. **162**, 82 % and **165**, 90 %). Therefore, these fragments were retained and different aryl cationic centers were evaluated at the 3-position of the chromone ring. To further develop the structural diversity of the series, a benzimidazole piperidine and ortho phenyl substituted phenyl or pyridine or pyrimidinopiperazines (**Table 7, 170-174**) were utilized. The chromone-based benzimidazole **170** exhibited weak binding at 23 % inhibition. Compounds **171 - 174** have an additional aryl/pyridyl or pyrimidinyl ring between the *o*-isopropylphenyl group and the piperazine. The pyridine and pyrimidine rings can serve as an additional hydrogen bonding centers. Compound **174** has *o*-isopropylphenyl ring at the para position to the pyridine nitrogen. Compounds **141-144** were found to be inactive based on the guidelines for interpretation of these binding data.

Compounds found to have high % inhibition values were selected for further evaluation in IC₅₀ determinations and receptor subtype selectivity assays. Hence, compound **147** was found to have an IC₅₀ of 280 nM. Compounds **146, 148** and **151** were selected for muscarinic subtype selectivity determinations at concentrations of 500, 100 and 500 nM, respectively. The % inhibition values at the five muscarinic receptor subtypes are shown in **Figure 15** and **Table 8**. Compound **146** shows no binding at M₁, M₃ and M₅ but modest binding is seen at M₂ (49 %) and M₄ (59 %) subtype. Compound **148** show no binding at M₁, M₂, M₄ and M₅ subtype and low binding at M₃ subtype (39 %). Compound **151** shows no binding at M₁-M₃ and M₅ subtypes but modest binding at M₄

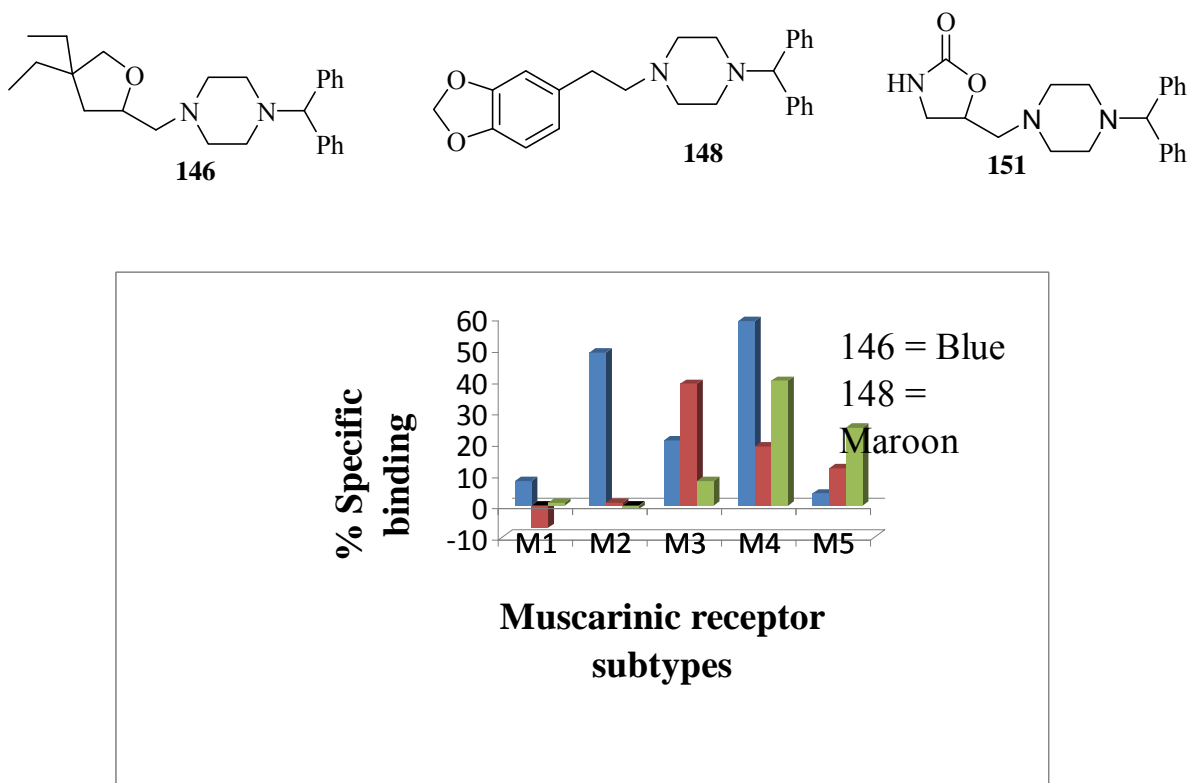
subtype (40 %). None of the above compounds show any selectivity towards any of the subtypes examined.

Table 8: Subtype selectivity data at hM₁-hM₅ for compounds **146**, **148** and **151**.

Compound #	Structure	% specific inhibition				
		M ₁	M ₂	M ₃	M ₄	M ₅
146		8	49	21	59	4
148		7	1	39	19	12
151		1	-1	8	40	25

Compounds **146**, **148** and **151** were tested at concentration of 500, 100 and 500 nM, respectively.

Figure 15: Subtype selective profile of compound **146** (at 500 nM), **148** (at 100 nM) and **151** (at 500 nM).



The test compounds were also evaluated in solubility assays to examine possible influences of solubility on the binding characteristics of the compounds (**Table 9**). The assay was performed in the high throughput screening facility of Moulder Center for Drug Discovery Research (MCDDR). The kinetic solubility was determined after solubilizing test compounds in DMSO and diluting with universal buffer (45 mM ethanolamine, 45 mM potassium dihydrogen phosphate and 45 mM potassium acetate) at pH 7.4. After 90 min the solution is filtered in 96 well collection plates. The filtered sample is then analyzed by absorbance (UV) (or by UPLC/mass spectrometer in case of samples with insufficient absorbance). Compounds exhibiting good solubility did not necessarily correlate with high binding but compounds with low solubility can correlate

with low binding or inactivity. In the CEREP binding assay, the lactone based compounds **127**, **131**, **132-134** and **141** had % inhibition values ranging from 9-46 % (see **Table 10** in **Chapter 5**). Hence these compounds were either inactive or had low binding. When evaluated in the solubility assay, they were found to have solubilities ranging from 180-200 μM . Based on these data, the lactones did not exhibit any solubility issues and hence physicochemical properties of the compounds is likely responsible for the lack of binding observed. A similar profile was seen in case of oxazolidinone-based compounds **150-152**, **155** and **156** which had solubilities ranging from 14-200 μM and showed modest binding (46-87 %). The profiles for the chromone-based ligands were not as straightforward. The solubilities of chromone series ranged from 2-100 μM . Chromones **162-164**, **166**, **169-170** did not exhibit any solubility issue (solubility 17-200 μM). Chromone **165** had modest solubility of 8 μM and exhibited 90 % inhibition. Chromones **167 - 168**, **171-174** had low solubility of 2-4 μM and exhibited binding between 14-74 %. Several of those compounds were found to have limited solubility that may help to explain poor binding in the receptor assays and will require further discussion in the next section of the thesis.

Table 9: Solubility profile for target compounds.

Compound #	Solubility (μM)	Compound #	Solubility (μM)
127	184	163	20
131	200	164	17.1
132	194	165	7.9
133	200	166	57.6
134	198	167	5.5
141	180	168	4
151	200	169	52.2
148	83	170	200
152	198	171	4
155	14.2	172	3
156	200	173	2
162	43.9	174	3

The structures for the above compounds along with their binding and solubility values are given in the discussion section

CHAPTER 5

DISCUSSION

It is evident from the literature and from work in our laboratory that the lactone nucleus can serve as an H-bonding center in our newly designed muscarinic ligands. Phenylpiperazines have been widely utilized as aryl cationic centers in muscarinic ligands. Hence we hypothesized that designing lactone-based ligands containing appropriately substituted phenylpiperazines would result in an improvement in affinity and ultimately may lead to selectivity towards muscarinic receptor subtypes.

The present work also focused on identifying suitable replacements for the lactone ring due to its metabolic instability. Thus the compounds designed and synthesized herein possess several potential lactone bioisosteres. These compounds were screened in preliminary binding assays and promising ligands were evaluated for subtype selectivity..

5.1. Chemistry:

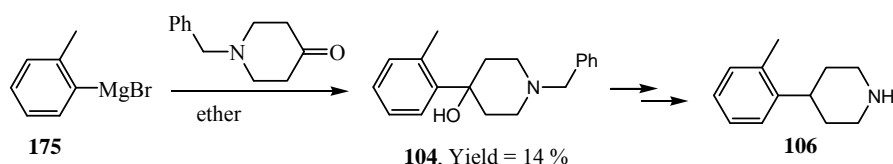
A structurally diverse library of compounds has been synthesized as potential muscarinic ligands by coupling amines (commercially available or synthesized) with H-bonding fragments. Thermal and microwave techniques were adopted for the synthesis of intermediates and final products.

5.1.1. Synthesis of ortho-substituted phenylpiperidines.

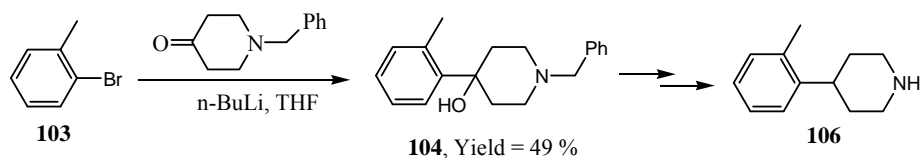
The 4 fold improvement in binding observed for unsubstituted phenylpiperidine-based lactones over the piperazine-based lactone suggested that the synthesis of additional ortho

substituted phenylpiperidines was warranted. Therefore efforts to prepare ortho substituted phenylpiperidines were undertaken as shown below. **Schemes 25** and **26** depict the synthesis of intermediate **104** by two methods.

Scheme 25: Synthesis of 1-Benzyl-4-*o*-tolyl-piperidin-4-ol (**104**) using Grignard reagent

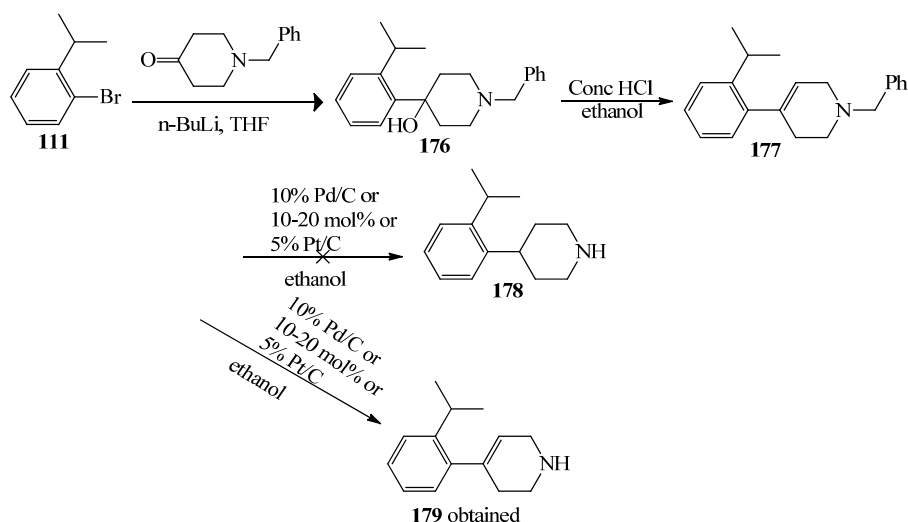


Scheme 26: Synthesis of 1-Benzyl-4-*o*-tolyl-piperidin-4-ol (**104**) using n-BuLi



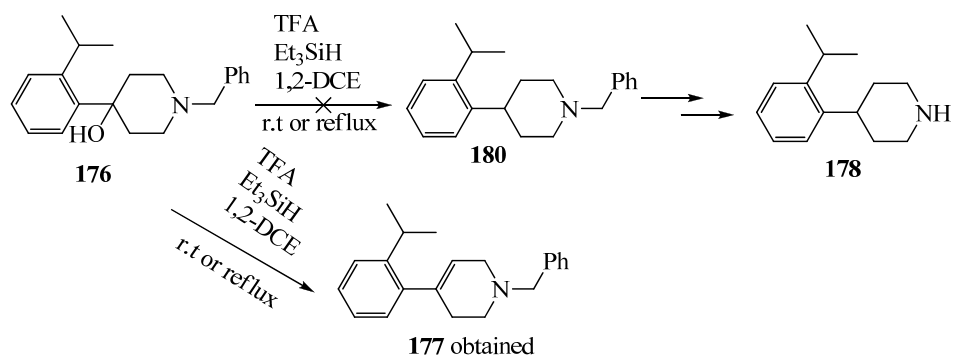
Scheme 25 utilized the use of Grignard reagent **175** in anhydrous ether to obtain intermediate **104**. The product on purification was found to have a yield of 14 %. Reaction of 2-bromotoluene **103** with N-benzyl-4-piperidone in the presence of n-BuLi in THF (**Scheme 26**) provided **104** in much higher yield (49 %) and this route was chosen for the syntheses of this intermediate.

Scheme 27: Attempted synthesis of 4-(2-isopropylphenyl)piperidine (**178**) and synthesis of 4-(2-isopropylphenyl)-1,2,3,6-tetrahydropyridine (**179**)



The routes used in attempts to prepare ortho isopropyl substituted intermediates **178** and **179** are shown in Scheme 27. Precursors **176** and **177** were synthesized using methods similar to those reported earlier for intermediates **104**, **105** (Scheme 13). Standard hydrogenation conditions using 10% Pd/C (10 mol%) gave the deprotected intermediate **179**. Attempts to deprotect and reduce **177** to provide **178** were unsuccessful. Increasing the amount of catalyst (20 mol%) and changing the catalyst from palladium to platinum proved to be futile as **179** was isolated in all cases. Steric hindrance provided by the ortho isopropyl group may contribute to the failure of these reduction reactions

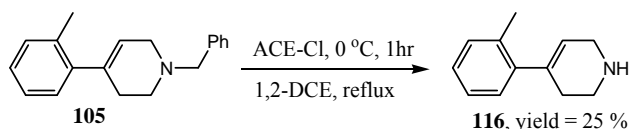
Scheme 28: Synthesis of 1-benzyl-4-(2-isopropylphenyl)-1,2,3,6-tetrahydropyridine (**177**) and attempted synthesis of 4-(2-isopropylphenyl)piperidine (**178**).



Another route was undertaken (**Scheme 28**) in efforts to prepare intermediate **178**. Precursor **176** was treated with trifluoroacetic acid and triethylsilylhydride in 1,2-dichloroethane at r.t (or reflux). The intermediate **180** would then be deprotected as shown in **Scheme 13**. The only product recovered when the reaction was run at r.t or at reflux was **177**.

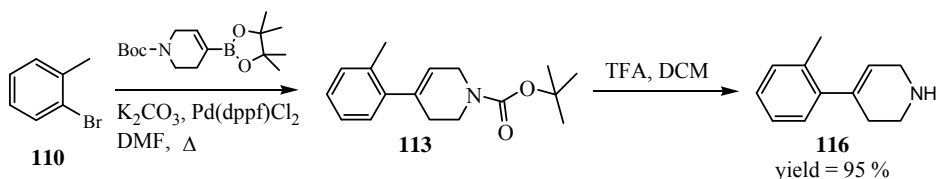
In spite of the failure to prepare **178**, SAR studies proceeded using 1-benzyl-4-(2-isopropylphenyl)-1,2,3,6-tetrahydropyridine (**177**), in order to investigate the influence of the double bond on binding. The presence of the double bond would conformationally restrict the piperidine ring and may lead to interesting binding characteristics. Following up on this approach, intermediate **116** was prepared using precursor **105** (see **Scheme 13** Chapter 4: Results section) which was N-debenzylated using 1-chloroethylchloroformate (ACE-Cl) to obtain 1,2,3,6-tetrahydro-pyridine **116**. The reaction was run for 1 hrs at 0° C and then allowed to warm to r.t and refluxed overnight. Work up and purification afforded **116** in 25 % yield (**Scheme 29**).

Scheme 29: Synthesis of 4-*o*-Tolyl-1,2,3,6-tetrahydro-pyridine (**116**)



Due to the low yield achieved using this method, an alternative approach was utilized (**Scheme 30**). Intermediate **113** was obtained under Suzuki conditions by reacting 2-bromotoluene **110** with the boronic acid ester shown in the presence of $\text{PdCl}_2(\text{dppf})/\text{K}_2\text{CO}_3$ in DMF. The *t*-Boc group was removed under standard conditions using TFA in DCM at 0 °C to r. t to obtain **116** in 95 % yield. Based on the higher yields obtained with the Suzuki reaction, this route was used for future syntheses of intermediate **116**.

Scheme 30: Synthesis of 4-*o*-Tolyl-1,2,3,6-tetrahydro-pyridine (**116**)



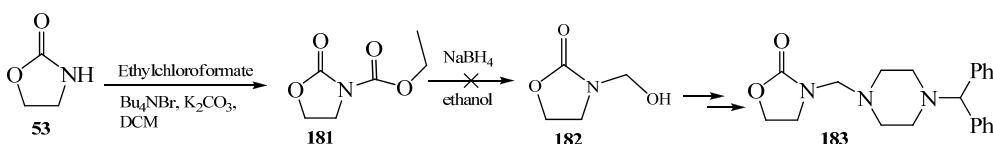
5.1.2. Synthesis of N₃-substituted oxazolidinones.

The oxazolidinones synthesized and tested in the present study fall into 3 structural classes. One class had the biphenylpiperazine fragment attached to the 3N position of the ring with a two carbon spacer (e.g., **150**). A second class has the biphenylpiperazine fragment attached at the 5 position of the ring (**one carbon spacer**) and the N3 position is substituted (alkyl, aryl; e.g., **153**, **154**) or unsubstituted (H; e.g., **151**). A third class has biphenylpiperazine fragment attached at the 4 position of the ring (**two carbon spacer**) and the N3 position is unsubstituted (H; e.g., **191**). The promising binding data obtained

for unsubstituted oxazolidinone **151** (87% inhibition) suggested that N3-substituted analogs of this ligand should be synthesized. This series of compounds are shown in **Scheme 31-34**. Examples of the three structural classes of oxazolidinones prepared and evaluated here.

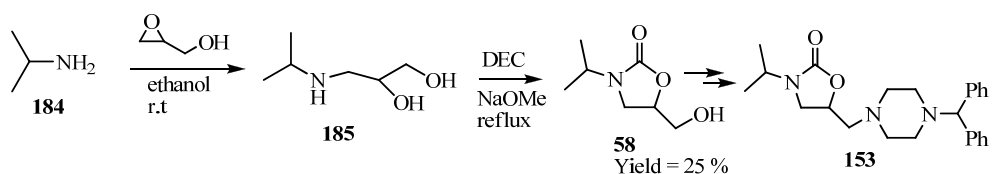
Schemes 31, 32, 33 and 34 describe the attempted synthesis of oxazolidinone intermediates.

Scheme 31: Synthesis of 3-(hydroxymethyl)oxazolidin-2-one (**182**).



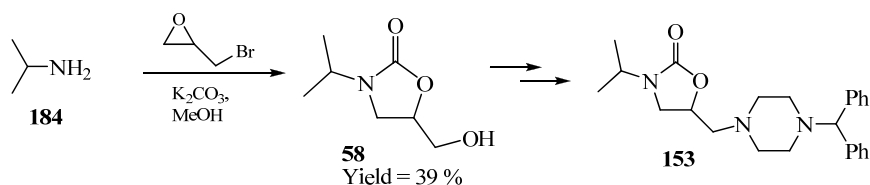
Attempted synthesis of **182** involved the reaction of 2-oxazolidinone with ethylchloroformate in the presence of tetrabutylammonium bromide (TBAF) and K_2CO_3 to obtain the N3 substituted **181**. Reduction of dicarbamate **181** using $NaBH_4$ (3/1.5/1/0.5 Eq) in ethanol did not yield the desired alcohol. Reaction of **181** with 1 Eq of $LiAlH_4$ produced multiple spots on TLC. The failure of the reduction reactions for this compound might be due to the presence of dicarbamate. Literature evidence cites this susceptibility of such groups to ring opening under basic conditions.^{91,92} Hence a two carbon linker was chosen which was later coupled to biphenylmethylpiperazine. The compound **150** (see Chapter 4, **Table 5**) when tested was found to have % inhibition of 81 %.

Scheme 32: Synthesis of 5-(hydroxymethyl)-3-isopropylloxazolidin-2-one (**58**) from glycidol.



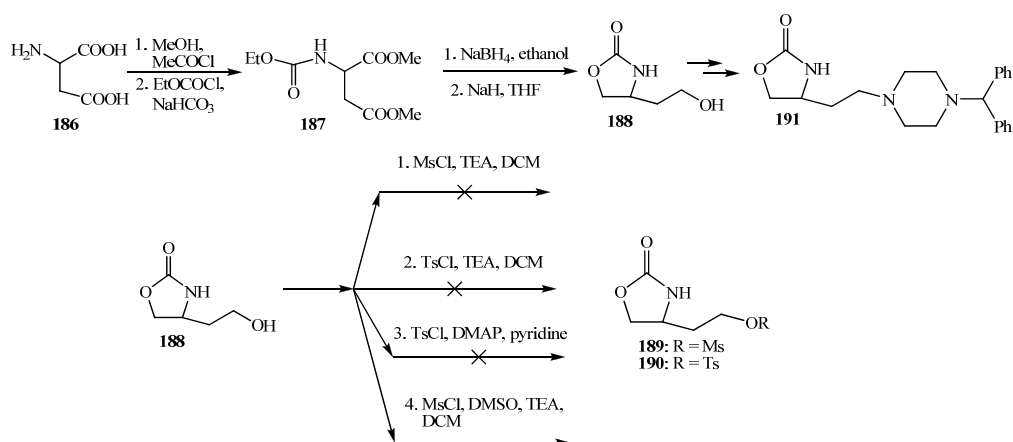
The intermediate **58** was synthesized by two methods as shown in **Schemes 32** and **33**. Trial reactions were carried out in order to determine the most efficient route to the target compound. In the above route, isopropylamine **184** was reacted with glycidol to obtain the aminodiol **185** which was cyclized to oxazolidinone **58** using diethylcarbonate in 25 % yield.

Scheme 33: Synthesis of 5-(hydroxymethyl)-3-isopropylloxazolidin-2-one (**58**) from epibromohydrin.



In **Scheme 33**, isopropylamine **184** was reacted with epibromohydrin under basic conditions in one pot to obtain intermediate **58** in 39 % yield. Considering the advantages of the one step reaction and the higher yield obtained, the above method was utilized for the preparation of other N3 substituted oxazolidinones.

Scheme 34: Synthesis of 2-(2-oxooxazolidin-4-yl)ethyl methanesulfonate (**189**) and 2-(2-oxooxazolidin-4-yl)ethyl 4-methylbenzenesulfonate (**190**)



Scheme 34 denotes the synthesis of target oxazolidinone **191**. The intermediate alcohol **188** was synthesized from DL-aspartic acid **186** by treating it with methanolic acetyl chloride and ethylchloroacetate under basic conditions to obtain N-protected dimethylaspartic acid methyl ester **187**. The methyl ester was reduced to alcohol using standard conditions and the alcohol was cyclized to oxazolidinone **188** using NaH in refluxing THF.

The alcohol **188** was mesylated to afford **189** which was coupled with biphenylmethylpiperazine. The LC-MS of the reaction mixture did not show the presence of product **191**. Re-inspection of the mesylation reaction revealed that alcohol **188** was insoluble in DCM.

Efforts to solubilize the starting material by sonication during the mesylation step proved futile. The same reaction was carried out with tosylchloride as this could aid in detection and isolation of tosylate **190**. Our initial attempt failed and a second route was attempted using DMAP and pyridine at -10 °C. Multiple attempts failed to provide the tosylate by this route. A final attempt at the tosylation reaction involved the use of DMSO as a co-

solvent in DCM in order to aid in solubilization of alcohol **188**. On addition of DMSO to a suspension of **188** in DCM, a translucent mixture was observed. The reaction was allowed to run with stirring for 24 hrs. LC-MS analysis revealed a peak at **286** ($M + 1$) which indicated the presence of the tosylate. However the amount of the product obtained was low based on the LC-MS data. These results suggest that the limited solubility of alcohol **188** prevents the formation of the desired mesylate or tosylate analogs. Converting the alcohol to a halide (bromine; e.g., PBr_3) was considered as an alternative to introduce a leaving group at this position. The reaction could be carried out in variety of solvents such as DMF, diethylether, THF, ACN. Hence the solubility of the alcohol **188** was evaluated in different solvents (THF, ether, ACN, DMF, CHCl_3) and found to exhibit limited solubility in all of these solvents.

In conclusion, different methods were investigated for the synthesis of intermediates (H-bonding/ amine fragments) necessary for the preparation of target compounds. In efficient reactions were revised to improve yields or reduce the number of steps. Side products of some of reactions were identified based on ^1H -NMR or literature reports (carbamate **181**, Scheme 31). Attempts to prepare 2-(2-oxooxazolidin-4-yl)ethyl methanesulfonate (**189**) and 2-(2-oxooxazolidin-4-yl)ethyl 4-methylbenzenesulfonate (**190**) were unsuccessful and the target ligands with a 2 carbon spacer were not synthesized. In spite of these drawbacks, the majority of intermediates attempted were prepared in moderate to good yields and coupled to the appropriate fragments to afford the target ligands.

5.2 Biological activity of target compounds

Lactone-based muscarinic leads were subjected to molecular modifications in an effort to increase affinity. The original lead lactones contained various substituted amines and amine containing heterocycles and were found to have IC₅₀ values in 1 - 2 μ M. The compounds reported herein differ from the leads in that all possess substituted or unsubstituted aromatic rings. The electronic nature of substituents on the test compounds vary from electron donating groups (eg. **134**; OH) to strong electron withdrawing groups (eg. **129**; NO₂). The position of the functional groups was also varied (eg. **127**, **132** and **133**).

The newly designed lactones were prepared in modest yields using well precedented literature routes. The ligands reported herein have pharmacophoric features in common but are structurally different in potentially important ways. Compounds **127-130** and **132-135** share a lactone ring coupled to phenylpiperazines containing a variety of electron withdrawing (NO₂, CN) or electron donating (OCH₃, OH) aromatic substituents. Compound **144** possess a lactone attached to an unsubstituted diphenylmethylpiperazine. Lactones **136-140** have piperidine nitrogen or benzimidazole nitrogens as potential cationic centers. Compounds **139** and **140** are ortho substituted phenylpiperidines having unsaturation in the piperidine ring. Compounds **136-137**, **139-141** are similar in that each compound has only one nitrogen capable of forming a cationic center. The amide and carbamate moieties in **142** and **145** provide additional opportunities for H-bonding with the receptor. Compound **145** is unique within the present series of ligands as its nitrogen containing heterocycle is on the opposite side of the aromatic group.

Preliminary binding studies were performed at test concentration of 10 μ M in rat cerebral cortical membranes at CEREP. For the lactone-based test compounds these assays revealed that both piperidine and piperazine-containing compounds exhibited modest affinity for muscarinic receptors. Piperazines **127**, **132**, **135** and **143** and piperidinyl phenyl carbamate **145** inhibited [3 H]-QNB binding to rat cerebral cortex membranes by 26 to 32 %. Piperazines **134**, **144** and piperidines (unsubstituted, substituted and benzimidazole) **136-140** and 1,2,3,4-tetrahydroisoquinoline **141** were inhibitors of specific binding also with percent inhibition values ranging from 44 to 97 %. Within the present series, compounds **136** and **144** exhibited the highest % inhibition values (68 % and 97 %, respectively). Based on the guidelines suggested by CEREP for interpretation of these data (baseline = -20 - 20 %, considered inactive; 20 % - 49 %, considered marginally active; > 50 % considered active), the remaining piperazines (**128**, **129-131** and **142**) were considered inactive.

A closer look at the binding data for this set of aromatic heterocycles suggests that the position of an aromatic substituent may hold precedent over its electronic nature. For example, the ortho substituted compounds **132** (OMe, electron donating; 32 %), **134** (OH, electron donating; 46 %) and **135** (CN, electron withdrawing; 31 %) were marginally active and were the only compounds in **Table 1** to inhibit binding by more than 30 %. The corresponding derivatives with substituents at the para position (**128-130**) were inactive (7 % to 18 %). Introduction of an additional hydrogen bond acceptor in the form of a carbamate in **145** did not improve activity. The addition of a benzimidazole ring in **138** resulted in marginal activity (46 %). Fusing the piperidine with an aromatic ring in **141** did not improve activity and the introduction of an additional H - bond acceptor

group (amide carbonyl) in **142** proved deleterious to binding. A comparison of the % inhibition for piperazine **131** with that for piperidine **136** reveals an improvement in activity for the piperidine. These results suggest that further evaluation of piperidine containing lactones was needed. Hence ortho - substituted piperidine based lactones **137**, **139** and **140** were synthesized and tested. Substitution at the ortho position did not show any improvement in the activity over the unsubstituted piperidine **136** (68 %). The presence or absence of a double bond in the piperidine ring did not result in a change in activity (57 % in compound **137** and **139**). Of all the test compounds assayed, diphenylmethylpiperazine **144** was found to exhibit the highest % inhibition (97 % at 10 μ M). Further evaluation to determine the IC₅₀ (non-selective) value revealed **144** to be the highest affinity lactone - based ligand identified in this series (IC₅₀ = 340 nM).

Compared to our previously reported ligands (IC_{50s} of 1-2 μ M) the data reported herein confirm that the lactone nucleus is a useful scaffold for the design of muscarinic ligands and indicate that the addition of appropriately positioned aromatic substituents can improve affinity. The % inhibition studies reported herein suggest that further structural modification to these lactone derivatives is warranted and may provide higher affinity compounds. Further work on this series has been accomplished and will be reported by a colleague in our lab.⁹⁰

For the next series of compounds, we decided to retain the biphenylmethyl piperazine, the *o*-isopropyl phenylpiperazine or the *o*-isopropyl phenyl tetrahydro-pyridine fragments and to change the H-bonding lactone ring. The ortho substitution was selected based on the modest improvement in the % inhibition data reported above. Four different groups

were evaluated as bioisosteric replacements for the lactone ring. Two of the proposed bioisosteres (tetrahydrofuran and oxazolidinone) were structurally related to the lactone ring whereas 1,3-benzodioxoles and substituted chromones were structurally unrelated but had the pharmacophoric features required for the binding to the muscarinic receptors.

Tetrahydrofuran **146** was made in order to improve the metabolic stability of lactone **144**. The substituted tetrahydrofuran **146** retained the activity of the parent lactone (98 % inhibition) indicating that the carbonyl of lactone ring is not required for binding to mAChRs.

The 1,3-benzodioxole ring was also investigated as a lactone bioisostere and was substituted at the 2 and 6 positions. A two carbon linker was utilized to assess the effect of homologation on the muscarinic binding of **148**. Compounds **147** and **148** showed similar values in the binding assay % (98 and 97 %, respectively) suggesting that homologation does not improve binding. Substitution at the 2 position of the 1,3-benzodioxole ring as seen in **149** caused a significant drop in the % inhibition value (17 %). Thus based on the limited data in this small series (**147**, **148**, **149**) substitution at position 6 is preferred for binding possibly due to less steric hindrance in the area of the hydrogen bonding center.

The oxazolidinone was also evaluated as a possible bioisostere as it has structural similarities to the lactone ring. Oxazolidinone **150** has a biphenylmethylpiperazine coupled directly to the nitrogen of the heterocyclic ring with an ethyl spacer. This compound did not show improved binding (% inhibition 81%) over the lactone lead **144**. The oxazolidinone series (**151-159**) has amine side chains attached at the five (5) position while the three (3) position has different substituents (e.g., alkyl, cycloalkyl and aryl) and

exhibited % inhibition values between 46-80 %. Among the different N3 substituents, cyclopropyl gave the highest % inhibition value (80 %) while the unsubstituted oxazolidinone **151** gave the highest % inhibition in this series (87 %). In general, changing the size of alkyl substituents on the N3 position had minimal effects on binding. The same was true of the one aromatic substituent included in the series (**153**). None of the oxazolidinones synthesized herein compared favorably with the binding reported for our lead lactone **144** (97 %). The data collected for this oxazolidinone series suggest a limited tolerance for steric bulk at N3 of the oxazolidinone ring system.

In an effort to improve the structural variability in the compound library, the *o*-isopropyl phenylpiperazine fragment was utilized in the design of tetrahydrofuran based compounds **160-161**. Compound **161**, a homolog was synthesized to investigate the effect of homologation on binding to muscarinic receptors. Compound **160** showed modest affinity for muscarinic receptors with a % inhibition of 54. The % inhibition observed for homolog **161** (87 %) indicates homologation was successful in improving affinity and that a 2 carbon spacer may be preferred in future ligands in this series. The chromone fragment has pharmacophoric features required for binding to the muscarinic receptors. For example, the ring system has H-bond acceptors at both carbonyl or ether oxygens, an aromatic ring (with or without substituents) and a degree of lipophilicity that might contribute to improved binding to muscarinic receptors. An ortho substituted phenylpiperidine was chosen as the fragment to couple to the chromone nucleus due to previous SAR data reported above (67 % inhibition for lactone **144**) and similar data obtained in a related project in our lab.⁹⁰ In addition, the biphenylmethyl piperazine

fragment is found in many known drugs/ligands and appears widely in the patent literature. The chromone-based ligands **162-169** differ in terms of lipophilicity, electronic properties, conformational rigidity and steric bulk. In compounds **162-168**, the aryl cationic center was attached at the 3 position, whereas in compound **169**, the attachment is at the 2 position of the chromone ring. Position 6 of the ring was substituted with different alkyl groups having varying degree of lipophilicity, steric bulk (**163-165**, **167-168**) and electronic property (**166**). Different alkyl substitutions gave % inhibition values between 82 - 90 % with the highest inhibition value reported for **165** (90%). An increase in the lipophilicity, steric bulk and rigidity exhibited by compound **168** resulted in a decrease in binding (74 %) when compared to **165**. To investigate the effect of influence of electronic property of the chromone ring on binding, the 6 position was substituted with nitro group. Compound **166** has a nitro group at position 6 of the chromone ring and was found to have a % inhibition value of 80 %; similar to the alkyl substituted analogs. Hence, it appears that the electronic properties of substituents at this position do not influence binding. Substitution of the ortho isopropyl group in **165** (90% inhibition) with a benzyl group (**167**), resulted in a decrease in the % inhibition value (61 %). These limited data suggest that steric and/or lipophilic influences may be responsible for the decrease in binding. Compound **169** was synthesized to investigate the optimal position for attachment of the aryl cationic centers to the chromone ring. The % inhibition value for **169** was 50 % as compared to 82 % for compound **162**. This indicates that the 3 position is the preferred position for attachment of the aryl cationic centers in this series of chromones.

The unsubstituted and isopropyl substituted chromones (**162** and **165**) gave the highest % inhibition values in the series of chromones tested thus far. Consequently, this fragment was retained within a series of different aryl cationic centers attached to the 3 position of the chromone ring. In order to further the structural diversity of the library, benzimidazole piperidine and aryl aryl/pyrido/pyrimidopiperazines were utilized. The % specific inhibition values for compounds **170-174** were in the range of 14-38 % making them inactive (**171** and **174**) or marginally active (**170**, **172**, **173**) based on criteria provided by Cerep and mentioned earlier (See **Table 7**, Chapter 4: Results section).

Several of the final compounds (lactone and bioisosteres) were chosen for further evaluation to determine IC₅₀ values and subtype selectivity profiles. A full binding curve generated for compound **147** revealed an IC₅₀ (non-selective) of 280 nM. Based on the IC₅₀ values of **147** (280nM) and **144** (**340 nM**), it can be said that the benzodioxole ring system is a suitable bioisostere for the lactone ring.

Compounds **146**, **148** and **151** were selected for evaluation in muscarinic subtype selectivity assays (hM₁-hM₅) and were evaluated at CEREP, France at concentrations of 500 nM, 100 nM and 500 nM (see **Table 8** and **Figure 15** in Chapter 4: Results section). On the basis of % inhibition values, no receptor subtype selectivity was observed for these ligands. However, compound **146** shows some modest preference for hM₂ and hM₄ receptors (49 and 59 % inhibition, respectively) and no binding at the hM₁, hM₃ and hM₅ subtypes. Compound **148** shows weak binding at hM₃ (39 % inhibition) and did not bind to hM_{1,2} and hM_{4,5} subtypes; compound **151** has weak binding to hM_{4,5} (40 and 25 % inhibition, respectively) but is inactive at hM_{1,3}, and hM₂.

Over the course of our investigations, compounds with similar pharmacophoric elements were shown to have different binding profiles. Since solubility differences could help to explain these observations, solubility assays were performed on compounds exhibiting low to modest binding in CEREP binding assays. In order for test compounds to bind target receptors, they must be soluble in the solutions used in the binding assays. In general, compounds that are soluble in the test solution up to 10 μ M are considered to have good solubility and binding data may be viewed as acceptable. Compounds showing solubility of less than 10 μ M are considered low to modest solubility and concentrations below 4 μ M were considered insoluble. The final DMSO concentration in the solubility assay was 2 %.

Tables 10, 11 and 12 show the solubility profiles and the preliminary binding profiles of test compounds with low to modest affinity. **Table 10** indicates the solubility profile for lactone based compounds. Many lactone based piperazines when tested were found to be inactive or weakly active. When evaluated in the solubility assay, their solubilities were found to be between 180-200 μ M. Based on the solubility data in **Table 10**, the lactone-based compounds had good solubility in the binding assay and the data should reflect the ability of the ligands to displace radioligand from the target receptor at 10 μ M. The electronic properties and position of substituents on the aromatic ring did not influence their solubility characteristics. The low binding affinity of these compounds to may be due to poor complementarity to the muscarinic receptors. In fact, a series of homologous lactone-based ligands have been shown to have much higher affinity for the receptor.⁹⁰

Table 10: Solubility profile for lactone based compounds

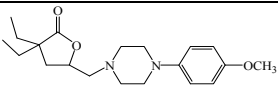
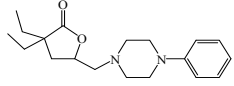
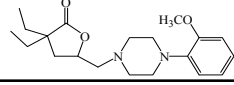
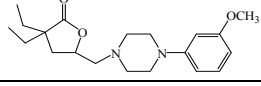
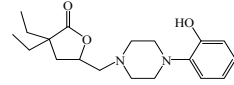
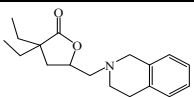
Compound #	Structure	% specific inhibition at 10 μ M	Solubility (μ M)
127		26	184
131		16	200
132		32	194
133		9	200
134		46	198
141		44	180

Table 11 indicates the solubility profiles for oxazolidinone-based compounds **150-152**, and **155-156**. These compounds showed inhibition values ranging from 46-87 % (20 % - 49 %, considered marginally active; > 50 % considered active). When evaluated in solubility assay, these compounds were found to have solubilities ranging from 14-200 μ M. The nature of the substituent at N₃ does affect the solubility as indicated by compound **155**. However, the differences in binding observed in this series did not appear to be related to solubility issues.

Table 11: Solubility profile for oxazolidinone based compounds

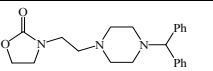
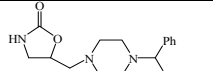
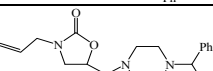
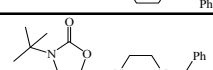
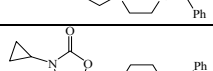
Compound #	Structure	% specific inhibition at 10 μ M	Solubility (μ M)
150		81	83
151		87	200
152		53	198
155		74	14.2
156		46	200

Table 12 shows the solubility profiles for chromone-based compounds **162-174**. These compounds showed inhibition values ranging from 14-90 % (20 % - 49 %, considered marginally active; > 50 % considered active). The solubilities of the compounds ranged from 2-200 μ M. Chromones **162-165** and **168** were similar except for the substituent at position 6 of the chromone ring (H to alkyl) leading to different degrees of lipophilicity and steric bulk. The increase in lipophilicity for these compounds was reflected in their solubility profiles with the highest solubility observed for compound **162** and modest to low solubility for **165** and **168** (8-4 μ M). Substitution of the ortho-isopropyl group in **165** with a benzyl group in **167** resulted in decreased solubility and a corresponding decrease in binding. The low solubility of compounds **165**, **167** and **168**, suggest that the % inhibition values for these compounds may be under estimated. Compound **169** (% inhibition value of 50 %) had a solubility of 52.2 μ M as against compound **162** (% inhibition of 82 %) with solubility of 43.9 μ M. A difference in binding characteristics

between **162** and **169** could be due to the substitution position on the chromone ring (2 Vs 3) and not the solubility issue.

Compound **170** had good solubility (200 μ M) but was found to be inactive in the binding assay. Chromones **171-174** were shown to have limited solubilities bringing the binding data for these compounds into question. Should the chromone-based ligands be chosen for further evaluation, these compounds and others with limited solubility should be re-evaluated as salts to improve solubility. ($IC_{50s} > 50 \mu$ M in CISBIO assay; unpublished data).

Table 12: Solubility profile for chromone based compounds

Compound #	Structure	% specific inhibition at 10 μ M	Solubility (μ M)
162		82	43.9
163		82	20
164		75	17.1
165		90	7.9
166		80	57.6
167		61	5.5
168		74	4
169		50	52.2
170		23	200
171		14	4
172		33	3
173		38	2
174		15	3

In conclusion, lactone-based, THF-based, 1,3-benzodioxole-based, oxazolidinone-based and chromone-based ligands were prepared and tested in preliminary binding assays as muscarinic ligands. The present work identified a novel lactone-based muscarinic ligand with the highest affinity reported to date (**144; 340 nM**). In addition, the 1,3-benzodioxole ring was identified as a lactone bioisostere that provided a moderate affinity, muscarinic ligand (**147; 280 nM**). The data suggest that replacement of the lactone fragment with other hydrogen bonding centers (tetrahydrofuran, 1,3-benzodioxole, oxazolidinone and chromone) provides ligands that retain affinity for the target receptors.

Solubility was shown to play a possible role in the binding data for compounds of limited solubility. In most cases, compounds were shown to be soluble under the assay conditions. In these cases, the low or modest binding of compounds in the assays may be attributed to structural features and/or physicochemical properties of the ligands. The compound library prepared as described in this work will be screened for activity in a wide range of assays that could provide new lead compounds for yet unknown targets.

5.3 Future directions

Evaluation of compounds at single point concentrations provides preliminary data regarding the binding of the test compounds to muscarinic receptors. However, these data provide no information on how the compounds act at the receptor (agonist, antagonists, inverse agonist) their selectivity for muscarinic receptors or other GPCRs. Efforts have been made to obtain additional data on the test compounds by determining IC_{50s} and subtype selectivity in a CISBIO assay. This assay is based on homogenous time resolved

fluorescence (HTRF) technology and uses whole cells rather than the membrane homogenates used by CEREP. Preliminary experiments have been performed but the data is not available at this time. Compounds found to have interesting profiles in these experiments would be considered for future modification and further testing.

Many of the compounds reported herein have also been sent to the PDSP (Psychoactive Drug Screening Program) screening center at the University of North Carolina, Chapel Hill. The center has begun screening the compounds at different protein targets including muscarinic, serotonin receptors, dopamine receptors, and other GPCRs. The compounds are evaluated first in preliminary binding assays at concentrations of 10 μ M. Compounds exhibiting > 50 % inhibition are investigated further to determine IC₅₀/ EC₅₀ values. The preliminary data provided by PDSP are very encouraging and a new target for several of the novel compounds described herein has been identified. A patent application covering these compounds has been filed.

CHAPTER 6

EXPERIMENTAL

Proton Magnetic Resonance spectra (^1H - NMR) were measured in CDCl_3 on a Bruker WM-400 MHz instrument, data are presented as follows: chemical shift in parts per million (ppm) on the δ scale relative to internal tetramethylsilane (TMS) (coupling constant(s) in hertz). The following abbreviations are used to denote signal patterns: s = singlet, d = doublet, t = triplet, m = multiplet. Elemental analyses were performed by Atlantic Microlabs, Inc., Atlanta, GA, and were within $\pm 0.4\%$ of the theoretical values. All TLC was run using Silicycle precoated 60-F-254 silica plates (0.25 mm) with dichloromethane in methanol (9 : 1) or hexane in ethyl acetate (7 : 3) solvent system and the components were visualized with iodine vapor and/or UV-light. Extractive workups culminated in washing the organic layer with brine, drying over MgSO_4 , and evaporating the solvent at reduced pressure on a rotary evaporator. Flash column chromatography was carried out on Silia-P flash silica gel (40 - 63 μm) using methanol (0 - 3 %) in dichloromethane solvent system. Combiflash systems using Redisep silica prepacked columns and C_{18} columns were also utilised when required using dichloromethane - methanol, hexane - ethyl acetate and acetonitrile-water (containing 0.1 % formic acid) gradient system. LC-MS (ESI) analyses were done on an Agilent technologies 1200 series instrument on target compounds using 5 - 95 % acetonitrile in water (containing 0.1 % formic acid) gradient solvent system and was found to be $> 95\%$. HPLC analysis was performed on Gilson 215 reversed phase chromatographic system equipped with Sepax GP 5 μm C-18 column; using 10-90 % acetonitrile in water solvent gradient containing 0.1 % formic acid and; 10-90 % methanol in water solvent gradient containing 0.1 % trifluoroacetic acid.

6.1.1 Procedure for 2,2-Diethyl-pent-4-enoic acid ethyl ester (37)

Anhydrous tetrahydrofuran (THF, 75 ml) was added to a 500 ml round bottom flask having a pressure equalizing dropping funnel under nitrogen atmosphere and maintained at $-76\text{ }^\circ\text{C}$. Lithium diisopropylamide (LDA; 2M solution in heptanes, THF and ethylbenzene; 1Eq) was introduced via a syringe. Ethyl 2-ethyl-butyrate (1 Eq) dissolved in anhydrous THF (120 ml) was transferred to the dropping funnel and was added dropwise and was added for a period of 30 mins, and after the addition was complete, it was stirred for 1 hr. Allyl bromide (1.3 Eq) dissolved in hexamethyl phosphoramidate (0.5 Eq) was added dropwise and the reaction was stirred at $-78\text{ }^\circ\text{C}$ for additional 4 hours, brought to room temperature and allowed to stir overnight. The reaction was quenched with 10 % HCl and then made strongly acidic with conc. HCl. THF was evaporated under reduced pressure. The aqueous layer was extracted with hexane (5 x 100 ml), washed with 10 % sodium bicarbonate (NaHCO_3) solution. The organic layer was dried over MgSO_4 , concentrated under reduced pressure distilled under vacuum to obtain a colorless liquid **37**.

6.1.2 Procedure for 2,2-Diethyl-pent-4-enoic acid (38)

To a 250 ml r.b.f containing the ester **37** (1 Eq) was added 10 % ethanolic solution of NaOH (200 ml). The ester is saponified by refluxing for 2 days. 100 ml of ice water was added and the ethanol was removed under reduced pressure. The basic aqueous solution was extracted with hexane (1 x 100 ml). The aqueous layer was then made strongly acidic with conc. HCl, extracted with ethyl acetate (3 x 100 ml). The combined organic extracts were dried over MgSO₄, concentrated under reduced pressure and distilled under vacuum to obtain light yellow liquid **38**.

6.1.3 Procedure for 3,3-Diethyl-5-iodomethyl-dihydro-furan-2-one (39)

To a solution of acid **38** (1 Eq) in diethyl ether (50 ml) in 250 ml r.b.f., was added saturated aqueous sodium bicarbonate solution (50 ml). The flask was covered with aluminum foil and kept in ice bath. A chilled solution of iodine (3 Eq) dissolved in tetrahydrofuran (50 ml) was added. The reaction was stirred in ice bath for 5 hrs, quenched with saturated aqueous sodium sulfite solution (50 ml) diluted with saturated aqueous NaHCO₃ (100 ml) extracted with ether (2 x 100 ml). The ethereal layer was dried over MgSO₄, concentrated under reduced pressure to obtain orange color liquid which was chromatographed on silica gel using ethyl acetate in hexane (0 - 40 %) to obtain light yellow color liquid **39**.

6.1.4 Procedure for 3,3-Diethyl-5-hydroxymethyl-dihydro-furan-2-one (40)

The acid **38** (1 Eq) was transferred to a 50 ml r.b.f. containing formic acid (98 % solution), and hydrogen peroxide (30 % w/w). The contents were refluxed for 20 mins. After cooling, the reaction was stirred for 9 hrs. Formic acid was removed under reduced pressure, the contents were dissolved in ether (50 ml), washed with saturated aqueous Na₂CO₃ and dried over MgSO₄. The organic layer was concentrated under reduced pressure to obtain a yellow colored liquid. This liquid was refluxed for 7 mins with 5 % KOH solution (100 ml) in absolute ethanol, followed by dilution with ice and acidification with conc H₂SO₄. Ethanol was removed under reduced pressure, and the residue was ethyl acetate (1 x 100 ml), washed with aqueous Na₂CO₃, dried over MgSO₄, concentrated under reduced pressure to obtain a light yellow colored liquid **40**.

6.1.5 Procedure for 2,2-diethyl-pent-4-en-1-ol (41)

From a solution of lithium aluminum hydride (LAH) in ether (1.6 M), 1.2 Eq of LAH is transferred to a 25 ml round bottom flask containing 2.5 ml anhydrous ether. The ester **37** (1 Eq) was dissolved in 10 ml of anhydrous ether and transferred to the above solution. The mixture was stirred in ice for 1 hr and later refluxed overnight. The reaction was quenched by dropwise addition of 10 % NaOH. The organic layer was decanted off and the residue was washed with EtOAc. The combined organic layer was washed with water, brine and dried over MgSO₄ and evaporated to obtain a clear colorless liquid **52**.

6.1.6 Procedure for 4,4-diethyl-2-iodomethyl-tetrahydrofuran (42)

To a solution of alcohol **41** (1 Eq) in ether (10 ml) was added saturated NaHCO₃ (30 ml) and the mixture was cooled to 0 °C in ice. To the above solution was added a chilled solution of iodine (3 eq) in THF 11 ml and the flask was protected from light. The

reaction was stirred for 5 hrs at 0 °C, quenched with saturated aqueous sodium sulfite, diluted with saturated aqueous NaHCO₃, extracted with ether, washed with brine and dried over MgSO₄ to obtain a yellow clear liquid **42**.

6.1.7 Procedure for Toluene-4-sulfonic acid 2-(4,4-diethyl-tetrahydro-furan-2-yl)-ethyl ester (44)

To an anhydrous chloroform (10 ml) in a screw capped vial fitted with nitrogen balloon was added the lactone tosylate **43** (20 Eq), InBr₃ (1 Eq) and Et₃SiH (80 Eq). The mixture was stirred at 60 °C, the solution turned from colorless to yellow to orange. The reaction was stirred for 3 hrs. Water (5 ml) was added till the color disappeared. The aqueous layer was extracted with DCM (50 ml) and the combined organic phase was dried over anhydrous Mg₂SO₄, filtered and evaporated under reduced pressure. The residue was then purified over silica gel columns using ethyl acetate in hexane (0 – 100 %) to obtain **44** as colorless liquid.

6.1.8 General procedure for precursors (47 and 48).

Sodium iodide (15 Eq) in acetone (35 ml) was added to a round bottom flasks containing **45** and **46** and the mixture were refluxed for 48 hrs. The reaction was later quenched with water and extracted with ether. The organic layer was washed with water, brine and dried over MgSO₄ to obtain compounds **47** and **48** as light yellow solids and were utilized for the next step without purification.

6.1.9 Procedure for Benzo[1,3]dioxole-2-carboxylic acid methyl ester (50)

A mixture of catechol **49** (1 Eq), sodium methoxide (25 % w/w in MeOH; 2 Eq) and methyl dichloroacetate (1 Eq) in anhydrous methanol (50 ml) was refluxed overnight. The reaction after cooling was acidified with conc HCl, concentrated under vacuum. The residue was diluted with water and the mixture was extracted with diethyl ether (3 x 100 ml). The organic layer was dried over MgSO₄, concentrated under reduced pressure and purified on redisp silicagel column using ethyl acetate in hexane (0 – 100 %) to obtain a colorless oil **50**.

6.2.0 Procedure for Benzo[1,3]dioxol-2-yl-methanol (51)

The methyl ester **50** (1 Eq) was dissolved in anhydrous tetrahydrofuran (THF, 20 ml) and transferred to 100 ml r.b.f. To it was added 1M solution of lithium aluminum hydride in THF (1 Eq). The reaction was stirred for 1 hr and quenched with sat. aq. NaHCO₃ solution. The organic solution was evaporated in vacuum to obtain a white solid. Water (100 ml) was added to it and the residue was extracted with ethyl acetate (3 x 100 ml). The organic layer was separated, dried over MgSO₄, concentrated under reduced pressure and purified on redisp silicagel column using ethyl acetate in hexane (0 – 100 %) to obtain colorless oil **51**.

6.2.1 Procedure for intermediate (52).

Toluenesulfonylchloride (2 Eq) was added to a chilled solution of respective alcohol **51** (1 Eq) and triethylamine (1.59 Eq) in DCM (20 ml). The reaction was stirred in ice at 0 °C for 1 hr followed by overnight stirring at room temperature. It was later quenched with ice water and the organic layer was washed successfully with 10 % HCL, saturated aqueous sodium bicarbonate and brine. The organic layer was dried over MgSO₄ and concentrated under reduced pressure to obtain a solid/oil which was purified by silicagel using hexane: ethylacetate (0 - 90 %) to obtain colorless solid.

6.2.2 Procedure for (2-oxo-oxazolidin-3-yl) acetic acid ethyl ester (54)

To a suspension of NaH (60 % dispersion in mineral oil, 1.2 Eq) in anhydrous THF (15 ml), was added a solution of 2-oxazolidinone **53** (1 Eq) in anhydrous THF (10 ml) (1 Eq) at 0 °C. After stirring the mixture at 0 °C for 1 hr, ethyl bromoacetate (1 Eq) was added. The resulting mixture was warmed to room temperature and stirred overnight. The mixture was cooled to 0 °C, quenched with ethanol and water, evaporated under reduced pressure to remove ethyl acetate. The crude mixture was later diluted with CH₂Cl₂, washed with brine, dried over MgSO₄, concentrated in vacuum. The crude product was purified on combiflash system with Redisep silica column using ethyl acetate (0 - 100 %) in hexane to obtain a colorless clear liquid **54**.

6.2.3 Procedure for 3-(2-hydroxyethyl)-oxazolidin-2-one (55)

To a solution of ethyl ester **54** (1 Eq) in absolute ethanol (10 ml) was added slowly NaBH₄ (1.5 Eq) at 0 °C. The reaction was then warmed to room temperature and stirred for 11 hrs. 3 ml of saturated solution of NH₄Cl was added. The solids were filtered off and the solvent was removed under reduced pressure. Purification was made on silica using methanol (0 - 2 %) in dichloromethane to obtain colorless clear liquid **55**.

6.2.4 General procedure for N-substituted-5-hydroxymethyl-2-oxazolidinones (56-63)

To a suspension of K₂CO₃ (1 Eq) in anhydrous methanol (30 ml) containing epibromohydrin (2 Eq) was added the respective amine (2 Eq) and the reaction was stirred overnight. The reaction mixture was later filtered and the organic solvent was stripped off under reduced pressure to obtain a liquid residue. It was chromatographed on silica gel using methanol (0 - 2 %) in dichloromethane to obtain the N3-substituted oxazolidinones.

6.2.5 Procedure for 2,5-Dichloro-2,5-dimethyl-hexane (65)

To 2,5-dimethyl-2,5-hexanediol **64** (1 Eq) was added conc. HCl (20 ml), and the contents were vigorously stirred for 6 hrs. Chloroform (CHCl₃, 30 ml) was added to the solution and the stirring was continued overnight. The two layers were separated. The aqueous layer was extracted with CHCl₃ (2 x 100 ml), the organic layers were combined, dried over MgSO₄ and concentrated under reduced pressure. The residue was purified on silica gel using ethyl acetate in hexane (0 – 10 %) to obtain **65**.

6.2.6 Procedure for 5,5,8,8-Tetramethyl-5,6,7,8-tetrahydro-naphthalen-2-ol (66)

To a solution of **65** (1 Eq) and phenol (1.2 Eq) in anhydrous dichloromethane (DCM, 30 ml) was added dry aluminum chloride (AlCl_3 , 1.5 Eq) in portions. The mixture was stirred at room temperature overnight. The reaction was quenched by dropwise addition of water, extracted with ethyl acetate (3 x 100 ml). The organic layer was dried over MgSO_4 , concentrated under reduced pressure, purified on silica gel using ethyl acetate in hexane (0 – 50 %) to obtain **66**.

6.2.7 Procedure for 1-(3-Hydroxy-5,5,8,8-tetramethyl-5,6,7,8-tetrahydronaphthalen-2-yl)-ethanone (67)

A solution of **66** in anhydrous DCM (30 ml) was added slowly to AlCl_3 (1 Eq). To this was added acetyl chloride (1.2 Eq) dropwise and the reaction was refluxed overnight. The reaction was quenched with slow addition of water and the aqueous phase was extracted with ethyl acetate (2 x 100 ml), dried over MgSO_4 , concentrated under reduced pressure and purified on silica gel using ethyl acetate in hexane (0 – 20 %) to afford **67**.

6.2.8 Procedure for 6,6,9,9-Tetramethyl-4-oxo-6,7,8,9-tetrahydro-4H-benzo[g]chromene-3-carbaldehyde (68)

To a solution of **67** (1 Eq) in anhydrous dimethyl formamide (DMF, 20 ml), freshly distilled phosphorous oxychloride (POCl_3 , 5 Eq) was added dropwise. The mixture was refluxed overnight. Solvent was removed under reduced pressure and ice cold water was added. The aqueous phase was extracted with DCM, dried over MgSO_4 , concentrated under reduced pressure and purified on silica gel using ethyl acetate in hexane (0 – 10 %) to obtain **68**.

6.2.9 General procedure for Hydroxymethylchromene-4-one (74-79).

To a chilled solution of 6-substituted-3-formyl chromones **68-73** (1 Eq) in anhydrous THF (20 ml) was added 9-BBN (0.5 M solution in THF, 1.1 Eq). The solution was stirred in ice for 6 hr, and warmed to room temperature and stirred for additional 6 hr. The reaction was quenched with saturated aqueous ammonium chloride solution and extracted with ethyl acetate, dried over magnesium sulfate, evaporated under reduced pressure to obtain a residual liquid. It was chromatographed on redisepp silica gel using ethyl acetate in hexane (0 - 100 %) to obtain **74-79**.

6.3.0 Procedure for methyl 4-oxo-4H-chromene-2-carboxylate (81).

10 ml of conc H_2SO_4 was added to a solution of the acid **80** (0.95 gm) in methanol (50 ml). The reaction mixture was refluxed for 12 hrs. After the reaction is cooled, the solvent is evaporated under reduced pressure. Water (100 ml) is added and the acid is neutralized with 200 ml of 10 % NaHCO_3 . The aqueous phase is extracted with ethyl acetate. The organic phase is dried over MgSO_4 , concentrated under reduced pressure to obtain **81** as white solid (0.88 gm).

6.3.1 Procedure for 2-(hydroxymethyl)-4H-chromen-4-one (82).

To a solution of the methyl ester **81** (1 Eq) in methanol 10 ml, was slowly added sodium borohydride (1.5 Eq). The reaction was stirred overnight. The solvent is removed under reduced pressure and water 20 ml is added. The aqueous phase is extracted with ethyl acetate (3 x 200 ml), dried over MgSO₄, concentrated and purified on combiflash normal phase system using hexane:ethyl acetate (5-100%) to obtain colorless white solid **82**.

6.3.2 General procedure for intermediates (84-100).

Methanesulfonylchloride (1.25 Eq) in DCM (10 ml) was added dropwise to a chilled solution of respective alcohols (1 Eq) and triethylamine (1.59 Eq) in DCM (20 ml). The reaction was stirred in ice at 0 °C for 1 hr followed by overnight stirring at room temperature. It was later quenched with ice water and the organic layer was washed successfully with 10 % HCL, saturated aqueous sodium bicarbonate and brine. The organic layer was dried over MgSO₄ and concentrated under reduced pressure to obtain a solid/oil which was used for the next step without further purification.

6.3.3 Procedure for 2-Piperidin-4-yl-1H-benzoimidazole (102)

In a 100 ml r.b.f was transferred 1,2-diaminobenzene **101** (1 Eq), isonipecotinic acid (1 Eq) and polyphosphoric acid (2 Eq). The contents were heated at 180 °C for 4 hrs. The reaction mixture after cooling was dissolved in ethyl acetate and loaded on small bed of silica gel column and eluted with ethyl acetate (100 %) to obtain pink color solid **102**.

6.3.4 Procedure for 1-Benzyl-4-*o*-tolyl-piperidin-4-ol (104)

A solution of 2-bromotoluene **103** (1 Eq) in THF (25 ml) was added dropwise to a solution of n-BuLi (1.08 Eq of 1.6 M) in hexane over a period of 30 mins at -78 °C. The mixture was stirred for 1 h at -78 °C, and a solution of 1-benzylpiperidone (1 Eq) in THF (20 ml) was added dropwise over a period of 30 mins. The reaction temperature was maintained at -78 °C. The resulting mixture was stirred at -78 °C overnight and later quenched with saturated solution of ammonium chloride (20 ml) was added. The reaction mixture was extracted with dichloromethane (3 x 120 mL). The combined organic extracts were washed with water, dried (MgSO₄), and filtered. The solvent was removed under reduced pressure to yield crude product which was purified by silicagel using hexane: ethyl acetate (0-90 %) and reversed phase using acetonitrile in water (5-90 %), solvent was stripped of using genevac to obtain colorless liquid **104**.

6.3.5 Procedure for 1-Benzyl-4-*o*-tolyl-1,2,3,6-tetrahydro-pyridine (105)

To a solution of 4-*o*-tolylpiperidin-4-ol **104** (1 Eq) in ethanol (15 ml) was added concentrated HCl (10 ml) and the mixture was heated at reflux temperature for 1 h. The reaction mixture was cooled and the solvent removed under reduced pressure and the crude residue was diluted with 20 ml of water, washed with sat. aq. NaHCO₃ and the aqueous phase was extracted with dichloromethane (2 x 50 ml), dried over MgSO₄ and concentrated to obtain a liquid crude product which was purified on silicagel using hexane: ethyl acetate (0-90 %) to obtain colorless liquid **105**.

6.3.6 Procedure for 4-*o*-Tolyl-piperidine (106)

To a solution of **105** (1Eq) in anhydrous ethanol (10 ml), was added 10 % Pd/C (5 mol%) and the mixture was hydrogenated at 50 psi for 24 hr. The mixture was then filtered and the filtrate was evaporated under reduced pressure to obtain light yellow liquid which was utilized without purification for coupling with the iodolactone (**39**).

6.3.7 Procedure for 1-(2-Isopropyl-phenyl)-4-(4-nitro-benzenesulfonyl)-piperazine (108)

The nosylprotected diethanolamine **107** (1 Eq), the representative aniline (1.2 Eq), DIPEA (4 Eq), and CH₃CN (3 mL) were mixed in a microwave reaction vial (10 mL) fitted with a vial cap. The mixture was reacted in the microwave for 1 h at 175 °C. After 1 hr, the solvent was removed under reduced pressure. The residue was dissolved in dichloromethane (DCM) and washed with HCl (10 %, 3 X 30 mL) and saturated NaHCO₃ (40 mL). The organic phase was dried over MgSO₄ and concentrated in vacuo to afford the crude product. This crude product was purified by silica gel using hexane: ethyl acetate (0 - 100 %) to obtain a yellow solid.

6.3.8 Procedure for 1-(2-Isopropyl-phenyl)-piperazine (109)

Potassiumcarbonate (12.01 Eq) was added to a mixture of acetonitrile and dimethyl sulfoxide (CH₃CN/DMSO = 49:1) and heated to 50 °C. Thiophenol (10.01 Eq) was added dropwise via syringe to the mixture with stirring. After 30 min, a solution of the nosyl-protected N-arylpiperazine **108** (1 Eq) in CH₃CN and DMSO (CH₃CN/DMSO = 49:1) was added dropwise. The reaction mixture was stirred for 3 hr, quenched with excess NaOH solution (40 %), and concentrated under reduced pressure. The residue was extracted with DCM (5 x 40 mL), and the organic phase was dried over MgSO₄ and concentrated in vacuo to give a crude oil. The oil was purified by reversed-phase chromatography (CH₃CN in H₂O, gradient from 5 % to 100% containing 0.1% formic acid) to afford the light yellow solid **109**.

6.3.9 General procedure for thermal based Suzuki reaction for intermediates 4-*o*-tolyl-3, 6-dihydro-2H-pyridine-1-carboxylic acid tert-butyl ester (113), 4-(2-isopropyl-phenyl)-3,6-dihydro-2H-pyridine-1-carboxylic acid tert-butyl ester (114) and tert-butyl 4-(2-benzylphenyl)-5,6-dihydropyridine-1(2H)-carboxylate (115)

To three separate nitrogen flashed flasks containing 3, 6-dihydro-2H-1-N-Boc-4-boronic acid pinacol ester (0.949 Eq), anhydrous K₂CO₃ (2.84 Eq) and PdCl₂(dppf) (6 mol %) was added a solution of 2-bromotoluene **110**, isocumene **111** and 2-benzyl bromobenzene **112** in DMF (15 ml). The mixture was heated at 80 °C overnight. The mixture was later passed thru a plug of celite and washed with ethyl acetate. The solvent (EtOAc) was evaporated under reduced pressure and the crude product was purified over C₁₈ combiflash system using acetonitrile (0 - 90 %) in water (containing 0.1 % formic acid). Solvent was removed using genevac to obtain boc-protected intermediates **113**, **114** and **115**.

6.4.0 General procedure for microwave promoted Suzuki reaction for tert-butyl 4-(2'-isopropylbiphenyl-4-yl)piperazine-1-carboxylate (119), tert-butyl 4-(5-(2-

isopropylphenyl)pyridin-2-yl)piperazine-1-carboxylate (120), tert-butyl 4-(5-(2-isopropylphenyl)pyrimidin-2-yl)piperazine-1-carboxylate (121), tert-butyl 4-(4-(2-isopropylphenyl)pyridin-2-yl)piperazine-1-carboxylate (125)

Isocumene **111** (1 Eq), corresponding boronic acid pinacol ester (1.25 Eq), potassium or sodium carbonate (2M, 2 Eq) and trans-dichlorobis(triphenyl phosphine) palladium (II) (10 mol %) were placed in a microwave vial (10 ml) with a magnetic stirrer. Tetrahydrofuran and water (1:1) were added as solvents and the vial was capped and subjected to microwave heating at 140 °C for 30 mins. At the end of 30 mins, the reaction mixtures were passed thru a plug of silica and washed with ethyl acetate and concentrated under reduced pressure. Intermediate **119** was purified on reverse phase chromatography using acetonitrile-water (5 - 95 %) containing 0.1 % formic acid. Intermediates **120**, **121** and **125** were taken to next step without purification.

6.4.1 General procedure for N-tertbutoxy carbonyl (t-boc) group deprotection for intermediates (116-118, 122-124, 126).

To the N-tertbutoxy carbonyl protected piperidines **113-115** and piperazines **119-121** and **125** (1 Eq) in anhydrous dichloromethane (30 ml), was added trifluoroacetic acid (50 Eq). The reaction mixture were stirred at 0 °C in ice for 2 hrs The acid was neutralized with saturated aqueous NaHCO₃ and the crude product was extracted in dichloromethane. The product was purified using acetonitrile (0 - 90 %) in water using C₁₈ combiflash system. Solvent was stripped off using genevac, the crystalline materials were redissolved in dichloromethane, washed with saturated bicarbonate solution. The organic layer was separated, dried over MgSO₄, concentrated under reduced pressure to obtain light yellow crystalline solids **116-118**, **122** and reddish viscous liquids **123**, **124** and **126**.

6.4.2 General procedure for compounds (127-144).

Iodomethyl lactone **39** (1 Eq) and the appropriate secondary amine (5 Eq) in anhydrous tetrahydrofuran (THF; 35 mL) was stirred at reflux under a nitrogen atmosphere for 48 hrs. The mixture was filtered (when appropriate), concentrated under reduced pressure and the residue was dissolved in dichloromethane and purified by flash silica gel chromatography using methanol (0 - 3%) in dichloromethane.

6.4.3 Procedure for compound (145).

To a solution of hydroxymethyl lactone **40** (1 Eq) in anhydrous dichloromethane (5 mL) was added 1-(4-isocyanatophenyl) piperidine (1 Eq) in dichloromethane (5 ml) with stirring. The reaction was stirred overnight, filtered, and the residue chromatographed on silica gel using methanol (0 - 1 %) in dichloromethane.

6.4.4 General procedure for compounds (146, 148, 151, 160).

The respective iodides **39**, **42**, **47** and **48** (1 Eq) and the diphenylmethylpiperazine (5 Eq)/ *o*-methylphenyl piperazine **116** and *o*-isopropylphenyl piperazine **117** in anhydrous THF (50 ml) was stirred at reflux under a nitrogen atmosphere for 48 hrs. The mixture was filtered (when appropriate), concentrated under reduced pressure and the residue was

dissolved in dichloromethane and purified by flash silica gel chromatography using methanol (0-3 %) in dichloromethane.

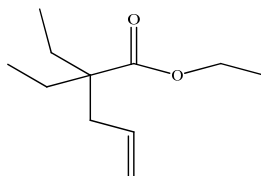
6.4.5 General procedure for compounds (147, 150).

The respective mesylates **55** and **84** (1 Eq) and the diphenylmethylpiperazine (5 Eq) in anhydrous THF (50 ml) were stirred at reflux under nitrogen atmosphere for 24 hrs. The mixture was cooled and concentrated under reduced pressure and the residue was dissolved in dichloromethane and purified by redisepp silica gel columns using dichloromethane-methanol gradient system or C₁₈ columns using acetonitrile - water (containing 0.1 % formic acid) when required.

6.4.6 General procedure for compounds (149, 151-159, 161-174).

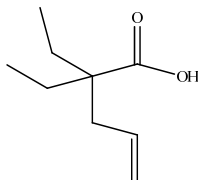
The respective tosylates **44**, **52**, mesylates **86-100** (1 Eq) and diphenylmethylpiperazine and other secondary amines **102**, **109**, **116-117**, **122-124** and **126** (2 Eq) in anhydrous THF (5ml) and triethyl amine (4 Eq) were stirred under microwave at 120 °C for 1 hr. After 1 hr, the solvent was stripped off, residue was dissolved in dichloromethane and purified by redisepp silica gel columns using dichloromethane-methanol gradient system or C₁₈ columns using acetonitrile-water (0.1 % formic acid) when required.

1. 2,2-Diethyl-pent-4-enoic acid ethyl ester (**37**)



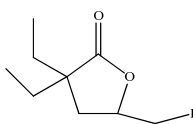
Colorless liquid. Yield: 41.22 %. ¹H - NMR {CDCl₃, 400 MHz, δ (ppm)} 0.77 - 0.83 (m, 6H), 1.22 (t, 3H), 1.11.51 - 1.60 (m, 4H), 2.10 - 2.15 (m, 2H), 4.11 - 4.16 (q, 4H), 5.01 - 5.08 (m, 2H), 5.62 - 5.72 (m, 1H).

2. 2,2-Diethyl-pent-4-enoic acid (**38**)



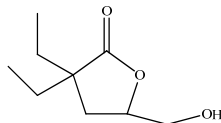
Light yellow liquid. Yield: 70.79 %. ¹H - NMR {CDCl₃, 400 MHz, δ (ppm)} 0.75 - 0.79 (m, 6H), 1.47 - 1.60 (m, 4H), 2.27 (d, 2H), 4.98 - 5.05 (m, 2H), 5.59 - 5.69 (m, 1H).

3. 3,3-Diethyl-5-iodomethyl-dihydro-furan-2-one (**39**)



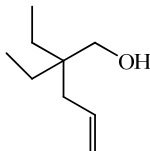
Light yellow liquid. Yield: 87 %. ^1H - NMR $\{\text{CDCl}_3, 400 \text{ MHz}, \delta \text{ (ppm)}\}$ 0.89 – 0.96 (m, 6H), 1.59 – 1.66 (m, 4H), 1.82 – 1.88 (m, 1H), 2.21 – 2.27 (m, 1H), 3.38 – 3.41 (m, 1H), 3.21 – 3.25 (m, 1H), 4.37 – 4.44 (m, 1H).

4. 3,3-Diethyl-5-hydroxymethyl-dihydro-furan-2-one (**40**)



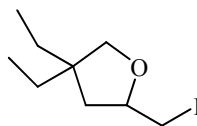
Light yellow liquid. Yield: 46.03 %. ^1H - NMR $\{\text{CDCl}_3, 400 \text{ MHz}, \delta \text{ (ppm)}\}$ 0.75 (t, 3H), 0.80 (t, 3H), 1.45 - 1.52 (m, 4H), 1.80 - 1.95 (m, 2H), 3.42 - 3.46 (dd, 1H, $J = 12.48 \text{ Hz}$), 3.70 - 3.74 (dd, 1H, $J = 12.48, 12.52 \text{ Hz}$), 4.32 - 4.36 (m, 1H).

5. 2,2-diethyl-pent-4-en-1-ol (**41**)



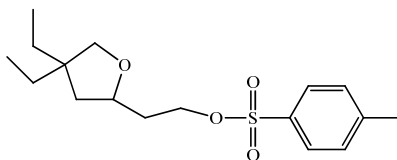
Clear colorless liquid. Yield: 56.18 %. ^1H - NMR $\{\text{CDCl}_3, 400 \text{ MHz}, \delta \text{ (ppm)}\}$ 0.82 (t, 6H), 1.22 - 1.32 (m, 4H), 1.58 (s, 1H), 2.01 (d, 2H), 3.38 (s, 2H), 5.03 - 5.15 (m, 2H), 5.79 - 5.89 (m, 1H).

6. 4,4-diethyl-2-iodomethyl-tetrahydrofuran (**42**)



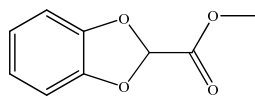
Pale yellow liquid. Yield: 90.37 %. ^1H - NMR $\{\text{CDCl}_3, 400 \text{ MHz}, \delta \text{ (ppm)}\}$ 0.84 (t, 6H), 1.34 - 1.52 (m, 5H), 1.92 - 1.98 (m, 1H), 3.18 - 3.27 (m, 2H), 3.57 - 3.65 (m, 2H), 4.02 - 4.09 (m, 1H), 7.13 - 7.19 (m, 2H), 7.23 - 7.27 (m, 4H), 7.41 - 7.43 (m, 4H).

7. Toluene-4-sulfonic acid 2-(4,4-diethyl-tetrahydro-furan-2-yl)-ethyl ester (**44**)



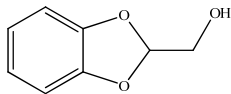
Colorless liquid. Yield: 42.9 %. ^1H - NMR $\{\text{CDCl}_3, 400 \text{ MHz}, \delta \text{ (ppm)}\}$ 7.77 – 7.79 (d, 2H), 7.32 – 7.34 (d, 2H), 4.14 (t, 2H), 3.85 – 3.95 (m, 1H), 3.47 – 3.49 (m, 1H), 3.37 – 3.39 (m, 1H), 2.44 (m, 3H), 1.83 – 1.88 (m, 1H), 1.73 – 1.78 (m, 1H), 1.29 – 1.41 (m, 4H), 1.17 – 1.23 (m, 1H), 0.78 – 0.83 (m, 6H). LC-MS (ESI) (m/z) 327.0 ($M + 1$)⁺.

8. Benzo[1,3]dioxole-2-carboxylic acid methyl ester (**50**)



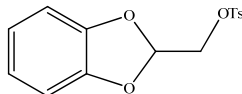
Colorless liquid. Yield: 28.47 %. ^1H - NMR $\{\text{CDCl}_3, 400 \text{ MHz}, \delta (\text{ppm})\}$ 3.86 (s, 3H), 6.32 (s, 1H), 6.87 – 6.89 (m, 4H). LC-MS (ESI) (m/z) 181.0 (M+1) $^+$.

9. Benzo[1,3]dioxol-2-yl-methanol (**51**)



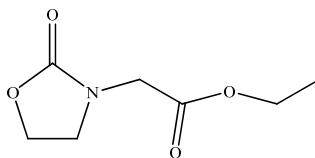
Colorless liquid. Yield: 99.71 %. ^1H - NMR $\{\text{CDCl}_3, 400 \text{ MHz}, \delta (\text{ppm})\}$ 6.79 – 6.81 (m, 4H), 6.17 (t, 1H), 3.90 – 3.92 (dd, $J = 6.84 \text{ Hz}$, 2H), 2.03 (t, 1H). LC-MS (ESI) (m/z) 153.1 (M+1) $^+$.

10. Toluene-4-sulfonic acid benzo[1,3]dioxol-2-ylmethyl ester (**52**)



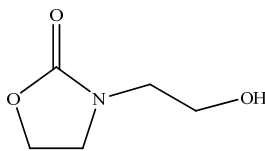
Colorless solid. Yield: 85.77 %. ^1H - NMR $\{\text{CDCl}_3, 400 \text{ MHz}, \delta (\text{ppm})\}$ 7.77 – 7.79 (d, 2H), 7.33 – 7.35 (d, 2H), 6.78 – 6.81 (m, 2H), 6.73 – 6.76 (m, 2H), 6.23 – 6.25 (t, 1H), 4.24 – 4.25 (d, 2H), 2.45 (s, 3H).

11. (2-Oxo-oxazolidin-3-yl) acetic acid ethyl ester (**54**)



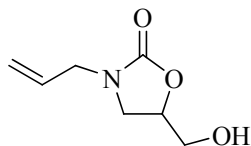
Clear colorless liquid. Yield: 26.7 %. ^1H - NMR $\{\text{CDCl}_3, 400 \text{ MHz}, \delta (\text{ppm})\}$ 1.29 (t, 3H), 3.69 - 3.76 (m, 2H), 4.03 (s, 3H), 4.21 (q, 2H), 4.37 - 4.43 (m, 2H).

12. 3-(2-hydroxyethyl)-oxazolidin-2-one (**55**)



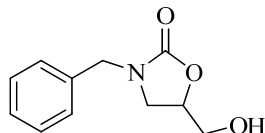
Clear colorless liquid. Yield: 23.9 %. ^1H - NMR $\{\text{CDCl}_3, 400 \text{ MHz}, \delta (\text{ppm})\}$ 3.14 (bs, 1H), 3.40 (t, 2H), 3.71 (t, 2H), 3.79 (t, 2H), 4.36 (t, 2H).

13. 3-allyl-5-hydroxymethyl-oxazolidin-2-one (**56**)



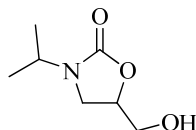
Light yellow solid. Yield: 20.44 %. ^1H - NMR $\{\text{CDCl}_3, 400 \text{ MHz}, \delta \text{ (ppm)}\}$ 2.94 (s, 1H), 3.42 - 3.46 (m, 1H), 3.54 (t, 1H), 3.62 - 3.66 (m, 1H), 3.85 - 3.91 (m, 3H), 4.59 - 4.62 (m, 1H), 5.23 - 5.30 (m, 2H), 5.72 - 5.82 (m, 1H).

14. 3-Benzyl-5-hydroxymethyl-oxazolidin-2-one (**57**)



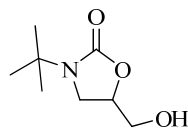
Colorless solid. Yield: 87.95 %. ^1H - NMR $\{\text{CDCl}_3, 400 \text{ MHz}, \delta \text{ (ppm)}\}$ 2.17 (t, 1H), 3.23 - 3.27 (m, 1H), 3.34 - 3.39 (m, 1H), 3.52 - 3.57 (m, 1H), 3.74 - 3.79 (m, 1H), 4.29 - 4.42 (m, 2H), 4.47 - 4.53 (m, 1H), 7.19 - 7.30 (m, 5H). LC - MS (ESI) (m/z) 208.1(M + 1) $^+$.

15. 5-Hydroxymethyl-3-isopropyl-oxazolidin-2-one (**58**)



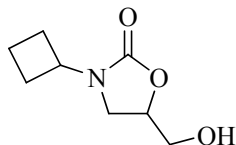
Colorless solid. Yield: 38.42 %. ^1H - NMR $\{\text{CDCl}_3, 400 \text{ MHz}, \delta \text{ (ppm)}\}$ 1.10 - 1.12 (m, 6H), 3.32 - 3.36 (m, 1H), 3.41 - 3.47 (m, 1H), 3.56 - 3.60 (m, 1H), 3.78 - 3.81 (m, 1H), 3.95 - 4.07 (septet, 1H), 4.49 - 4.54 (m, 1H).

16. 3-*t*-butyl-5-hydroxymethyl-oxazolidin-2-one (**59**)



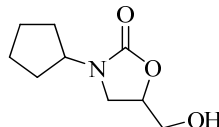
Clear colorless liquid. Yield: 20.34 %. ^1H - NMR $\{\text{CDCl}_3, 400 \text{ MHz}, \delta \text{ (ppm)}\}$ 1.39 (s, 9H), 2.46 (t, 1H), 3.48 - 3.53 (m, 1H), 3.60 - 3.66 (m, 2H), 3.82 - 3.87 (m, 2H), 4.45 - 4.49 (m, 1H).

17. 3-cyclobutyl-5-hydroxymethyl-oxazolidin-2-one (**60**)



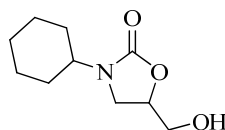
Clear colorless liquid. Yield: 24.8 %. ^1H - NMR $\{\text{CDCl}_3, 400 \text{ MHz}, \delta (\text{ppm})\}$ 1.64 - 1.72 (m, 2H), 2.12 - 2.19 (m, 4H), 2.79 (t, 1H), 3.50 - 3.54 (dd, 8.4 Hz, 2H), 3.61 - 3.69 (m, 2H), 3.84 - 3.89 (m, 1H), 4.32 - 4.40 (pentet, 1H), 4.56 - 4.62 (m, 1H).

18. 3-cyclopentyl-5-hydroxymethyl-oxazolidin-2-one (**61**)



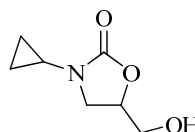
Clear colorless liquid. Yield: 21.43 %. ^1H - NMR $\{\text{CDCl}_3, 400 \text{ MHz}, \delta (\text{ppm})\}$ 0.92 (d, 6H), 1.84-1.95 (septet, 1H), 3.05 (d, 2H), 3.14 (t, 1H), 3.47 - 3.49 (m, 1H), 3.57 (t, 1H), 3.61 - 3.67 (m, 1H), 3.85 - 3.90 (m, 1H), 4.57 - 4.62 (m, 1H).

19. 3-cyclohexyl-5-hydroxymethyl-oxazolidin-2-one (**62**)



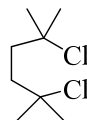
Colorless solid. Yield: 11.28 %. ^1H - NMR $\{\text{CDCl}_3, 400 \text{ MHz}, \delta (\text{ppm})\}$ 0.89 - 1.01 (m, 1H), 1.11 - 1.30 (m, 4H), 1.44 - 1.68 (m, 5H), 3.20 - 3.24 (m, 1H), 3.32 - 3.43 (m, 3H), 3.50 - 3.54 (m, 1H), 4.33 - 4.39 (m, 1H).

20. 3-cyclopropyl-5-hydroxymethyl-oxazolidin-2-one (**63**)



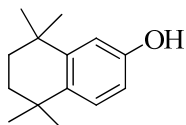
Clear colorless liquid. Yield: 29.5 %. ^1H - NMR $\{\text{CDCl}_3, 400 \text{ MHz}, \delta (\text{ppm})\}$ 0.69-0.84 (m, 4H), 2.51 - 2.57 (m, 1H), 2.71 (t, 1H), 3.44 - 3.48 (dd, 8.6 Hz, 1H), 3.55 (t, 1H), 3.61 - 3.66 (m, 1H), 3.83 - 3.88 (m, 1H), 4.51 - 4.55 (m, 1H).

21. 2,5-Dichloro-2,5-dimethyl-hexane (**65**)



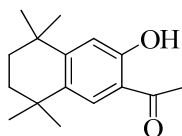
Pink color solid. Yield 50.43 %. ^1H - NMR $\{\text{CDCl}_3, 400 \text{ MHz}, \delta (\text{ppm})\}$ 1.88 (s, 4H), 1.53 (s, 12H).

22. 5,5,8,8-Tetramethyl-5,6,7,8-tetrahydro-naphthalen-2-ol (**66**)



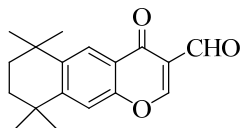
Light yellow solid. Yield 62.8 %. ^1H - NMR (CDCl_3 , 400 MHz, δ (ppm)) 7.09 (d, J = 8.52, 1H), 6.68 (d, J = 2.76 Hz, 1H), 6.54 (dd, 8.52 Hz, 1H), 4.49 (s, 1H), 1.58 (m, 4H), 1.17 (d, 3.6 Hz, 12H). LC-MS (ESI) (m/z) 205.1 ($M + 1$) $^+$.

23. 1-(3-Hydroxy-5,5,8,8-tetramethyl-5,6,7,8-tetrahydro-naphthalen-2-yl)-ethanone (**67**)



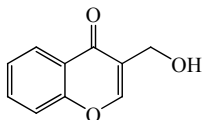
Light yellow solid. Yield 55.6 %. ^1H - NMR (CDCl_3 , 400 MHz, δ (ppm)) 7.57 (s, 1H), 6.82 (s, 1H), 2.53 (s, 3H), 1.61 (m, 4H), 1.20 (d, 6.88 Hz, 12H). LC-MS (ESI) (m/z) 247.1 ($M + 1$) $^+$.

24. 6,6,9,9-Tetramethyl-4-oxo-6,7,8,9-tetrahydro-4H-benzo[g]chromene-3-carbaldehyde (**68**)



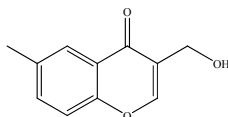
Light yellow solid. Yield 51 %. ^1H - NMR (CDCl_3 , 400 MHz, δ (ppm)) 10.39 (s, 1H), 8.50 (s, 1H), 8.22 (s, 1H), 7.44 (s, 1H), 1.76 (m, 4H), 1.35 (d, J = 6.84 Hz, 12 H); LC-MS (ESI) (m/z) 285.1 ($M + 1$) $^+$.

25. 3-Hydroxymethyl-chromen-4-one (**74**)



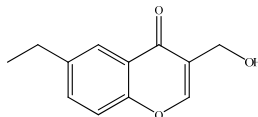
Cream colored solid. Yield 55 %. ^1H - NMR (CD_3OD , 400 MHz, δ (ppm)) 4.55 (s, 2H), 7.47-7.51 (m, 1H), 7.58 - 7.61 (m, 1H), 7.77 - 7.81 (m, 1H), 8.16 - 8.18 (m, 1H), 8.21 - 8.22 (m, 1H); LC - MS (ESI) (m/z) 177.1 ($M + 1$) $^+$.

26. 3-(hydroxymethyl)-6-methyl-4H-chromen-4-one (**75**)



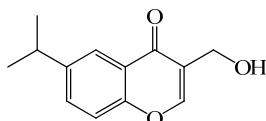
Yellow colored solid.: Yield: 37.0 %. ^1H - NMR $\{\text{CDCl}_3, 400 \text{ MHz}, \delta (\text{ppm})\}$ 2.46 (s, 3H), 3.03 (t, 1H), 4.57 (d, 2H), 7.36-7.38 (m, 1H), 7.48-7.51 (m, 1H), 7.92 (s, 1H), 8.00 (s, 1H). LC-MS (ESI) (m/z) 191.0 ($\text{M} + 1$) $^+$.

27. 6-ethyl-3-(hydroxymethyl)-4H-chromen-4-one (**76**)



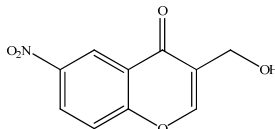
Yellow colored solid.: Yield: 49.73 %. ^1H - NMR $\{\text{CDCl}_3, 400 \text{ MHz}, \delta (\text{ppm})\}$ 1.28 (t, 3H), 2.73-2.79 (q, 2H), 3.15 (t, 1H), 4.58 (d, 2H), 7.38-7.40 (m, 1H), 7.51-7.54 (m, 1H), 7.93 (s, 1H), 8.02 (d, 1H). LC-MS (ESI) (m/z) 205.1 ($\text{M} + 1$) $^+$.

28. 3-Hydroxymethyl-6-isopropyl-chromen-4-one (**77**)



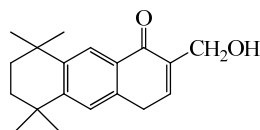
Yellow colored solid. Yield 39.10 %. ^1H - NMR $\{\text{CDCl}_3, 400 \text{ MHz}, \delta (\text{ppm})\}$ 1.30 (d, 6H), 2.98 - 3.10 (sep, 1H), 3.17 (bs 1H), 4.58 (s, 2H), 7.39 - 7.41 (m, 1H), 7.55 - 7.57 (m, 1H), 7.93 (s, 1H), 8.05 (d, 1H); LC-MS (ESI) (m/z) 219.1 ($\text{M} + 1$) $^+$.

29. 3-(hydroxymethyl)-6-nitro-4H-chromen-4-one (**78**)



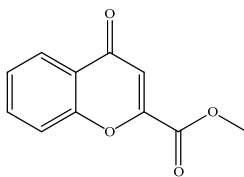
Yellow colored solid.: Yield: 19.30 %. ^1H - NMR $\{\text{CDCl}_3, 400 \text{ MHz}, \delta (\text{ppm})\}$ 2.64 (t, 1H), 4.63 (d, 2H), 7.64 (d, 1H), 8.02 (m, 1H), 8.51-8.54 (dd, $J = 9.2, 9.16 \text{ Hz}$, 1H), 9.10 (d, 1H). LC-MS (ESI) (m/z) 222.0 ($\text{M} + 1$) $^+$.

30. 3-Hydroxymethyl-6,6,9,9-tetramethyl-6,7,8,9-tetrahydro-benzo[g]chromen-4-one (**79**)



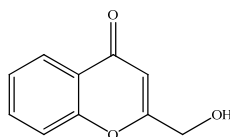
Yellow colored solid. Yield: 39.49 %. ^1H - NMR $\{\text{CDCl}_3, 400 \text{ MHz}, \delta (\text{ppm})\}$ 8.15 (s, 1H), 7.87 (s, 1H), 7.38 (s, 1H), 4.55 (d, 1H), 1.75 (m, 4H), 1.27 (d, 12H). LC-MS (ESI) (m/z) 286.1 ($\text{M} + 1$) $^+$.

31. Methyl 4-oxo-4H-chromene-2-carboxylate (**81**)



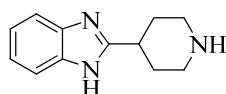
Creamish white colored solid. Yield: 86.55 %. ^1H - NMR {MeOD₄, 400 MHz, δ (ppm)} 3.90 (s, 3H), 6.93 (s, 1H), 7.40-7.44 (m, 1H), 7.56-7.58 (m, 1H), 7.71-7.77 (m, 1H), 8.01-8.04 (dd, J = 1.44, 8.84 Hz, 1H). LC-MS (ESI) (m/z) 205.1 ($M + 1$)⁺.

32. 2-(hydroxymethyl)-4H-chromen-4-one (**82**)



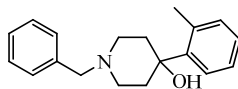
Creamish white colored solid.: Yield: 45.42 %. ^1H - NMR {MeOD₄, 400 MHz, δ (ppm)} 3.32-3.33 (m, 1H), 4.56 (d, 2H), 6.49 (s, 1H), 7.45-7.50 (m, 1H), 7.57-7.59 (m, 1H), 7.77 (7.84 (m, 1H), 8.12-8.14 (dd, J = 1.56, 7.98 Hz, 1H). LC-MS (ESI) (m/z) 177.1 ($M + 1$)⁺.

33. 2-Piperidin-4-yl-1H-benzoimidazole (**102**)



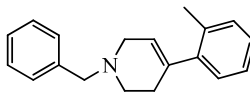
Pink colored solid. Yield: 21.76 %. ^1H - NMR: {CDCl₃, 400 MHz, δ (ppm)} 1.79 - 1.91 (m, 2H), 2.05 - 2.09 (m, 2H), 2.73 - 2.80 (m, 2H), 3.03 - 3.10 (m, 1H), 3.14 - 3.19 (m, 2H), 7.18 - 7.22 (m, 2H), 7.49 - 7.54 (m, 2H). LC-MS (ESI) (m/z) 202.1 ($M + 1$)⁺.

34. 1-Benzyl-4-*O*-tolyl-piperidin-4-ol (**104**)



Colorless solid. Yield: 49.02 %. ^1H - NMR {CDCl₃, 400 MHz, δ (ppm)} 2.03 - 2.06 (m, 2H), 2.45 - 2.53 (m, 2H), 2.55 (s, 3H), 3.12 - 3.19 (m, 2H), 3.30 - 3.33 (m, 2H), 4.10 (s, 2H), 7.11 - 7.19 (m, 3H), 7.28 - 7.31 (m, 1H), 7.36 - 7.40 (m, 5H). LC-MS (ESI) (m/z) 282.2 ($M + 1$)⁺.

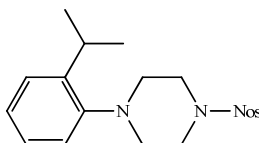
35. 1-Benzyl-4-*O*-tolyl-1,2,3,6-tetrahydro-pyridine (**105**)



Colorless solid. Yield: 54.99 %. ^1H - NMR {CDCl₃, 400 MHz, δ (ppm)} 2.30 (s, 3H), 2.53 - 2.57 (m, 2H), 3.10 (t, 2H), 3.48 - 3.50 (m, 2H), 4.06 (s, 2H), 5.51 - 5.53 (m, 1H),

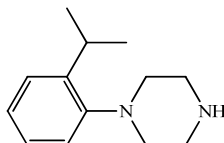
7.05 - 7.07 (m, 2H), 7.12 - 7.22 (m, 3H), 7.36 - 7.48 (m, 5H). LC-MS (ESI) (m/z) 264.2 (M + 1)⁺

36. 4-Nitro-benzenesulfonic acid 4-(2-isopropyl-phenyl)-piperazin-1-yl ester (**108**)



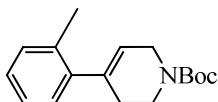
Yellow solid. Yield: 87.0 %. ¹H - NMR {CDCl₃, 400 MHz, δ (ppm)} 8.32 - 8.38 (m, 2H), 7.91 - 7.94 (m, 2H), 7.16 - 7.18 (m, 1H), 6.99 - 7.11 (m, 3H), 3.17 - 3.27 (m, 1H), 2.88 - 2.91 (m, 4H), 1.04 (d, 6H). LC - MS (ESI) (m/z) 390.1 (M + 1)⁺.

37. 1-(2-Isopropyl-phenyl)-piperazine (**109**)



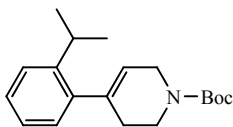
Pale yellow solid. Yield: 59.17 %. ¹H - NMR {CDCl₃, 400 MHz, δ (ppm)} 7.17 - 7.21 (m, 1H), 7.05 - 7.12 (m, 3H), 6.56 (s, 1H), 3.27 - 3.36 (m, 5H), 3.11 (m, 4H), 1.12 (d, 6H). LC - MS (ESI) (m/z) 205.1 (M + 1)⁺.

38. 4-*o*-Tolyl-3, 6-dihydro-2H-pyridine-1-carboxylic acid tert-butyl ester (**113**)



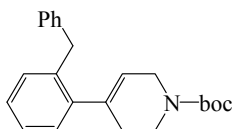
Brown color solid. Yield: 84.2 %. ¹H - NMR {CDCl₃, 400 MHz, δ (ppm)} 1.50 (s, 9H), 2.26 (s, 3H), 2.32 (bs, 2H), 3.59 (t, 2H), 4.02 (bs, 2H), 5.52 (bs, 1H), 7.04 - 7.07 (m, 1H), 7.10 - 7.15 (3H). LC-MS (ESI) (m/z) 218.0 (M + 1)⁺.

39. 4-(2-Isopropyl-phenyl)-3,6-dihydro-2H-pyridine-1-carboxylic acid tert-butyl ester (**114**)



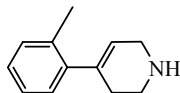
Brown color solid. Yield: 84.1 %. ¹H - NMR {CDCl₃, 400 MHz, δ (ppm)} 1.20 (d, 6H), 1.54 (s, 9H), 2.32 (bs, 2H), 2.99 - 3.09 (m, 1H), 3.62 (t, 2H), 4.02 (bs, 2H), 5.51 (bs, 1H), 7.01 - 7.03 (m, 1H), 7.11 - 7.15 (m, 1H), 7.22 - 7.30 (m, 2H). LC - MS (ESI) (m/z) 246.1 (M + 1)⁺.

40. tert-butyl 4-(2-benzylphenyl)-5,6-dihydropyridine-1(2H)-carboxylate (**115**)



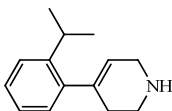
Brown colored solid.: Yield: 56.58 %. ^1H - NMR $\{\text{CDCl}_3, 400 \text{ MHz}, \delta \text{ (ppm)}\}$ 1.45 (s, 9H), 2.17 (m, 2H), 3.49 (m, 2H), 3.95-3.98 (m, 4H), 5.45 (s, 1H), 7.06-7.10 (m, 3H), 7.14-7.26 (m, 6H). LC-MS (ESI) (m/z) $(\text{M} + 1)^+$.

41. 4-*o*-Tolyl-1,2,3,6-tetrahydropyridine (**116**)



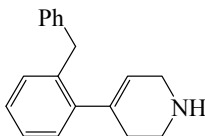
Light yellow solid. Yield: 95.3 %. ^1H - NMR $\{\text{CDCl}_3, 400 \text{ MHz}, \delta \text{ (ppm)}\}$ 2.28 (s, 3H), 2.61 - 2.62 (m, 2H), 3.41 (t, 2H), 3.81 (bs, 2H), 5.58 (bs, 1H), 7.06 - 7.08 (m, 1H), 7.14 - 7.23 (m, 3H). LC - MS (ESI) (m/z) 174.1 $(\text{M} + 1)^+$.

42. 4-(2-Isopropyl-phenyl)-1,2,3,6-tetrahydropyridine (**117**)



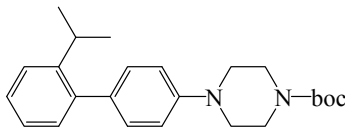
Light yellow solid. Yield: 98.30 %. ^1H - NMR $\{\text{CDCl}_3, 400 \text{ MHz}, \delta \text{ (ppm)}\}$ 1.22 (d, 6H), 2.55-2.58 (m, 2H), 3.03 - 3.17 (m, 1H), 3.45 (t, 2H), 3.80-3.82 (m, 2H), 5.55-5.65 (m, 1H), 7.04 - 7.06 (m, 1H), 7.12 - 7.16 (m, 1H), 7.25 - 7.34 (m, 2H). LC-MS (ESI) (m/z) 202.1 $(\text{M} + \text{H})^+$.

43. 4-(2-benzylphenyl)-1,2,3,6-tetrahydropyridine (**118**)



Pale yellow colored solid.: Yield: 43.92 %. ^1H - NMR $\{\text{CDCl}_3, 400 \text{ MHz}, \delta \text{ (ppm)}\}$ 2.35 (m, 2H), 3.14-3.17 (t, 2H), 3.65-3.66 (m, 2H), 3.98 (s, 2H), 5.42 (s, 1H), 7.04-7.10 (m, 3H), 7.14-7.17 (m, 1H), 7.20-7.29 (m, 6H). LC-MS (ESI) (m/z) 250.1 $(\text{M} + 1)^+$.

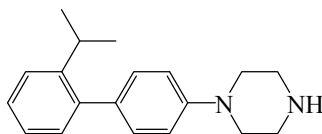
44. tert-butyl 4-(2'-isopropylbiphenyl-4-yl)piperazine-1-carboxylate (**119**)



Brown colored solid.: Yield: 69.75 %. ^1H - NMR $\{\text{CDCl}_3, 400 \text{ MHz}, \delta \text{ (ppm)}\}$ 1.15 (d, 6H), 1.49 (s, 9H), 3.04-3.14 (m, 1H), 3.18-3.20 (m, 4H), 3.60 (t, 4H), 6.94-6.99 (m, 2H),

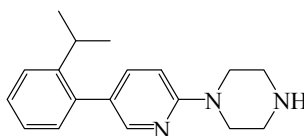
7.15-7.22 (m, 4H), 7.29-7.33 (m, 1H), 7.37-7.38 (m, 1H). LC-MS (ESI) (m/z) 381.2 (M + 1)⁺.

45. 1-(2'-isopropylbiphenyl-4-yl)piperazine (**122**)



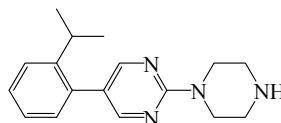
Pale yellow colored solid.: Yield: 73.91 %. ¹H - NMR {CDCl₃, 400 MHz, δ (ppm)} 1.15 (d, 6H), 3.06-3.16 (m, 5H), 3.20-3.23 (m, 4H), 6.94-6.99 (m, 2H), 7.15-7.23 (m, 4H), 7.29-7.33 (m, 1H), 7.35-7.37 (m, 1H). LC-MS (ESI) (m/z) 281.1 (M + 1)⁺.

46. 1-(5-(2-isopropylphenyl)pyridin-2-yl)piperazine (**123**)



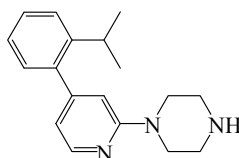
Reddish viscous liquid.: Yield: 26.99 %. ¹H - NMR {CDCl₃, 400 MHz, δ (ppm)} 1.17 (d, 6H), 1.83 (s, 1H), 3.01-3.14 (m, 5H), 3.58 (t, 4H), 6.70 (d, 1H), 7.13-7.16 (m, 1H), 7.19-7.24 (td, *J* = 2, 5.04 Hz, 1H), 7.40- (m, 2H), 7.43-7.46 (dd, *J* = 2.48, 8.6 Hz, 1H), 8.14-8.16 (m, 1H). LC-MS (ESI) (m/z) (M + 1)⁺.

47. 5-(2-isopropylphenyl)-2-(piperazin-1-yl)pyrimidine (**124**)



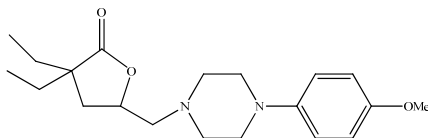
Brownish semi-solid.: Yield: 30.53 %. ¹H - NMR {CDCl₃, 400 MHz, δ (ppm)} 1.10 (d, 6H), 1.72 (s, 1H), 2.90 (t, 4H), 2.94-3.03 (m, 1H), 3.77 (t, 4H), 7.04-7.06 (dd, *J* = 1.12, 7.52 Hz, 1H), 7.14-7.18 (td, *J* = 2.12, 9.4 Hz, 1H), 7.26-7.34 (m, 2H), 8.21 (s, 2H). LC-MS (ESI) (m/z) (M + 1)⁺.

48. 1-(4-(2-isopropylphenyl)pyridin-2-yl)piperazine (**126**)



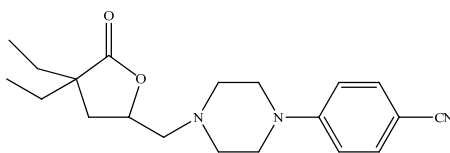
Brownish semi-solid.: Yield: 33.93 %. ¹H - NMR {CDCl₃, 400 MHz, δ (ppm)} 1.17 (d, 6H), 1.76 (s, 1H), 2.99-3.09 (m, 5H), 3.53-3.56 (m, 4H), 7.13-7.15 (m, 1H), 7.20-7.24 (m, 1H), 7.34-7.40 (m, 2H), 8.21 (d, 1H). LC-MS (ESI) (m/z) (M + 1)⁺.

49. 3,3-diethyl-4,5-dihydro-5-(4-[4-methoxyphenyl]piperazinylmethyl)-2(3H)-furanone (**127**)



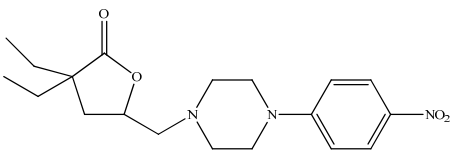
Pale yellow solid. Yield: 31.33 %. ^1H NMR: $\{\text{CDCl}_3, 400 \text{ MHz}, \delta (\text{ppm})\}$ 0.88 - 0.96 (m, 6H), 1.59 - 1.65 (m, 4H), 1.88 - 1.94 (m, 1H), 2.04 - 2.09 (m, 1H), 2.57 - 2.79 (m, 6H), 3.06 - 3.09 (m, 4H), 3.74 (s, 3H), 4.56 - 4.60 (m, 1H), 6.81 - 6.89 (m, 4H). Elemental analysis: calcd. for $\text{C}_{20}\text{H}_{30}\text{N}_2\text{O}_3$: C, 69.33; H, 8.73; N, 8.09; Found: C, 69.11; H, 8.81; N, 8.01 %.

50. 3,3-diethyl-4,5-dihydro-5-(4-[4-cyanophenyl]piperazinylmethyl)-2(3H)-furanone (**128**)



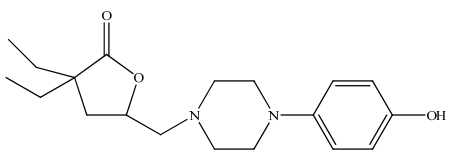
Pale yellow liquid. Yield: 15.78 %. ^1H - NMR $\{\text{CDCl}_3, 400 \text{ MHz}, \delta (\text{ppm})\}$ 0.80-0.90 (m, 6H), 1.53-1.61 (m, 4H), 1.83-1.88 (m, 1H), 1.99-2.04 (m, 1H), 2.49-2.71 (m, 6H), 3.24-3.26 (m, 4H), 4.49-4.55 (m, 1H), 6.76-6.80 (d, 2H), 7.41-7.44 (d, 2H). Elemental analysis: calcd. for $\text{C}_{20}\text{H}_{27}\text{N}_3\text{O}_2$: C, 70.35; H, 7.97; N, 12.31; Found: C, 70.07; H, 8.03; N, 12.11 %.

51. 3,3-diethyl-4,5-dihydro-5-(4-[4-nitrophenyl]piperazinylmethyl)-2(3H)-furanone (**129**)



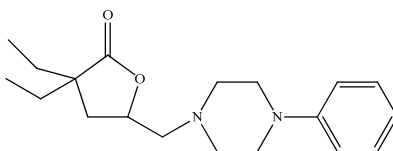
Pale yellow liquid. Yield: 25.97 %. ^1H - NMR $\{\text{CDCl}_3, 400 \text{ MHz}, \delta (\text{ppm})\}$ 0.87-0.97 (m, 6H), 1.59-1.66 (m, 4H), 1.89-1.94 (m, 1H), 2.05-2.10 (m, 1H), 2.56-2.78 (m, 6H), 3.37-3.42 (m, 4H), 4.55-4.61 (m, 1H), 6.77-6.82 (d, 2H), 8.07-8.12 (d, 2H). LC-MS (ESI) (m/z) 362.3 ($\text{M}+1$) $^+$.

52. 3,3-diethyl-4,5-dihydro-5-(4-[4-hydroxyphenyl]piperazinylmethyl)-2(3H)-furanone (**130**)



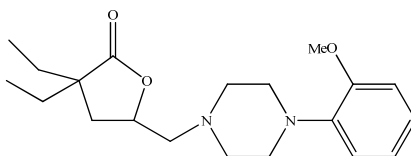
Pale yellow solid. Yield: 7.79 %. ^1H - NMR $\{\text{CDCl}_3, 400 \text{ MHz}, \delta (\text{ppm})\}$ 0.85-0.92 (m, 6H), 1.55-1.62 (m, 4H), 1.82-1.88 (m, 1H), 2.01-2.06 (m, 1H), 2.54-2.81 (m, 6H), 3.02-3.05 (m, 4H), 4.55-4.62 (m, 1H), 6.71 (d, 2H), 6.78 (d, 2H). LC-MS (ESI) (m/z) 333.0 ($\text{M}+1$) $^+$.

53. 3,3-diethyl-4,5-dihydro-5-(4-[4-phenyl]piperazinylmethyl)-2(3H)-furanone (**131**)



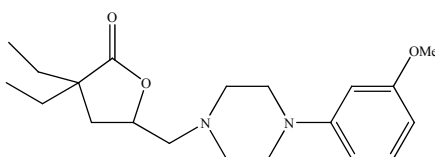
Pale yellow solid. Yield: 22.02 %. ^1H - NMR $\{\text{CDCl}_3, 400 \text{ MHz}, \delta (\text{ppm})\}$ 0.89-0.98 (m, 6H), 1.60-1.66 (m, 4H), 1.90-1.96 (m, 1H), 2.06-2.11 (m, 1H), 2.58-2.80 (m, 6H), 3.14-3.21 (m, 4H), 4.57-4.63 (m, 1H), 6.85 (t, 1H), 6.92 (d, 2H), 7.26 (t, 2H). Elemental analysis: calcd. for: $\text{C}_{19}\text{H}_{28}\text{N}_2\text{O}_2$: C, 72.12; H, 8.92; N, 8.85; Found: C, 72.40; H, 9.13; N, 8.65 %.

54. 3,3-diethyl-4,5-dihydro-5-(4-[2-methoxyphenyl]piperazinylmethyl)-2(3H)-furanone (**132**)



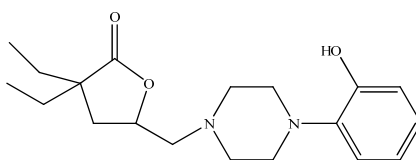
Pale yellow liquid. Yield: 17.04 %. ^1H - NMR $\{\text{CDCl}_3, 400 \text{ MHz}, \delta (\text{ppm})\}$ 0.89-0.97 (m, 6H), 1.60-1.65 (m, 4H), 1.88-1.91 (m, 1H), 2.05-2.10 (m, 1H), 2.60-2.81 (m, 6H), 3.08 (m, 4H), 3.85 (s, 3H), 4.58-4.62 (m, 1H), 6.84-7.01 (m, 4H). LC-MS (ESI) (m/z) 347.3 (M+H) $^+$. HPLC analysis: > 95 % purity using two different mobile phases.

55. 3,3-diethyl-4,5-dihydro-5-(4-[3-methoxyphenyl]piperazinylmethyl)-2(3H)-furanone (**133**)



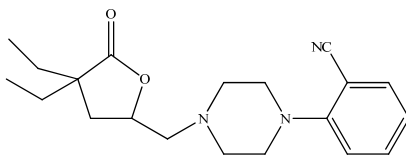
Pale yellow liquid. Yield: 40.54 %. ^1H - NMR $\{\text{CDCl}_3, 400 \text{ MHz}, \delta (\text{ppm})\}$ 0.87 - 0.96 (m, 6H), 1.58 - 1.64 (m, 4H), 1.88 - 1.93 (m, 1H), 2.03 - 2.08 (m, 1H), 2.55 - 2.76 (m, 6H), 3.12 - 3.18 (m, 4H), 3.76 (s, 3H), 4.56 - 4.59 (m, 1H), 6.38 - 6.53 (m, 3H), 7.12 - 7.16 (t, 1H). LC-MS (ESI) (m/z) 347.3 (M+1) $^+$.

56. 3,3-diethyl-4,5-dihydro-5-(4-[2-hydroxyphenyl]piperazinylmethyl)-2(3H)-furanone (**134**)



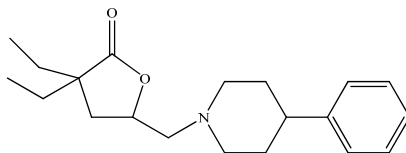
Pale yellow liquid. Yield: 18.38 %. ^1H - NMR $\{\text{CDCl}_3, 400 \text{ MHz}, \delta (\text{ppm})\}$ 0.89 - 0.97 (m, 6H), 1.62 - 1.67 (m, 4H), 1.88 - 1.94 (m, 1H), 2.07 - 2.12 (m, 1H), 2.60 - 2.78 (m, 6H), 2.88 - 2.90 (m, 4H), 4.57 - 4.64 (m, 1H), 6.83 - 6.88 (m, 1H), 6.93 - 6.95 (m, 1H), 7.05 - 7.09 (m, 1H), 7.14 - 7.17 (m, 1H). LC-MS (ESI) (m/z) 333.3 (M+1)⁺. HPLC analysis: > 95 % purity using two different mobile phases.

57. 3,3-diethyl-4,5-dihydro-5-(4-[2-cyanophenyl]piperazinylmethyl)-2(3H)-furanone (**135**)



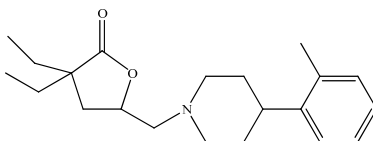
Pale yellow liquid. Yield: 15.80 %. ^1H - NMR $\{\text{CDCl}_3, 400 \text{ MHz}, \delta (\text{ppm})\}$ 0.85-0.93 (m, 6H), 1.55-1.61 (m, 4H), 1.84-1.90 (m, 1H), 2.01-2.06 (m, 1H), 2.57-2.80 (m, 6H), 3.14-3.21 (m, 4H), 4.52-4.57 (m, 1H), 6.93-6.97 (m, 2H), 7.41-7.45 (m, 1H), 7.49 (dd, 8Hz and 4Hz, 1H). LC-MS (ESI) (m/z) 342.2 (M+1)⁺. HPLC analysis: > 95 % purity using two different mobile phases.

58. 3,3-diethyl-4,5-dihydro-5-(4-[4-phenyl]piperidinylmethyl)-2(3H)-furanone (**136**)



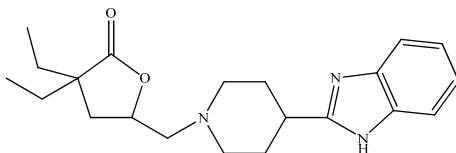
Pale yellow liquid. Yield: 23.74 %. ^1H - NMR $\{\text{CDCl}_3, 400 \text{ MHz}, \delta (\text{ppm})\}$ 0.93-1.01 (m, 6H), 1.63-1.69 (m, 4H), 1.81-1.95 (m, 5H), 2.09-2.14 (m, 1H), 2.23-2.29 (m, 2H), 2.51 (m, 1H), 2.64-2.67 (m, 2H), 3.05 (d, 11.2Hz, 1H), 3.19 (d, 12.4Hz, 1H), 4.62-4.63 (m, 1H), 7.22-7.34 (m, 5H). LC-MS (ESI) (m/z) 316.3 (M+H)⁺. HPLC analysis: > 95 % purity using two different mobile phases.

59. 3,3-diethyl-5-(4-*O*-tolyl-piperazin-1-ylmethyl)-dihydro-furan-2-one (**137**)



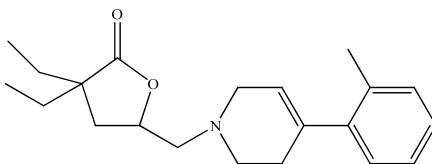
Pale yellow liquid. Yield: 15.9 % ^1H - NMR $\{\text{CDCl}_3, 400 \text{ MHz}, \delta (\text{ppm})\}$ 0.90-0.94 (t, 3H), 0.96-1.0 (t, 3H), 1.58-1.73 (m, 4H), 1.81-1.94 (m, 3H), 2.24-2.31 (m, 1H), 2.35 (s, 3H), 2.66-2.91 (m, 4H), 3.38 (d, 1H), 3.49 (s, 1H), 3.71 (s, 1H), 4.85-4.92 (m, 1H), 7.12-7.37 (m, 4H). LC-MS (ESI) (m/z) 330.3 (M+1)⁺. HPLC analysis: > 95 % purity using two different mobile phases.

60. 3,3-diethyl-4,5-dihydro-5-(2-[4-piperidinyl]benzimidazolylmethyl)-2(3H)-furanone (**138**)



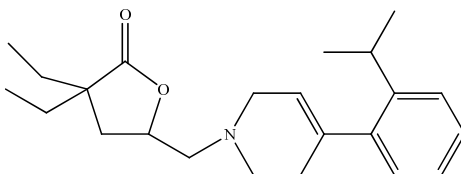
Pale yellow solid. Yield: 10.15 %. ^1H - NMR $\{\text{CDCl}_3, 400 \text{ MHz}, \delta (\text{ppm})\}$ 0.85-0.96 (m, 6H), 1.57-1.65 (m, 4H), 1.86-2.28 (m, 9H), 2.51-2.64 (m, 2H), 2.88-3.09 (m, 3H), 4.52-4.58 (m, 1H), 7.15-7.25 (m, 2H), 7.51-7.54 (m, 2H). LC-MS (ESI) (m/z) 356.0 ($\text{M}+1$) $^+$. HPLC analysis: > 95 % purity using two different mobile phases.

61. 3,3-diethyl-5-(4-(4-tolyl-3,6-dihydro-2H-pyridin-1-yl)methyl)-dihydrofuran-2-one
(139)



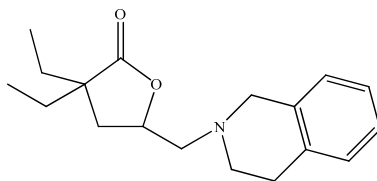
Pale yellow liquid. Yield: 18.12 %. ^1H - NMR $\{\text{CDCl}_3, 400 \text{ MHz}, \delta (\text{ppm})\}$ 1H 0.91 (t, 3H), 0.96 (t, 3H), 1.57 - 1.69 (m, 4H), 1.84 - 1.90 (dd, 13.2 Hz, 2H), 2.18 - 2.23 (m, 2H), 2.28 (t, 3H), 2.44 - 2.56 (m, 2H), 2.79 - 2.84 (m, 2H), 2.99 - 3.05 (m, 2H), 3.44 - 3.55 (m, 2H), 4.78 - 4.84 (m, 1H), 5.53 - 5.54 (m, 1H), 7.07 - 7.10 (m, 1H), 7.12 - 7.17 (m, 3H). LC - MS (ESI) (m/z) 327.0 ($\text{M}+\text{H}$) $^+$. HPLC analysis: > 95 % purity using two different mobile phases.

62. 1-[2-(4,4-diethyl-tetrahydro-furan-2-yl)-ethyl]-4-(2-isopropylphenyl)-piperazine
(140)



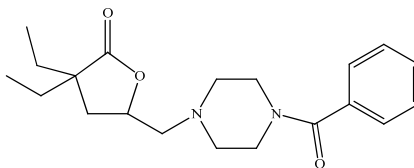
Pale yellow semisolid. Yield: 10 %. ^1H - NMR ($\text{CDCl}_3, 400 \text{ MHz}, \delta (\text{ppm})\}$ 0.84 - 0.92 (m, 6h), 1.12 (d, 6H), 1.53 - 1.61 (m, 4H), 1.85 - 1.90 (m, 1H), 2.02 - 2.10 (m, 1H), 2.31 (m, 2H), 2.61 - 2.87 (m, 3H), 2.98 - 3.08 (septet, 1H), 3.12 - 3.28 (m, 2H), 4.56 - 4.69 (m, 1H), 5.42 - 5.44 (m, 1H), 6.97 - 7.07 (m, 2H), 7.14 - 7.16 (1H), 7.20 - 7.22 (m, 1H). LC - MS (ESI) (m/z) 356.1 ($\text{M}+1$) $^+$.

63. 3,3-diethyl-4,5-dihydro-5-([1,2,3,4-tetrahydroisoquinolyl]methyl)-2(3H)-furanone
(141)



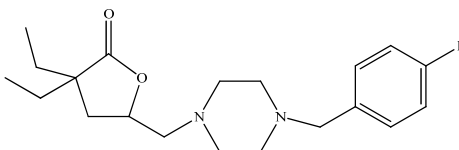
Pale yellow liquid. Yield: 7.4 %. ^1H - NMR $\{\text{CDCl}_3, 400 \text{ MHz}, \delta \text{ (ppm)}\}$ 0.90 (t, 3H), 0.96 (t, 3H), 1.59 - 1.66 (m, 4H), 1.91-1.97 (m, 1H), 2.08 - 2.13 (m, 1H), 2.72 - 2.90 (m, 6H), 3.70 (d, 1H), 3.81 (d, 1H), 4.62 - 4.68 (m, 1H), 7.01 - 7.03 (m, 1H), 7.03 - 7.13 (m, 3H). LC-MS (ESI) (m/z) 288.3 (M+1)⁺.

64. 3,3-diethyl-4,5-dihydro-5-(4-[4-phenylcarbonyl]piperazinylmethyl)-2(3H)-furanone (**142**)



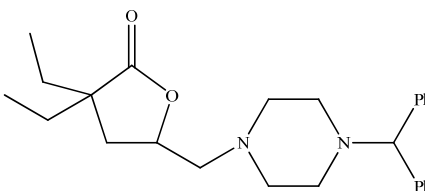
Pale yellow liquid. Yield: 22.5 %. ^1H - NMR $\{\text{CDCl}_3, 400 \text{ MHz}, \delta \text{ (ppm)}\}$ 0.75-0.83 (m, 6H), 1.45-1.52 (m, 4H), 1.71-1.79 (m, 1H), 1.91-1.96 (m, 1H), 2.34-2.56 (m, 6H), 3.28-3.34 (m, 2H), 3.58-3.64 (m, 2H), 4.40-4.44 (m, 1H), 7.24-7.27 (m, 5H). LC-MS (ESI) (m/z) 345.3 (M+1)⁺. HPLC analysis: > 95 % purity using two different mobile phases.

65. 3,3-diethyl-5-[4-(4-fluoro-benzyl)-piperazin-1-ylmethyl]-dihydro-furan-2-one (**143**)



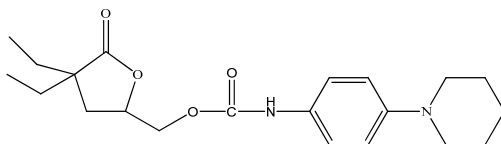
Pale yellow liquid. Yield: 12.32 %. ^1H - NMR ($\text{CDCl}_3, 400 \text{ MHz}$): 0.85-0.96 (m, 6H), 1.58-1.64 (m, 4H), 1.81-1.90 (m, 1H), 2.02-2.07 (m, 1H), 2.45-2.63 (m, 8H), 3.45 (d, 2H), 4.51-4.58 (m, 1H), 5.30 (s, 2H), 6.96-7.01 (m, 2H), 7.21-7.31 (m, 2H); LC-MS (ESI) (m/z) 349.2 (M+1)⁺. HPLC analysis: > 95 % purity using two different mobile phases.

66. 3,3-diethyl-4,5-dihydro-5-(4-[4-biphenylmethyl]piperazinylmethyl)-2(3H)-furanone (**144**)



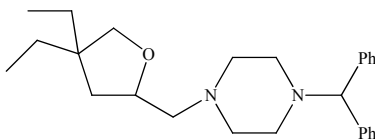
Pale yellow liquid. Yield: 8.72 %. ^1H - NMR $\{\text{CDCl}_3, 400 \text{ MHz}, \delta \text{ (ppm)}\}$ 0.87-0.95 (m, 6H), 1.57-1.63 (m, 4H), 1.83-1.88 (m, 1H), 2.01-2.06 (m, 1H), 2.42-2.64 (m, 10H), 4.22 (s, 1H), 4.52-4.55 (m, 1H), 7.14-7.18 (m, 2H), 7.24-7.27 (m, 4H), 7.40-7.42 (m, 4H). LC-MS (ESI) (m/z) 407.3 (M+1)⁺.

67. (4-piperidinylphenyl)-1-carbamic acid 3, 3-diethyl-4,5-dihydro-2(3H)-furanone methylester (**145**)



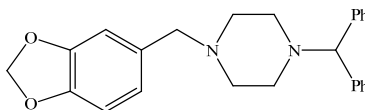
Pale yellow solid. Yield: 52.66 %. ^1H - NMR $\{\text{CDCl}_3, 400 \text{ MHz}, \delta (\text{ppm})\}$ 0.89-0.97 (m, 6H), 1.52-1.72 (m, 10H), 1.90-1.95 (m, 1H), 2.06-2.11 (m, 1H), 3.07-3.10, 4.12-4.16 (m, 1H), 4.38-4.42 (m, 1H), 4.61-4.67 (m, 1H), 6.57 (s, 1H), 6.89 (d, 2H), 7.22-7.23 (m, 2H). LC-MS (ESI) (m/z) 376.2 (M+1) $^+$. HPLC analysis: > 95 % purity using two different mobile phases.

68. 1-benzhydryl-4-(4,4-diethyl-tetrahydro-furan-2-ylmethyl)-piperazine (**146**)



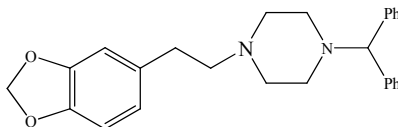
Pale yellow liquid. Yield: 22.40 %. ^1H - NMR $\{\text{CDCl}_3, 400 \text{ MHz}, \delta (\text{ppm})\}$ 0.79 - 0.83 (m, 6H), 1.20 - 1.26 (dd, 1H), 1.30 - 1.42 (m, 4H), 2.62 - 2.74 (m, 4H), 2.89 - 3.15 (m, 4H), 3.47 - 3.54 (m, 2H), 4.27 - 4.33 (m, 2H), 7.15 - 7.19 (m, 2H), 7.24 - 7.31 (m, 4H), 7.38 - 7.45 (m, 2H); LC - MS (ESI) (m/z) 393.3 (M+1) $^+$. HPLC analysis: > 95 % purity using two different mobile phases.

69. 1-Benzydryl-4-benzo [1,3]dioxol-5-ylmethyl-piperazine (**147**)



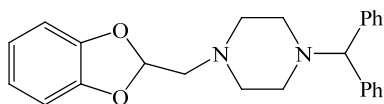
White solid. Yield: 57.6 %. ^1H - NMR $\{\text{CDCl}_3, 400 \text{ MHz}, \delta (\text{ppm})\}$ 2.45 (m, 8H), 3.42 (s, 2H), 4.24 (s, 1H), 5.86 (s, 2H), 6.72 (d, 2H), 6.84 (s 1H), 7.13 - 7.19 (m, 2H), 7.23 - 7.27 (m, 4H), 7.41 - 7.43 (m, 4H). LC - MS (ESI) (m/z) 387.2 (M+1) $^+$. HPLC analysis: > 95 % purity using two different mobile phases.

70. 1-Benzydryl-4-(2-benzo [1,3] dioxol-5-yl-ethyl)-piperazine (**148**)



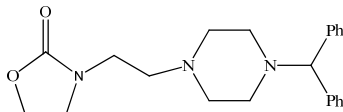
Pale yellow solid. Yield: 57.2%. ^1H - NMR (CDCl₃, 400 MHz, δ (ppm)) 2.46 - 2.56 (m, 4H), 2.68 - 2.72 (m, 2H), 4.23 (s, 1H), 5.87 (s, 2H), 6.61 - 6.64 (dd, 1H), 6.69 - 6.72 (m, 2H), 7.14 - 7.18 (m, 2H), 7.22 - 7.27 (m, 4H), 7.41 - 7.43 (m, 4H); LC - MS (ESI) (m/z) 401.2 (M+H) $^+$. HPLC analysis: > 95 % purity using two different mobile phases.

71. 1-Benzydryl-4-benzo[1,3]dioxol-2-ylmethyl-piperazine (**149**)



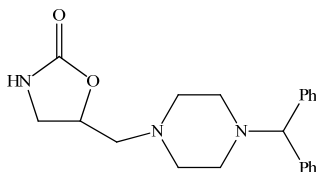
Colorless solid. Yield: 4.1 %. ^1H - NMR $\{\text{CDCl}_3, 400 \text{ MHz}, \delta \text{ (ppm)}\}$ 7.33 – 7.35 (m, 4H), 7.17 – 7.21 (m, 4H), 7.08 – 7.12 (m, 2H), 6.68 – 6.72 (m, 4H), 6.15 – 6.17 (s, 1H), 4.17 (s, 1H), 2.84 – 2.85 (d, 2H), 2.53 – 2.56 (m, 4H), 2.42 (m, 4H). LC - MS (ESI) (m/z) 387.0 (M+1) $^+$.

72. 3-[2-(4-Benzhydryl-piperazin-1-yl)-ethyl]-oxazolidin-2-one (**150**)



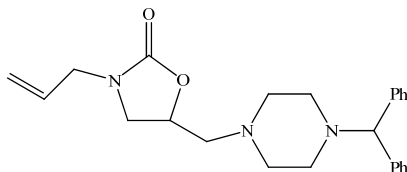
Pale yellow liquid. Yield: 51.90 %. ^1H - NMR $\{\text{CDCl}_3, 400 \text{ MHz}, \delta \text{ (ppm)}\}$ 2.39 - 2.54 (m, 10H), 3.36 (t, 2H), 3.60 - 3.66 (m, 2H), 4.19 (s, 2H), 4.27 - 4.31 (m, 2H), 7.14 - 7.18 (m, 2H), 7.24 - 7.27 (m, 4H), 7.38 - 7.42 (m, 4H). LC - MS (ESI) (m/z) 366.2 (M+1) $^+$.

73. 5-(4-Benzhydryl-piperazin-1-ylmethyl)-oxazolidin-2-one (**151**)



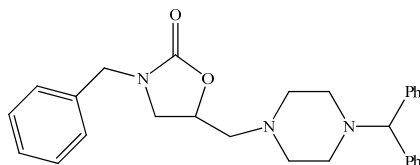
Colorless solid. Yield: 17.9 %. ^1H -NMR $\{\text{CDCl}_3, 400 \text{ MHz}, \delta \text{ (ppm)}\}$ 2.32 – 2.52 (m, 8H), 2.59 – 2.64 (m, 1H), 3.21 (t, 1H), 3.50 (t, 1H), 4.13 (s, 1H), 4.61 – 4.68 (m, 1H), 6.08 (s, 1H), 7.06 – 7.10 (m, 2H), 7.16 – 7.19 (m, 4H), 7.31 – 7.33 (m, 4H). LC - MS (ESI) (m/z) 352.2 (M+1) $^+$.

74. 3-allyl-5-(4-benzhydryl-piperazin-1-ylmethyl)-oxazolidin-2-one (**152**)



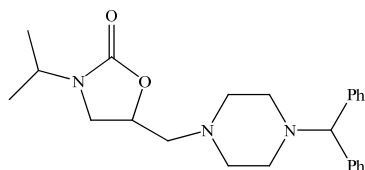
Pale yellow solid. Yield: 29.9 %. ^1H - NMR $\{\text{CDCl}_3, 400 \text{ MHz}, \delta \text{ (ppm)}\}$ 2.55 (bs, 4H), 2.78 - 2.95 (m, 5H), 3.07 - 3.11 (dd, 3H, 1H), 3.14 - 3.19 (dd, 9Hz, 1H), 3.63 (t, 1H), 3.77 - 3.90 (m, 2H), 4.26 (s, 1H), 4.80 - 4.87 (m, 1H), 5.16 - 5.25 (m, 2H), 5.69 - 5.79 (m, 1H), 7.16 - 7.22 (m, 2H), 7.25 - 7.29 (m, 4H), 7.38 - 7.40 (m, 4H). LC - MS (ESI) (m/z) 392.1 (M+1) $^+$. HPLC analysis: > 95 % purity using two different mobile phases.

75. 5-(4-benzhydryl-piperazin-1-ylmethyl)3-benzyl-oxazolidin-2-one (**153**)



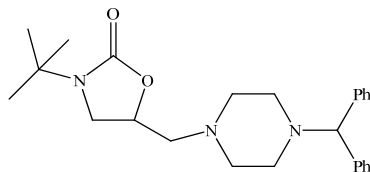
Pale yellow solid. Yield: 44.7 %. ^1H - NMR $\{\text{CDCl}_3, 400 \text{ MHz}, \delta \text{ (ppm)}\}$ 2.50 (bs, 4H), 2.71 - 2.95 (m, 6H), 3.05 - 3.09 (m, 1H), 3.50 (t, 1H), 3.99 - 4.13 (heptet, 1H), 4.24 (s, 1H), 4.39 (d, 2H), 4.73 - 4.80 (m, 1H), 7.15 - 7.22 (m, 2H), 7.24 - 7.41 (m, 13H). LC - MS (ESI) (m/z) 443.1 (M+1) $^+$.

76. 5-(4-benzhydryl-piperazin-1-ylmethyl)-3-isopropyl-oxazolidin-2-one (**154**)



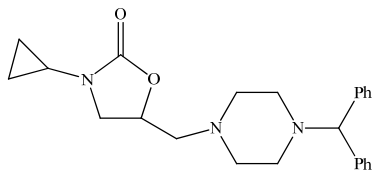
Pale yellow solid. Yield: 64.2 %. ^1H - NMR $\{\text{CDCl}_3, 400 \text{ MHz}, \delta \text{ (ppm)}\}$ 1.13 - 1.16 (m, 6H), 2.24 - 2.68 (m, 10H), 3.16 - 3.20 (t, 1H), 3.48 - 3.53 (t, 1H), 3.99 - 4.13 (heptet, 1H), 4.59-4.65 (m, 1H), 7.14 - 7.18 (m, 2H), 7.23 - 7.27 (m, 4H), 7.38 - 7.40 (m, 4H). LC - MS (ESI) (m/z) 394.1 (M+1) $^+$. HPLC analysis: > 95 % purity using two different mobile phases.

77. 5-(4-benzhydryl-piperazin-1-ylmethyl)-3-tert-butyl-oxazolidin-2-one (**155**)



Pale yellow solid. Yield: 33.27 %. ^1H - NMR $\{\text{CDCl}_3, 400 \text{ MHz}, \delta \text{ (ppm)}\}$ 1.36 (s, 9H), 2.57 (bs, 4H), 2.78 - 2.83 (dd, 13.5Hz, 1H), 2.88 - 3.08 (m, 4H), 3.11 - 3.15 (m, 1H), 3.23 (t, 1H), 3.69 - 3.76 (m, 2H), 4.27 (s, 1H), 4.69 - 4.75 (m, 1H), 7.16 - 7.20 (m, 2H), 7.25 - 7.29 (m, 4H), 7.38 - 7.40 (m, 4H). LC -MS (ESI) (m/z) 408.1 (M+1) $^+$.

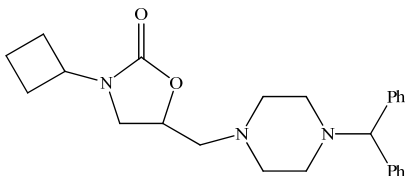
78. 5-(4-benzhydryl-piperazin-1-ylmethyl)-3-cyclopropyl-oxazolidin-2-one (**156**)



Pale yellow solid. Yield 37.2%. ^1H - NMR $\{\text{CDCl}_3, 400 \text{ MHz}, \delta \text{ (ppm)}\}$ 0.63 - 0.83 (m, 4H), 2.46 - 2.58 (m, 5H), 2.81 - 3.01 (m, 5H), 3.16 - 3.21 (m, 2H), 3.65 (t, 1H), 4.27 (s, 1H), 4.77 - 4.84 (m, 1H), 7.18 - 7.20 (m, 2H), 7.25 - 7.29 (m, 4H), 7.38 - 7.40 (m, 4H).

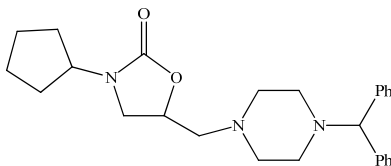
LC - MS (ESI) (m/z) 392.1 (M+1)⁺. HPLC analysis: > 95 % purity using two different mobile phases.

79. 5-(4-benzhydryl-piperazin-1-ylmethyl)-3-cyclobutyl-oxazolidin-2-one (**157**)



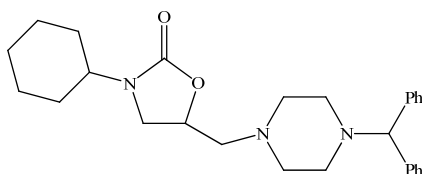
Pale yellow solid. Yield 38.4 %. ¹H - NMR {CDCl₃, 400 MHz, δ (ppm)} 1.61 - 1.72 (m, 2H), 2.09 - 2.15 (m, 4H), 2.40 - 2.69 (m, 10H), 3.28 - 3.32 (dd, 8.4 Hz, 1H), 3.61 (t, 1H), 4.21 (s, 1H), 4.31 - 4.40 (m, 1H), 4.55 - 4.62 (m, 1H), 7.14 - 7.16 (m, 2H), 7.23 - 7.27 (m, 4H), 7.38 - 7.40 (m, 4H). LC - MS (ESI) (m/z) 406.1 (M+1)⁺. HPLC analysis: > 95 % purity using two different mobile phases.

80. 5-(4-benzhydryl-piperazin-1-ylmethyl)-3-cyclopentyl-oxazolidin-2-one (**158**)



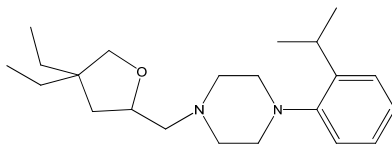
Pale yellow solid. Yield: 37.84 %. ¹H - NMR {CDCl₃, 400 MHz, δ (ppm)} 0.90 (d, 6H), 1.79 - 1.93 (m, 1H), 2.39 - 2.68 (m, 10H), 2.97 - 3.08 (m, 2H), 3.24 - 3.28 (m, 1H), 3.54 (t, 1H), 4.20 (s, 1H), 4.56 - 4.63 (m, 1H), 7.14 - 7.18 (m, 2H), 7.23 - 7.27 (m, 4H), 7.38 - 7.40 (m, 4H). LC - MS (ESI) (m/z) 408.2 (M+1)⁺. HPLC analysis: > 95 % purity using two different mobile phases.

81. 5-(4-benzhydryl-piperazin-1-ylmethyl)-3-cyclohexyl-oxazolidin-2-one (**159**)



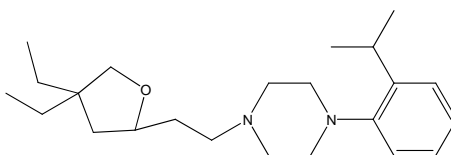
Pale yellow solid. Yield: 11.7 %. ¹H NMR: {CDCl₃, 400 MHz, δ (ppm)} 1.01 - 1.09 (m, 1H), 1.25 - 1.39 (m, 4H), 1.65 (d, 1H), 1.77 (m, 4H), 2.39 - 2.66 (m, 10H), 3.21 (t, 1H), 3.50 (t, 1H), 3.62 - 3.70 (m, 1H), 4.21 (s, 1H), 4.53 - 4.60 (m, 1H), 7.14 - 7.17 (m, 2H), 7.23 - 7.27 (m, 4H), 7.38 - 7.40 (m, 4H). LC - MS (ESI) (m/z) 434.1 (M+1)⁺. HPLC analysis: > 95 % purity using two different mobile phases.

82. 1-(4,4-diethyl-tetrahydro-furan-2-ylmethyl)-4-(2-isopropyl-phenyl)-piperazine (**160**).



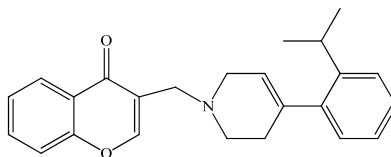
Pale yellow liquid. Yield: 11.7 %. ^1H NMR: $\{\text{CDCl}_3, 400 \text{ MHz}, \delta \text{ (ppm)}\}$; 7.16 – 7.18 (m, 1H), 6.98 – 7.07 (m, 3H), 4.07 – 4.14 (m, 1H), 3.51 – 3.53 (m, 1H), 3.37 – 3.42 (m, 2H), 2.84 – 2.86 (m, 4H), 2.61 (m, 3H), 2.49 – 2.54 (m, 1H), 2.39 – 2.43 (m, 1H), 1.29 – 1.44 (m, 4H), 1.20 – 1.26 (m, 1H), 1.12 (d, 6H), 0.75 – 0.80 (m, 6H). LC - MS (ESI) (m/z) 345.3 (M + 1) $^+$.

83. 1-[2-(4,4-Diethyl-tetrahydro-furan-2-yl)-ethyl]-4-(2-isopropyl-phenyl)-piperazine (**161**).



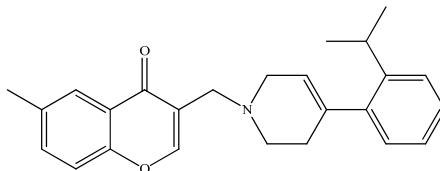
Light yellow liquid. Yield: 14.2 %. ^1H NMR: $\{\text{CDCl}_3, 400 \text{ MHz}, \delta \text{ (ppm)}\}$; 7.25 – 7.26 (m, 1H), 7.10 – 7.18 (m, 3H), 3.89 – 3.96 (m, 1H), 3.54 – 3.56 (m, 1H), 3.41 – 3.47 (m, 2H), 2.81 – 3.06 (m, 8H), 1.84 – 1.97 (m, 3H), 1.36 – 1.48 (m, 4H), 1.27 – 1.33 (m, 1H), 1.19 – 1.20 (d, 6H), 0.81 – 0.88 (m, 6H). LC - MS (ESI) (m/z) 359.2 (M + 1) $^+$.

84. 3-[4-(2-Isopropyl-phenyl)-3,6-dihydro-2H-pyridin-1-ylmethyl]-chromen-4-one (**162**)



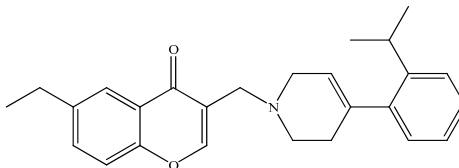
Yellow colored solid: Yield: 83.3 %. ^1H - NMR $\{\text{CDCl}_3, 400 \text{ MHz}, \delta \text{ (ppm)}\}$ 1.12 (d, 6H), 2.31-2.32 (m, 2H), 2.71 - 2.73 (m, 2H), 2.99 - 3.09 (septet, 1H), 3.18 - 3.19 (m, 2H), 3.59 (s, 2H), 5.45 - 5.55 (m, 2H), 6.98 - 7.07 (m, 2H), 7.14 - 7.18 (m, 1H), 7.20 - 7.22 (m, 1H), 7.32 - 7.41 (m, 2H), 7.58 - 7.62 (m, 1H), 8.08 (s, 1H), 8.17 - 8.19 (m, 1H). LC - MS: 360.2 (M+1) $^+$.

85. 3-((4-(2-isopropylphenyl)-5,6-dihydropyridin-1(2H)-yl)methyl)-6-methyl-4H-chromen-4-one (**163**)



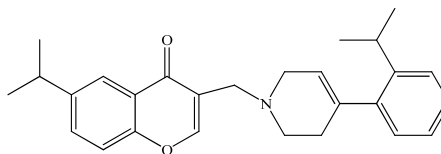
Yellow colored solid.: Yield: 45.6. ^1H - NMR $\{\text{CDCl}_3, 400 \text{ MHz}, \delta (\text{ppm})\}$ 1.19 (d, 6H), 2.37-2.38 (m, 2H), 2.46 (s, 3H), 2.78 (t, 2H), 3.06-3.16 (septet, 1H), 3.23-3.25 (m, 2H), 3.65 (s, 2H), 5.51-5.53 (m, 1H), 7.05-7.14 (m, 2H), 7.21-7.25 (m, 1H), 7.27-7.29 (m, 1H), 7.35-7.37 (m, 2H), 7.46-7.49 (m, 1H), 8.03 (s, 1H), 8.05 (1H). LC-MS (ESI) (m/z) 374.2 ($\text{M} + 1$) $^+$.

86. 6-ethyl-3-((4-(2-isopropylphenyl)-5,6-dihydropyridin-1(2H)-yl)methyl)-4H-chromen-4-one (**164**)



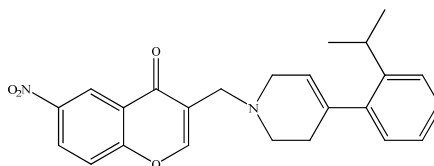
Yellow colored semi-solid.: Yield: 37.2 %. ^1H - NMR $\{\text{CDCl}_3, 400 \text{ MHz}, \delta (\text{ppm})\}$ 1.19 (d, 6H), 1.29 (t, 3H), 2.36-2.39 (m, 2H), 2.73-2.79 (m, 4H), 3.06-3.16 (septet, 1H), 3.23-3.25 (m, 2H), 3.65 (s, 1H), 5.52-5.53 (m, 1H), 7.05-7.14 (m, 2H), 7.21-7.25 (m, 1H), 7.27-7.29 (m, 1H), 7.38-7.40 (m, 1H), 7.49-7.52 (m, 1H), 8.03-8.06 (m, 2H). LC-MS (ESI) (m/z) 388.2 ($\text{M} + 1$) $^+$.

87. 6-Isopropyl-3-[4-(2-isopropyl-phenyl)-3,6-dihydro-2H-pyridin-1-ylmethyl]-chromen-4-one (**165**)



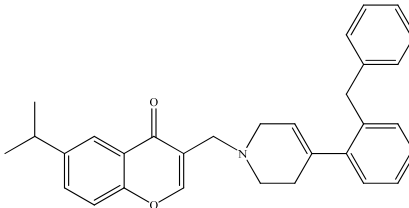
Yellow colored solid. Yield: 61.1 %. ^1H - NMR $\{\text{CDCl}_3, 400 \text{ MHz}, \delta (\text{ppm})\}$ 1.11-1.12 (d, 6H), 1.22 - 1.24 (d, 6H), 2.30 - 2.32 (m, 2H), 2.71 - 2.73 (m, 2H), 2.93 - 3.09 (m, 1H), 3.17 - 3.18 (m, 2H), 3.59 (s, 2H), 5.44 - 5.49 (m, 1H), 6.98 - 7.01 (m, 2H), 7.14 - 7.18 (m, 1H), 7.19 - 7.22 (m, 1H), 7.34 - 7.36 (m, 1H), 7.46 - 7.49 (m, 1H), 7.98 (s, 1H), 8.02 (d, 1H). LC - MS: 402.2 ($\text{M}+1$) $^+$.

88. 3-((4-(2-isopropylphenyl)-5,6-dihydropyridin-1(2H)-yl)methyl)-6-nitro-4H-chromen-4-one (**166**)



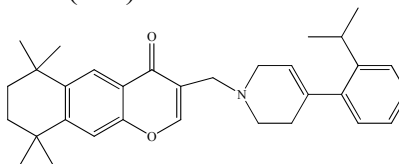
Yellow colored solid.: Yield: 6.4 %. ^1H - NMR $\{\text{CDCl}_3, 400 \text{ MHz}, \delta (\text{ppm})\}$ 1.21 (d, 6H), 2.39 (m, 2H), 2.79 (t, 2H), 3.05-3.16 (m, 1H), 3.25 (m, 2H), 3.66 (s, 2H), 5.52-5.54 (m, 1H), 7.06-7.15 (m, 2H), 7.22-7.24 (m, 1H), 7.28-7.30 (m, 2H), 7.64 (d, 1H), 8.13 (s, 1H), 8.49-8.52 (dd, $J = 9.2 \text{ Hz}$, 1H), 9.12 (d, 1H). LC-MS (ESI) (m/z) 405.1 ($\text{M} + 1$) $^+$.

89. 3-((4-(2-benzylphenyl)-5,6-dihydropyridin-1(2H)-yl)methyl)-6-isopropyl-4H-chromen-4-one (**167**)



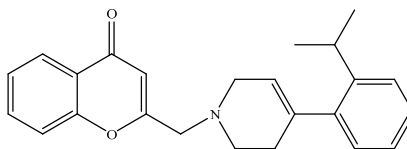
Yellow colored semi-solid.: Yield: 20.9 %. ^1H - NMR $\{\text{CDCl}_3, 400 \text{ MHz}, \delta (\text{ppm})\}$ 1.27 (d, 6H), 2.26 (m, 2H), 2.68 (t, 2H), 3.00-3.09 (m, 1H), 3.18 (m, 2H), 3.60 (m, 2H), 4.01 (m, 2H), 4.01 (m, 2H), 5.49 (s, 1H), 7.09-7.26 (m, 10H), 7.39 (d, 1H), 7.53-7.59 (m, 1H), 8.01 (s, 1H), 8.07-8.11 (m, 1H). LC-MS (ESI) (m/z) 450.2 ($\text{M} + 1$) $^+$.

90. 3-[4-(2-Isopropyl-phenyl)-3, 6-dihydro-2H-pyridin-1-ylmethyl]-6,6,9,9-tetramethyl-6,7,8,9-tetrahydro-benzo[g]chromen-4-one (**168**)



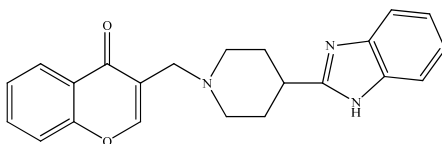
Creamish colored solid.: Yield: 22.1 %. ^1H - NMR $\{\text{CDCl}_3, 400 \text{ MHz}, \delta (\text{ppm})\}$ 1.12 (d, 6H), 1.27 (s, 6H), 1.31 (s, 6H), 1.66 (s, 4H), 2.29 - 2.30 (m, 2H), 2.68-2.71 (m, 2H), 2.98 - 3.09 (m, 1H) 3.16 - 3.17 (m, 2H), 3.55 (s, 2H), 5.44 - 5.49 (m, 1H), 6.98 - 7.06 (m, 2H), 7.14 - 7.18 (m, 1H), 7.19 - 7.21 (m, 1H), 7.30 (s, 1H), 7.92 (s, 1H), 8.11 (s, 1H). LC - MS: 470.2 ($\text{M}+1$) $^+$.

91. 2-((4-(2-isopropylphenyl)-5,6-dihydropyridin-1(2H)-yl)methyl)-4H-chromen-4-one (**169**)



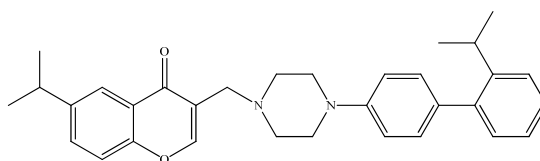
Yellow colored semi-solid.: Yield: 17.8 %. ^1H - NMR $\{\text{CDCl}_3, 400 \text{ MHz}, \delta (\text{ppm})\}$ 1.21 (d, 6H), 2.40-2.43 (m, 2H), 2.85 (t, 2H), 3.06-3.16 (septet, 1H), 3.29-3.31 (m, 2H), 3.66 (s, 2H), 5.52-5.53 (m, 1H), 6.49 (s, 1H), 7.05-7.07 (m, 1H), 7.12-7.18 (m, 1H), 7.22-7.30 (m, 2H), 7.39-7.43 (m, 1H), 7.50-7.52 (m, 1H), 7.65-7.69 (m, 1H), 8.20-8.22 (dd, J = 1.64, 7.96 Hz, 1H). LC-MS (ESI) (m/z) 360.2 ($\text{M} + 1$) $^+$.

92. 3-((4-(1H-benzo[d]imidazol-2-yl)piperidin-1-yl)methyl)-4H-chromen-4-one (**170**)



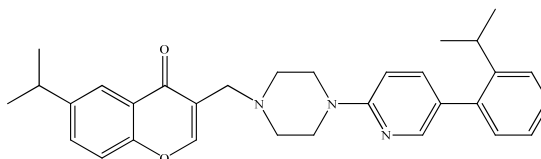
Creamish white colored solid.: Yield: 10.1 %. ^1H - NMR $\{\text{CDCl}_3, 400 \text{ MHz}, \delta (\text{ppm})\}$ 1.86-1.96 (m, 2H), 2.05-2.08 (m, 2H), 2.18-2.24 (m, 2H), 2.81-2.92 (m, 1H), 2.98-3.01 (m, 2H), 3.45 (s, 2H), 7.12-7.17 (m, 2H), 7.32-7.35 (m, 2H), 7.38-7.40 (m, 1H), 7.57-7.62 (m, 1H), 7.93 (s, 1H), 8.16-8.21 (m, 1H), 9.29 (s, 1H). LC-MS (ESI) (m/z) 360.1 ($\text{M} + 1$) $^+$.

93.6-isopropyl-3-((4-(2'-isopropylbiphenyl-4-yl)piperazin-1-yl)methyl)-4H-chromen-4-one (**171**)



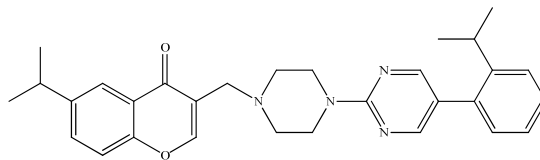
Yellow colored solid.: Yield: 17.19 %. ^1H - NMR $\{\text{CDCl}_3, 400 \text{ MHz}, \delta (\text{ppm})\}$ 1.15 (d, 6H), 1.28 (d, 6H), 2.72-2.75 (m, 4H), 3.00-3.18 (m, 2H), 3.26-3.38 (m, 4H), 3.57 (s, 2H), 6.93-6.96 (m, 2H), 7.15-7.22 (m, 4H), 7.27-7.41 (m, 4H), 7.53-7.56 (m, 1H), 8.01 (s, 1H), 8.08 (d, 1H). LC-MS (ESI) (m/z) 481.3 ($\text{M} + 1$) $^+$.

94. 6-isopropyl-3-((4-(5-(2-isopropylphenyl)pyridin-2-yl)piperazin-1-yl)methyl)-4H-chromen-4-one (**172**)



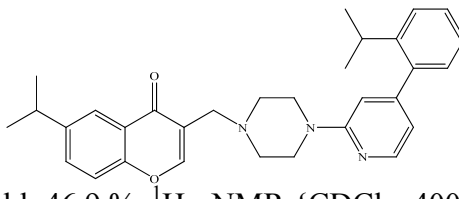
Creamish white solid.: Yield: 38.27 %. ^1H - NMR $\{\text{CDCl}_3, 400 \text{ MHz}, \delta (\text{ppm})\}$ 1.08 (d, 6H), 1.22 (d, 6H), 2.62 (t, 4H), 2.91-3.06 (m, 2H), 3.49 (s, 2H), 3.54 (t, 4H), 6.62 (d, 1H), 7.06-7.08 (m, 1H), 7.11-7.15 (m, 1H), 7.24-7.37 (m, 4H), 7.46-7.49 (m, 1H), 7.95 (s, 1H), 8.01 (d, 1H), 8.06 (d, 1H). LC-MS (ESI) (m/z) 481.3 ($\text{M} + 1$) $^+$.

95. 6-isopropyl-3-((4-(5-(2-isopropylphenyl)pyrimidin-2-yl)piperazin-1-yl)methyl)-4H-chromen-4-one (**173**)



Colorless white solid.: Yield: 55.15 %. ^1H - NMR $\{\text{CDCl}_3, 400 \text{ MHz}, \delta (\text{ppm})\}$ 1.17 (d, 6H), 1.29 (d, 6H), 2.65 (t, 4H), 2.99-3.09 (m, 2H), 3.56 (s, 2H), 3.90 (t, 4H), 7.21-7.25 (m, 1H), 7.33-7.41 (m, 3H), 7.53-7.56 (dd, $J = 2.68, 8.68 \text{ Hz}$, 1H), 8.02 (s, 1H), 8.08 (d, 1H), 8.28 (s, 2H). LC-MS (ESI) (m/z) 481.3 ($\text{M} + 1$) $^+$.

96. 6-isopropyl-3-((4-(4-(2-isopropylphenyl)pyridin-2-yl)piperazin-1-yl)methyl)-4H-chromen-4-one (**174**)



Creamish white solid.: Yield: 46.9 %. ¹H - NMR {CDCl₃, 400 MHz, δ (ppm)} 1.18 (d, 6H), 1.31 (d, 6H), 2.69 (t, 4H), 2.99-3.10 (m, 2H), 3.57 (s, 2H), 3.61 (t, 4H), 7.14-7.16 (m, 1H), 7.21-7.25 (m, 1H), 7.35-7.44 (m, 3H), 7.55-7.58 (m, 1H), 8.02 (s, 1H), 8.09 (d, 1H), 8.21 (d, 1H). (LC-MS (ESI) (m/z) 481.3 (M + 1)⁺.

6.4.7 Kinetic Compound Solubility Protocol.

Protocol Summary:

This is a 96 well plate based in vitro assay that determines the kinetic solubility of test compounds 90 minutes after a concentration solution of compound in neat DMSO is mixed with a universal buffer at pH 7.4 (45 mM ethanolamine, 45 mM potassium dihydrogen phosphate and 45 mM potassium acetate, pH 7.4). The final concentration of DMSO is 2 %. Soluble compound is separated from insoluble compound by filtering the samples into a 96 well collection plate. Soluble compound concentration is determined using either absorption (Spectramax plate reader; samples are read at 280, 300, 320, 340 and 360 nm and the absorbance values are summed) or by UPLC/Mass spectroscopy for compounds with insufficient absorbance at the test concentration. Standard curves are utilized for both analytical methods.

The solubilities are labeled “kinetic” solubilities because the values are determined for compounds already in solution in DMSO that are incubated for a specified period of time (90 minutes at room temperature) in aqueous buffer, rather than equilibrium solubilities (dry compound allowed to dissolve in aqueous buffer for an extended period of time).

REFERENCES

1. Karnik S. S, Gogonea C, Patil S, Saad Y and Takezako T; Activation of G-protein-coupled receptors: a common molecular mechanism; *Trends in Endocrinology and Metabolism* 14 (2003) 431-437.
2. Scarselli M, Li B, Kim S. K. and Wess J; Multiple residues in the second extracellular loops are critical for M₃ muscarinic acetylcholine receptor activation; *The Journal of Biological Chemistry*; 282 (2007) 7385-7396.
3. Hosey M. M; Diversity of structure, signaling and regulation within the family of muscarinic cholinergic receptors; *FASEB J*; 6 (1992) 845-852.
4. Felder C. C, Bymaster F. P, Ward J and DeLapp N; Therapeutic opportunities for muscarinic receptors in central nervous system; *Journal of Medicinal Chemistry*; 43 (2000) 4333-4353.
5. Felder C. C; Muscarinic acetylcholine receptors: signal transduction through multiple effectors; *FASEB J*; 9 (1995) 619-625.
6. Wess J, Eglen R. M and Gautam D; Muscarinic acetylcholine receptors:mutant mice provide new insights for drug development; *Nature Reviews: Drug Discovery*; 6 (2007) 721-733.
7. Caulfield M. P, Birdsall N. J. M., International Union of Pharmacology. XVII. Classification of muscarinic acetylcholine receptors; *Pharmacological Reviews*; 50 (1998) 279-290.
8. Wang, Z. S., El-Fakahany, E. E.; Application of transfected cell lines in studies of functional receptor subtype selectivity of muscarinic agonists; *Journal of Pharmacology and Experimental Therapeutics*; 266 (1993) 237-243.

9. Eglen R. M., Choppin A. and Watson N.; Therapeutic opportunities from muscarinic receptor research; *Trends in Pharmacological Sciences*; 22 (2001) 409-414.
10. Nathanson N. M.; A multiplicity of muscarinic mechanisms: Enough signaling pathways to take your breath away; *Proceedings of National Academy of Sciences*; 97 (2000) 6245-6247.
11. Koch H. J., Haas S. and Jurgens T.; On the physiological relevance of muscarinic acetylcholine receptors in alzheimer's disease; *Current Medicinal Chemistry*; 12 (2005) 2915-2921.
12. Lanzafame A. A., Christopoulos A. and Mitchelson F.; Cellular signaling mechanisms for muscarinic acetylcholine receptors; *Receptors and Channels*; 9 (2003) 241-260.
13. Shapiro S. M., Gomeza J., Hamilton S. E., Hille B., Loose M. D., Nathanson N. M., Roche J. P., Wess J.; Identification of subtypes of muscarinic receptors that regulate Ca^{2+} and K^{2+} channel activity in sympathetic neurons; *Life Sciences*; 68 (2001) 2481-2487.
14. Tense M., Cordier J., Premont J., Glowinski J.; Muscarinic cholinergic agonists stimulate arachidonic acid release from mouse striatal neurons in primary culture; *The Journal of Pharmacology and Experimental Therapeutics*; 269 (1994) 646-653.
15. Wotta R. D., Wattenberg V. E., Langason B. R., El-Fakahany E.; M1, M3 and M5 muscarinic receptors stimulate mitogen activated protein kinase; *Pharmacology*; 56 (1998) 175-186.

16. Liao C-F, Themmen A. P. N., Joho R., Barberis C., Birnbaumer M., and Birnbaumer L.; Molecular cloning and expression of the fifth muscarinic acetylcholine receptor; *The Journal of Biological Chemistry*; 264 (1989) 7328-7337.
17. Moncada S., Palmer J. M. R., Higgs A. E.; Nitric oxide: physiology, pathophysiology and pharmacology; *Pharmacological Reviews*; 43 (1991) 109-142.
18. Das S., Kumar N. K.; Nitric oxide: its identity and role in blood pressure control; *Life Sciences*; 57 (1995) 1547-1556.
19. Abrams P., Andersson K. E., Buccafusco J. J., Chapple C., Groat W. C., Fryer A. D., Kay G., Laties A., Nathanson N. M., Pasricha P. J. and Wein A. J.; Muscarinic receptors: their distribution and function in body systems and their implications for treating overactive bladder; *British Journal of Pharmacology*; 148 (2006) 565-578.
20. Eglen R. M.; Muscarinic receptor subtypes in neuronal and non-neuronal cholinergic function; *Autonomic & Autocoid Pharmacology*; 26 (2006) 219-233.
21. Yamada M., Basile A.S., Fedorova I., Zhang W., Duttaroy A., Cui Y., Lamping K. G., Faraci F. M., Deng C. X., Wess J.; Novel insights into M5 muscarinic acetylcholine receptor function by the use of gene targeting technology; *Life Sciences*; 74 (2003) 345-353.
22. (a) Eglen R. M., Choppin A., Dillon M. P. and Hegde S.; Muscarinic receptor ligands and their therapeutic potential; *Current Opinion in Chemical Biology*; 3 (1999) 426-432.

 (b) Prat M., Fernández D., Buil M. A, Crespo M. I, Casals G., Ferrer M., Tort L., Castro J., Monleón J. M., Gavalda A., Miralpeix M., Ramos I., Doménech T., Vilella D., Antón F., Huerta J. M., Espinosa S., López M., Sentellas S., González M., Albertí

- J., Segarra V., Cárdenas A., Beleta J. and Ryder H.; Discovery of novel quaternary ammonium derivatives of (3R)-quinuclidinol esters as potent and long-acting muscarinic antagonists with potential for minimal systemic exposure after inhaled administration: identification of (3R)-3-{[hydroxy(di-2-thienyl)acetyl]oxy}-1-(3-phenoxypropyl)-1-azoniabicyclo[2.2.2]octane bromide (aclidinium bromide); *Journal of Medicinal Chemistry*; 52 (2009) 5076-92.
23. Fisher A.; Muscarinic receptor agonists in Alzheimer's disease; *CNS Drugs*; 12 (1999) 197-214.
24. Simpson D. and Wagstaff A. J.; Solifenacin in overactive bladder syndrome; *Drugs Aging*; 22 (2005) 1061-1069.
25. Hills C. J., Winter S. A. and Balfour J. A.; Tolterodine; *Drugs*; 55 (1998) 813-820.
26. Croom K. J. and Keating G. M.; Darifenacin in the treatment of overactive bladder; *Drugs Aging*; 21 (2004) 885 - 892.
27. Brocks D. R.; Anticholinergic drugs used in Parkinson's disease: An overlooked class of drugs from a pharmacokinetic perspective; *Journal of Pharmacy & Pharmaceutical Sciences*; 2 (1999) 39 - 46.
28. Miller N. R., Daniels R. N., Lee D., Conn P. J., Lindsley C. W.; Synthesis and SAR of N-(4-(4-alkylpiperazin-1-yl)phenyl)benzamides as muscarinic acetylcholine receptor subtype (M1) antagonists; *Bioorganic & Medicinal Chemistry Letters*; 20 (2010) 2174-2177.
29. Johnson D. J., Forbes I. T., Watson S. P., Garzya V., Stevenson G. I., Walket G. R., Mudhar H. S., Flynn S. T., Wyman P. A., Smith P. W., Murkitt G. S., Lucas A. J.,

30. Budzik B., Garzya V., Shi D., Foley J. J., Rivero R. A., Langmead C. J., Watson J., Wu Z., Forbes I. T., Jin J.; Biaryl amides as novel and subtype selective M1 agonists. Part I: Identification, synthesis, and initial SAR; *Bioorganic & Medicinal Chemistry Letters*; 20 (2010) 3540–3544.
31. Budzik B., Garzya V., Shi D., Walker G., Lauchart Y., Lucas A. J., Rivero R. A., . Langmead C. J., Watson J., Wu Z., Forbes I. T., Jin J.; Biaryl amides as novel and subtype selective M1 agonists. Part II: Further optimization and profiling; *Bioorganic & Medicinal Chemistry Letters*; 20 (2010) 3545–3549.
32. Novelli F., Sparatore A., Tasso B., Sparatore F.; Quinolizidinyl derivatives of 5,11-dihydro-6H-pyrido[2,3-b][1,4]benzodiazepine-6-one as ligands for muscarinic receptors; *Bioorganic & Medicinal Chemistry Letters*; 9 (1999) 3031–3034.
33. Boyle C. D., Chackalamannil S., Chen L., Dugar S., Pushpavanam P., Billard W., Binch H., Crosby G., Williams M. C., Coffin V. L., Duffy R. A., Ruperto V. and Lachowicz J. E.; Benzylidene ketal derivatives as M2 muscarinic receptor antagonists; *Bioorganic & Medicinal Chemistry Letters*; 10 (2000) 2727–2730.
34. Wang Y., Chackalamannil S., Chang W., Greenlee W., Ruperto V., Duffy R. A., McQuade R., and Lachowicz J. E.; Design and synthesis of ether analogues as potent and selective M2 muscarinic receptor antagonists; *Bioorganic & Medicinal Chemistry Letters*; 11 (2001) 891–894.

- 35a. Kozlowski J. A., Zhou G., Tagat J. R., Lin S., McCombie S. W., Ruperto V. B., Duffy R. A., McQuade R. A., Crosby G., Taylor L. A., Billard W., Binch H., and Lachowicz J. E., Substituted 2-(*R*)-methyl piperazines as muscarinic M2 selective ligands; *Bioorganic & Medicinal Chemistry Letters*; 12 (2002) 791–794.
- 35b. McCombie S.W., Lin S. I., Tagat J. R., Nazareno D., Vice S., Ford J., Asberom T., Leone D., Kozlowski J. A., Zhou G., Ruperto V. B., Duffy R. A. and Lachowicz J. E.; Synthesis and structure–activity relationships of M2-selective muscarinic receptor ligands in the 1-[4-(4-arylsulfonyl)-phenylmethyl]-4-(4-piperidinyl)-piperazine family; *Bioorganic & Medicinal Chemistry Letters*; 12 (2002) 795–798.
36. Bohme T. M., Keim C., Dannhardt G., Mutschler E. and Lambrecht G.; Design and pharmacology of quinuclidine derivatives as M2-selective muscarinic receptor ligands; *Bioorganic & Medicinal Chemistry Letters*; 11 (2001) 1241–1243.
37. Kim M. G., Bodor E. T., Harden T. K., and Kohn H.; C(8)-Substituted 1-azabicyclo[3.3.1]non-3-enes: a novel scaffold for muscarinic receptor ligands; *Bioorganic & Medicinal Chemistry*; 12 (2004) 2357–2367.
38. Bohme T. M., Keim C., Kreutzmann K., Linder M., Dinger mann T., Dannhardt G., Mutschler E., and Lambrecht G.; Structure-activity relationships of dimethindene derivatives as new M2-selective muscarinic receptor antagonists; *Journal of Medicinal Chemistry*; 46 (2003) 856-867.
39. Wang Y., Chackalamannil S., Hu Z., Clader J. W., Greenlee W., Billard W., Binch H., Crosby G., Ruperto V., Duffy R. A., McQuade R. and Lachowicz J. E.; Design and synthesis of piperidinyl piperidine analogues as potent and selective M2 muscarinic receptor antagonists; *Bioorganic & Medicinal Chemistry Letters*; 10

- (2000) 2247-2250.
40. Minarini A., Marucci G., Bellucci C., Giorgi G., Tumiatti V., Bolognesi M. L., Matera R., Rosini M., Melchiorre C.; Design, synthesis, and biological evaluation of pirenzepine analogs bearing a 1,2-cyclohexanediamine and perhydroquinoxaline units in exchange for the piperazine ring as antimuscarinics; *Bioorganic & Medicinal Chemistry*; 16 (2008) 7311– 7320.
 41. Lachowicz J. E., Lowe D., Duffy R. A., Ruperto V., Taylor L. A., Guzik H., Brown J., Berger J. G., Tice M., McQuade R., Kozlowski J., Clader J., Strader C. D. and Murgolo N.; SCH 57790: a novel m, receptor selective antagonist; *Life Sciences*; 64 (1999) 535-539.
 42. Sabb A. L., Husbands G. M., Tokolics J., Stein R. P., Tasse P. P., Boast C. A., Moyer J. A., and Gharbia M. A.; Discovery of a highly potent, functionally-selective muscarinic M1 agonist, WAY-132983 using rational drug design and receptor modelling; *Bioorganic & Medicinal Chemistry Letters*; 9 (1999) 1895-1900.
 43. Lain D. I., McClelland B., Thomas S., Neipp C., Underwood B., Dufour J., Widdowson K. L., Palovich M. R., Blaney F. E., Foley J. J., Webb E. F., Luttmann M. A., Burman M., Belmonte K. and Salmon M.; Discovery of novel 1-Azoniabicyclo[2.2.2]octane muscarinic acetylcholine receptor antagonists; *Journal of Medicinal Chemistry*; 52 (2009) 2493–2505.
 44. (a) Mitsuya M., Ogino Y., Kawakami K., Uchiyama M., Kimura T., Numazawa T., Hasegawa T., Ohtake N., Noguchi K. and Mase T.; Discovery of a muscarinic M3 receptor antagonist with high selectivity for M3 Over M2 receptors among 2-[(1S,3S)-3-sulfonylaminocyclopentyl]phenylacetamide derivatives; *Bioorganic &*

- Medicinal Chemistry*; 8 (2000) 825-832.
- (b) Kaiser C., Audia V. H., Carter J. P., McPherson D. W., Waid P. P., Lowe V. C., Noronha-Blob L.; Synthesis and antimuscarinic activity of some 1-cycloalkyl-1-hydroxy-1-phenyl-3-(4-substituted piperazinyl)-2-propanones and related compounds; 36 (1993) 610–616.
45. Ogino Y., Ohtake N., Kobayashi K., Kimura T., Fujikawa T., Hasegawa T., Noguchi K. and Toshiaki Mase; Muscarinic M3 receptor antagonists with (2R)-2-[(1R)-3,3-difluorocyclopentyl]-2-hydroxyphenylacetamide structures. part 2; *Bioorganic & Medicinal Chemistry Letters*; 13 (2003) 2167–2172.
46. Sagara Y., Sagara T., Uchiyama M., Otsuki S., Kimura T., Fujikawa T., Noguchi K., and Norikazu Ohtake; Identification of a novel 4-Aminomethylpiperidine class of M3 muscarinic receptor antagonists and structural insight into their M3 selectivity; *Journal of Medicinal Chemistry*; 49 (2006) 5653-5663.
47. Sagara Y., Sagara T., Mase T., Kimura T., Numazawa T., Fujikawa T., Noguchi K. and Ohtake N.; Cyclohexylmethylpiperidinyltriphenylpropioamide: a selective muscarinic M3 antagonist discriminating against the other receptor subtypes; *Journal of Medicinal Chemistry*; 45 (2002) 984-987.
48. Diouf O., Gadeau S., Chelle F., Gelbcke M., Talaga P., Christophe B., Gillard M., Massinghamb R. and Guyauxb M.; A new series of M3 muscarinic antagonists based on the 4-amino-piperidine scaffold; *Bioorganic & Medicinal Chemistry Letters*; 12 (2002) 2535–2539.
49. Bohme T. M., Augelli-Szafran C. E., Hallak H., Pugsley T., Serpa K. and Schwarz R. D.; Synthesis and pharmacology of benzoxazines as highly selective antagonists at

- M4 muscarinic receptors; *Journal of Medicinal Chemistry*; 45(2002) 3094-3102.
50. Varoli L., Andreani A., Burnelli S., Granaiola M., Leoni A., Locatelli A., Morigi R., Rambaldi M., Bedini A., Faziob N. and Spampinato S.; Diphenidol-related diamines as novel muscarinic M4 receptor antagonists; *Bioorganic & Medicinal Chemistry Letters*; 18 (2008) 2972–2976.
51. Bridges T. M., Marlo J. E., Niswender C. M., Jones C. K., Jadhav S. B., Gentry P. R., Plumley H. C., Weaver C. D., Conn P. J. and Lindsley C. W.; Discovery of the first highly M5-preferring muscarinic acetylcholine receptor ligand, an M5 positive allosteric modulator derived from a series of 5-trifluoromethoxy N-benzyl isatins; *Journal of Medicinal Chemistry*; 52 (2009) 3445–3448.
52. Beers W. H, Reich E.; Structure and activity of acetylcholine; *Nature*; 228 (1970) 917-922.
53. Marriott D. P., Dougall I. G., Meghani P., Liu Y. J., Flower D. R., Lead generation using pharmacophore searching: application to muscarinic M3 receptor antagonists; *Journal of Medicinal Chemistry*; 42 (1999) 3210-3216.
54. (a) Haga K., Kruse A.C., Asada H., Kobayashi T.Y., Shiroishi M., Zhang C., Weis W.I., Okada T., Kobilka B.K., Haga T. and Kobayashi T., Structure of the human M2 muscarinic acetylcholine receptor bound to an antagonist; *Nature*; 482 (2012) 547-550.
- (b) Kruse A.C., Hu J., Pan A.C., Arlow D.H., Rosenbaum D.M., Rosemond E., Green H.F., Liu T., Chae P.S., Dror R.O., Shaw D.E., Weis W.I., Wess J. & Kobilka Brian K., Structure and dynamics of the M3 muscarinic acetylcholine receptor; *Nature*; 482 (2012) 552-556.

- (c) Nordvall G., Hacksell U.; Binding site modeling of muscarinic m1 receptor: a combination of homology-based and indirect approaches; *Journal of Medicinal Chemistry*; 36(1993) 967-976.
55. Peng J.Y., Vaidehi N., Hall S. E., Goddard W. A.; The predicted 3D structures of human M1 muscarinic acetylcholine receptor with agonist or antagonist bound; *ChemMedChem*; 1 (2006) 878-890.
56. Jöhren K., Holtje H. D.; A model of human M2 muscarinic acetylcholine receptor; *Journal Computer Aided Molecular Design*; 16 (2002) 795-801.
57. Ostapovici L., Mracec M., Mracec M., Borota A.; Exploring the binding site of human muscarinic M3 receptor: homology and docking study; *International Journal of Quantum Chemistry*; 107 (2007) 1794-1802.
58. Pedretti A., Vistoli G., Marconi C., Testa B.; Muscarinic receptors: a comparative analysis of structural features and binding modes through homology modelling and molecular docking; *Chemistry & Biodiversity*; 3 (2006) 481-501.
59. Vistoli G., Pedretti A., Dei S., Scapecchi S., Marconi C., Romanelli M. N.; Docking analyses on human muscarinic receptors: Unveiling the subtypes peculiarities in agonists binding; *Bioorganic & Medicinal Chemistry*; 16 (2008) 3049-3058.
60. Kaiser C., Spagnuolo C. J., Adams T. C., Audia V. H., Dupont A. C., Hatoum H., Lowe V. C., Prosser J. C., Sturm B. L., Noronha-Blob L.; Synthesis and antimuscarinic properties of some N-substituted 5-(aminomethyl)-3,3-diphenyl-2(3H)-furanones; *Journal of Medicinal Chemistry*; 35 (1992) 4415-4424.
61. Ahungena A., Gabriel J. L., Canney D. J.; Synthesis and evaluation of 5-substituted derivatives of 4,5-dihydro-3,3-diethyl-2(3H)-furanone as subtype-selective

- muscarinic leads; *Medicinal Chemistry Research*; 12 (2003) 481- 511.
62. Lewis L. M., Sheffler D., Williams R., Bridges T. M., Kennedy J. P., Brogan J. T., Mulder M. J, Williams L., Nalywajko N. T., Niswender C. M., Weaver C. D., Conn P. J., Lindsley C. W.; Synthesis and SAR of selective muscarinic acetylcholine receptor subtype 1(M1 mAChR) antagonist; *Bioorganic & Medicinal Chemistry Letters*; 18 (2008) 885-890.
63. Ahungena A., Canney D. J.; Synthesis and biological evaluation of aminomethyl derivatives of an anticonvulsant γ -butyrolactone; *Medicinal Chemistry Research*; 6 (1996) 618-634.
64. Orjales A., Bordell M. J., Rubio V.; Synthesis and structure-activity relationship of new piperidinyl and piperazinyl derivatives as antiallergics; *Heterocyclic Chemistry*; 32 (1995) 707-718.
65. Swanson D. M., Dubin A. E., Shah C., Nasser N., Chang L., Dax S. L., Jetter M., Breitenbucher J. G., Liu C., Mazur C., Lord B., Gonzales L., Hoey K., Rizzolio M., Bogenstaetter M., Codd E. E., Lee D. H., Zhang S. P., Chaplan S. R. and Carruthers N. I.; Identification and biological evaluation of 4-(3-trifluoromethylpyridin-2-yl)piperazine- 1-carboxylic acid (5-trifluoromethylpyridin-2-yl)amide, a high affinity TRPV1 (VR1) vanilloid receptor antagonist; *Journal of Medicinal Chemistry*, 48 (2005) 1857-1872.
66. Eastwood P. R.; A versatile synthesis of 4-aryl tetrahydropyridines via palladium mediated Suzuki cross-coupling with cyclic vinyl boronates; *Tetrahedron Letters*; 41 (2000) 3705-3708.
67. Zhao C.; Design, synthesis and evaluation of two-substituted quinuclidines: ligands

- for nicotinic acetylcholine receptors, Dissertation, 2001.
68. Richards M. H; Rat hippocampal muscarinic autoreceptors are similar to the M2 (cardiac) subtype: comparison with hippocampal M1, atrial M2 and ileal M3 receptors; *British Journal of Pharmacology*; 99 (1990) 753-761.
 69. Lima L. M. and Barreiro E. J.; Bioisosterism: A Useful Strategy for Molecular Modification and Drug Design; *Current Medicinal Chemistry*; 12 (2005) 23-49.
 70. Meanwell N. A.; Synopsis of Some Recent Tactical Application of Bioisosteres in Drug Design; *Journal of Medicinal Chemistry*; 54 (2011) 2529-91.
 71. Peretto I., Forlani R., Fossati C., Giardina G. A. M., Giardini A., Guala M., Porta E. L., Petrillo P., Radaelli S., Radice L., Raveglia L. F., Santoro E., Scudellaro R., Scarpitta F., Bigogno C., Misiano P., Dondio G. M., Rizzi A., Armani E., Amari G., Civelli M., Villetti G., Patacchini R., Bergamaschi M., Delcanale M., Salcedo C., Ferná'ndez A. G. and Imbimbo B. P.; Discovery of diaryl imidazolidin-2-one derivatives, a novel class of muscarinic M3 selective antagonists (Part 1); *Journal of Medicinal Chemistry*; 50 (2007) 1571-1583.
 72. Shahane S., Louafi F., Moreau J., Hurvois J. P., Renaud J. L., Weghe P. and Roisnel T.; Synthesis of alkaloids of *Galipea officinalis* by alkylation of and α - amino Nitrile," *European Journal of Organic Chemistry*, 2008 (2008) 4622-4631.
 73. Maryanoff B. E., McComsey D. F., Constanzo M. J., Hochman C., Swintosky V. S. and Shank R. P.; Comparison of sulfamate groups for the inhibition of carbonic anhydrase-II by using topiramate as structural platform; *Journal of Medicinal Chemistry*; 48 (2005) S4.
 74. MaGee D. I., Godineau E., Thornton P. D., Walters, M. A. and Sponholtz D. J;

- Diastereoselective [4+3] cycloadditions of enantiopure nitrogen-stabilized Oxyallyl Cations; *European Journal of Organic Chemistry*; 2006 (2006) 3667-3680.
75. Danielmeier K. and Steckhan E.; Efficient pathways to (R)- and (S)-5-hydroxymethyl-2-oxazolidinone and some derivatives; *Tetrahedron:Asymmetry*; 1995, Vol. 6, No. 5pp. 1181-1190.
76. Osa Y., Hikima Y., Sato Y., Takino K., Ida Y., Hirono S. and Nagase H.; Convenient synthesis of oxazolidinones by the use of halomethyloxirane, primary amine and carbonate salt; *Journal of Organic Chemistry*; 70 (2005) 5737-5740.
77. Weilin S., Carroll P. J., Soprano D. R. and Canney D. J.; Identification of a chromone-based retinoid containing a polyolefinic side chain via facile synthetic routes; *Bioorganic & Medicinal Chemistry Letters*; 19 (2009) 4339-4342.
78. Sakai N., Moriya T. and Konakahara T.; An efficient one-pot synthesis of unsymmetrical ethers: a directly reductive deoxygenation of esters using an InBr₃/Et₃SiH catalytic system; *Journal of Organic Chemistry*; 72 (2007) 5920-5922.
79. Gao R. and Canney D. J.; A versatile and practical microwave-assisted synthesis of sterically hindered N-arylpiperazines; *Journal of Organic Chemistry*; 75 (2010) 7451-7453.
80. Sun W., Desai S., Piao H., Carroll and Canney D. J.; Wittig-Horner-Emmons reactions of triethyl 3-methyl-phosphonocrotonate with 3-formylchromones en route to benzophenone- based retinoid candidates; *Heterocycles*; 71 (2007) 557 – 567.
81. (a) Desai S., Sun W., Gabriel J. L., and Canney D. J.; The synthesis and preliminary evaluation of substituted chromones, coumarins, chromanones, and benzophenones as retinoic acid receptor ligands; *Heterocyclic Communications*;

- 14:3 (2008) 129-137.
- (b) Khadem S. and Marles R. J.; Chromone and Flavonoid Alkaloids: Occurrence and Bioactivity; *Molecules*; 17 (2012) 191-206.
82. Choi. S., Pradhan A., Hammond N. L., Chittiboyina A. G., Tekwani B. L., and Avery M. A.; Design, synthesis, and biological evaluation of plasmodium falciparum lactate dehydrogenase inhibitors; *Journal of Medicinal Chemistry*; 50 (2007) 3841-3850.
83. Payard M., Couquelet J.; A new and facile synthesis of 2-hydroxymethyl chromone and 2-formylchromone; *Synthesis*; 11 (1979) 889.
84. Mouysset G., Payard M., Tronche P., Bastide J., Bastide P.; Synthesis and antiallergic activity of some benzopyronic and structurally related alcohols; *European Journal of Medicinal Chemistry*; 23 (1988) 199-202.
85. Levine J. A., Ferrendelli J. A. and Covey D. F.; Alkyl-substituted thio-, thiono-, and dithio- γ -butyrolactones: new classes of convulsant and anticonvulsant agents; *Journal of Medicinal Chemistry*; 29 (1986) 1996-1999.
86. Hou D. R., Reibenspies J. H. and Burgess K.; New, optically active phosphine oxazoline (JM-Phos) ligands: syntheses and applications in allylation reactions; *Journal of Organic Chemistry*; 66 (2001) 206-215.
87. Bensari A, Zaveri N.T.; Titanium(IV) Chloride-Mediated Ortho-Acylation of Phenols and Naphthols; *Synthesis*; 2 (2003) 267-271.
88. Isaad J., Achari A.; Biosourced 3-formyl chromenyl-azo dye as Michael acceptor type of chemodosimeter for cyanide in aqueous environment; *Tetrahedron*; 67 (2011) 5678-5685.

89. Annadurai S.; Lead generation using privileged structure based approach, Dissertation, 2011.
90. Gao R., Canney D. J.; Synthesis and evaluation of a homologous series of 3,5-trisubstituted gamma-butyrolactones as potential muscarinic ligands; Abstracts of Papers, 240th ACS National Meeting, Boston, MA, United States, August 22-26, 2010.
91. Ishizuka T. and Kunieda T.; Mild and selective ring cleavage of cyclic carbamates to amino alcohols; Tetrahedron letters; 28 (1987) 4185-4188.
92. List B., Pojarliev P., Biller W.T. and Martin H.J.; The proline-catalyzed direct asymmetric three-component mannich reaction: scope, optimization, and application to the highly enantioselective synthesis of 1,2-amino alcohols